STRUCTURAL INVESTIGATIONS OF SULPHONATED POLY(BUTYLENE TEREPHTHALATE) AND ITS BLEND WITH POLYCARBONATE USING THERMAL AND SCATTERING TECHNIQUES.

A thesis submitted for the degree of

Doctor of Philosophy

by

Khalid Mahmood

Department of Physics

Brunel University

May 1998

BRUNEL UNIVERSITY

PUBLICATION OF THESES

Please complete in block capitals

NAME: __KHALID MAHMOOD__

DEPARTMENT: INSTITUTE OF PHYSICAL AND ENVIRONMENTAL SCIENCES
__CENTRE FOR PHYSICAL SCIENCES__

TITLE OF THESIS: __STRUCTURAL INVESTIGATIONS OF SULPHONATED__
__POLY (BUTYLENE TEREPHTHALATE) AND ITS BLENDS WITH__
__POLYCARBONATE USING THERMAL AND SCATTERING__
TECHNIQUES

PLEASE COMPLETE __EITHER__ PART A __OR__ PART B

A. I agree that the abstract of my thesis may be published by the University without further reference to me.

In accordance with the University's Handbook of Procedures, the Head of Library Services may allow my thesis to be copied in whole or in part without further reference to me. Such Authority shall apply only to single copies made for study purposes and shall be subject to normal conditions of acknowledgement.

(See notes overleaf)

Signature: _Khalid Mahmood_

Date: __26/5/98__

B. I request that my thesis be held under confidential cover in the Library for a period of _____ years for the following reasons:

_____

_____

_____

_____

Once the period of confidentiality has expired, I agree that the conditions set down in Part A will apply without further reference to me

Signature: _____

Date: _____

Please pass this form to your supervisor who should sign below indicating his/her agreement to the retention of the thesis under confidential cover.

Signature of Supervisor: _____

Additional comments _____

_____

_____

_____

If you have completed Part A please return this form direct to the Library.

Part B, when complete, should be returned to the Assistant Registrar.

I dedicate this work to:

My parents for their never-ending moral support

My Family, especially my wife , Nuzhat Bano and my children
Shaftab Khalid, Areeba Khalid, Areej Khalid and Saifa Khalid

To those of you who care

ABSTRACT

The work described in this thesis aims at a better understanding of several ionomers and their blends on a microscopic level especially poly (butylene terephthalate) (PBT) and sulphonated poly (butylene terephthalate) (SPBT). The commercial importance of ionomer blends stems from the fact that the inclusion of sulphonate groups can improve or enhance the optical clarity of a blend made with non-sulphonated material. In particular, the present work investigates the optimum blend composition and level of sulphonation for a partially miscible sulphonated poly (butylene terephthalate) and polycarbonate (SPBT/PC) blend system. It has been found that the most transparent blends were SPBT/PC 7.9 mole % sulphonation 25/75 and 11.1 mole % sulphonation 50/50.

The principal part of this thesis deals with characterisation of polymer blends using primarily differential scanning calorimetery (DSC) and thermogravimetry analysis (TGA). The second part of the thesis contains an investigation of the structural and microstructural properties of the functionalized PBT both in the homopolymer and in a blend with PC, and polystyrene ionomers by wide angle X-ray diffraction, (WAXD) and light microscopy. For comparison, a series of polystyrene ionomers were studied. The similar behaviour of PS ionomers (which are model random ionomers) to that of PBT ionomers gives an additional support to this study.

It follows from the above studies that upon increase of the level of sulphonation a change in the structural properties of the material results in a reduced crystallinity of PBT. This leads to increased miscibility of the PBT/PC blend.

ACKNOWLEDGEMENTS

List of Tables

List of Figures

TABLE OF CONTENTS

CHAPTER 1

INTRODUCTION

1.1   The field of study

Functional polymers such as ionomers are some of the most important polymeric compounds used in the last decade. Their properties depend to a significant extent, or even entirely, on the functional group substituted on the macromolecule[1]. Polymers containing a small percentage (typically less than 10 mole %) of ionic groups chemically bound to a non-polar chain are termed *ionomers*. Their physical and mechanical properties such as viscosity or elasticity are often dramatically changed with respect to the starting material.

Further important field of study is the science of polymer blends and alloys. Polymer materials with desired physico-chemical properties can sometimes be obtained by modification of existing polymers by the incorporation of ionic groups or by blending with a second polymer. This procedure provides a cost efficient means of selectively improving polymer properties.

Understanding of the morphology and structure related properties of bulk polymer remains a challenging task, especially when a small alteration in their chemistry results in a substantial change in their physical properties. Such is the case of ionomers in some of the earliest studies Eisenberg has explained these property changes as due to a specific microphase structure of the ionic groups[2-3].

Over the past two decades, a considerable amount of research has been devoted to random ionomers due to their superior physical properties[4-15] such as combined heat and chemical resistance, dimensional stability and mechanical strength.

a

$$\left[\!-O-(CH_2)_4-O-\underset{\underset{O}{\|}}{C}-\bigcirc-\underset{\underset{O}{\|}}{C}\!-\right]_n$$

b

$$\left[\!-O-(CH_2)_4-O-\underset{\underset{O}{\|}}{C}-\bigcirc-\underset{\underset{O}{\|}}{C}\!-\right]_n$$

$$\left[\!-O-(CH_2)_4-O-\underset{\underset{O}{\|}}{C}-\underset{\underset{NaSO_3^{+-}}{\bigcirc}}{}-\underset{\underset{O}{\|}}{C}\!-\right]_m$$

c

$$\left[\!-O-\bigcirc-\underset{\underset{CH_3}{\overset{CH_3}{|}}}{C}-\bigcirc-O-\overset{\overset{O}{\|}}{C}\!-\right]_n$$

d

$$\left[\!-\underset{\bigcirc}{CH}CH_2-\right]_n \left[\!-\underset{\underset{NaSO_3^{+-}}{\bigcirc}}{CH}CH_2-\right]_m$$
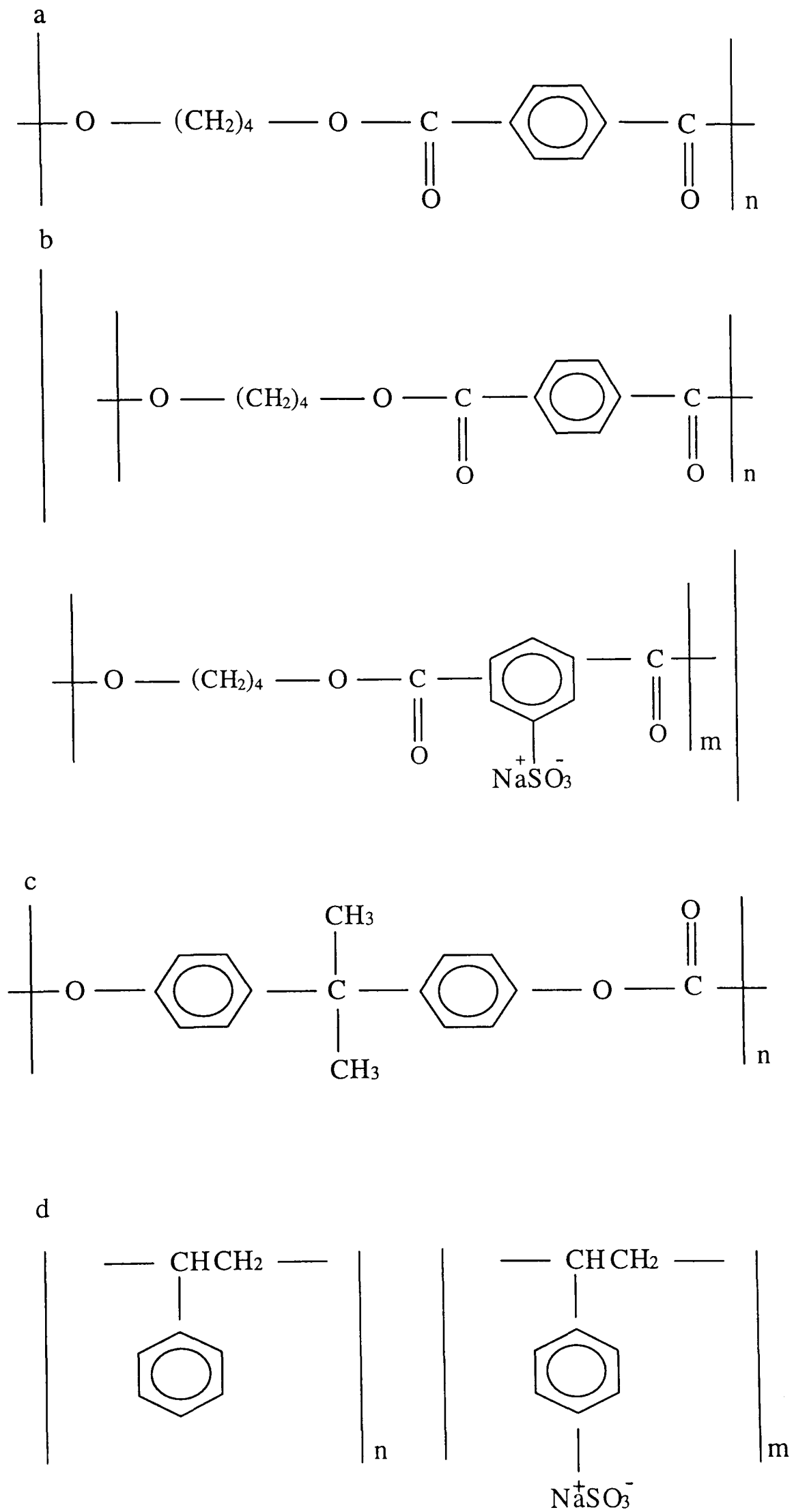
Figure 1.1 Molecular arrangements a) PBT, b) SPBT, c) PC, d) SPS

The term "random ionomer" denotes an ionomer in which the ionic species are randomly distributed along the chain. Figures 1.1 (b) and (d) display molecular arrangements of sulphonated poly (butylene terephthalate) (SPBT) and sulphonated isotactic polystyrene, respectively. The property enhancement is directly related to the incorporation of ionic moieties into the microphase-separated regions. This microphase phenomenon (Phases having different electron densities in the bulk) occurs in both wholly amorphous and semicrystalline polymers. In the latter materials, the crystalline regions add a further degree of complexity. Several of models for the morphology of random ionomers have been proposed, none of which is completely consistent with all experimental observations recorded for these materials. These models have recently been reviewed[11-12].

It is proposed that ion-rich regions termed *clusters* may also exist at sufficiently high ion content in some systems[16]. The clusters behave as a separate phase in that they exhibit their own glass transition temperature (T_g). However, the exact structures of the multiplets and clusters have not yet been fully elucidated. Extensive studies of ionomeric polymers have shown that the crystals formed in these systems, for example, consist entirely of copolymer segments similar to their homopolymers[17-18]. The polar substituents do not fit easily in the tight crystalline matrix and are excluded to the amorphous phase.

The interest in the polyester poly (butylene terephthalate)/polycarbonate (PBT/PC) blends arises from a favourable combination of fast crystallising polymer (PBT) that is partially miscible with a second, usually amorphous constituent polycarbonate (PC). The blend PBT/PC is widely used, for example for moulded automobile parts. It is produced from the semi-crystalline polymer PBT and has highly advantageous mechanical properties but is optically opaque due to the high level of crystallinity[18-20]. The primary aim of this work was to investigate the possibility of producing a new blend system, sulphonated poly (butylene terephthalate)/polycarbonate, (SPBT/PC), which could show equally advantageous mechanical properties as PBT/PC but with the added bonus of optical clarity. This would widely enhance its utility: it could be used for the production of car windscreens, for example. Firstly, it was necessary to gain an

improved understanding of the properties and behaviour of SPBT. Secondly, the miscibility and physical properties of the new blend were investigated with a view to optimising both the functionality of the homopolymer and the blend composition. To this end, the following techniques were used: wide angle X-ray diffraction (WAXD), differential scanning calorimetry (DSC), thermo-gravimetry analysis (TGA) and optical microscopy.

Since SPBT is a relatively new material, in addition a model type of ionomer, sulphonated polystyrene (SPS), was standard for comparison. In these random copolymers of PS and SPS, some hydrogen atoms from benzene rings are substituted by the SO_3^- group, and the sulphonate group is neutralised with a metal cation, such as Na^+ (Figure 1d). It was therefore interesting to compare the structure of SPS with that of SPBT. It is worth noting that while the SPS the sulphonate group is substituted on pending benzene ring, in SPBT the benzene ring is incorporated in the main chain.

1.2   Objectives

(i)   To characterise the thermal and structural properties of sulphonated poly (butylene terephthalate) (SPBT), sulphonated polystyrene (SPS) with different level of ionic content, and their unsulphonated counterparts.

(ii)   To investigate the possibility of producing a new blend system sulphonated poly (butylene terephthalate) (SPBT) and polycarbonate (PC) with a view to optimise both the functionality (ionic content) of the homopolymer and the blend composition, and to reduce crystallinity in the material in order to obtain optically clearer blends.

(iii)   To compare wide angle X-ray diffraction (WAXD) patterns and thermal data from *isotactic* polystyrene and its copolymer with sulphonated isotactic polystyrene (iso-SPS) with those obtained from PBT in order to gain a deeper understanding of the results obtained for the PBT/SPBT ionomers.

1.3   Outline of the thesis

This thesis comprises six chapters. Chapter two outlines the basic thermodynamic concepts such as the polymer solubility and lattice theory of polymer miscibility. In addition, the rudimental of models, which describe ion aggregation, are covered along with the concepts from polymer crystallinity. In chapter three the polymers used and experimental techniques employed during this research are described. These are thermal analysis, wide angle X-ray diffraction and optical microscopy. The experimental results are described and discussed in chapters four and five. The thermal behaviour of ionomers sulphonated poly (butylene teraphthalate (SPBT) and polystyrene (PS) studied by differential scanning calorimetery (DSC) and thermo-gravimetric analysis (TGA) techniques are discussed in chapter four along with the detailed description of DSC studies of SPBT/PC blends. Chapter five reports the results of wide angle X-ray diffraction measurements on the PBT, SPBT film and powder sample and the PS samples. The conclusions and recommendations for further work are presented in chapter six.

References

1   D E Bergbreiter and C R Martin, in "Functional Polymers", Plenum Press, London and New York (1991).

2   A Eisenberg and M King, in "Ion-Containing Polymers, Physical Properties and structure", Academic Press, New York (1977).

3   I S Miles and S Rostami, in "Multicomponent Polymer Systems", Longman Science & Technical, London and New York (1992).

4   A Eisenberg, in "Ions in Polymers" Advances in Chemistry Series 187, American Chemical Society, Washington DC (1980).

5   C G Bazuin and A Eisenberg, *Ind. Eng. Prod. Res. Dev*, **20** 271 (1981).

6   W J MacKnight and T R Earnest, *J. Polym. Sci. Macromol. Rev*, **16** 41 (1981).

7   A D Wilson, H J Prosser, in "Developments in Ionic Polymers" Applied Science, New York Vols 1 and 2 (1983).

8   A Eisenbereg and E F Bailey, "Coulombic Interactions in Macromolecular Systems", ACS Symposium Series 302, American Chemical Society, Washington DC (1986).

9   M Pineri and A Eisenberg, in "Structure and Properties of Ionomers", NATO Advanced Study Institute Series 198, D Reidel Publishing Co, Dordrecht, Holland (1987).

10   J J Fitzgerald and R A Weiss, *J. Macromol. Sci. Rev. Macromol. Chem. Phys*, **C28** 99 (1988).

11   K A Mauritz, *J. Macromol. Sci. Rev. Macromol. Chem. Phys*, **C28** 65 (1988).

12   A Eisenberg, B Hird and R B Moore, *Macromolecules*, **23** 18 (1990).

13   C G Bazuin, in "Multiphase Polymers Blends and Ionomers", L A Utracki, R A Weiss, ACS Symposium Series 395, American Chemical Society, Washington DC Chapter 21 (1989).

14   C W Lantman, W J Macknight and R D Lundberg, in "Comprehensive Polymer Science", G Allen, J C Bevington, Pergamon Press: Oxford, Vol. 2 Chapter 25.

15   K Hatada, T Kitayama and O Vogal, in "Macromolecular Design of Polymeric

Materials", M Dekker Inc, New York (1997).

16   Z Gao, X F Zhong and A Eisenberg, *Macromolecules,* **27** (1994).

17   K Tadano, E Hirasawa, H Yamamoto and S Yano, *Macromolecules,* **22** 226 (1989).

18   M R Tant, K A Mauritz and G L Wilkes, in "Ionomers, Synthesis, Structure, Properties and Applications", Blacki Academic & Professional London (1997).

19   S Datta and D J Lohse, in "Polymeric Compatibilizers", Hanser Publishers, Germany and New York (1996).

20   R G Griskey, in "Polymer Process Engineering", Champion & Hall, London and New York (1997).

CHAPTER 2

POLYMER MORPHOLOGY: THEORY AND BACKGROUND

2.1   Introduction

Polymer blends are physical mixtures of structurally different polymers which adhere together through the action of secondary bond forces, with no covalent bonding between them. They are of considerable scientific and industrial interest[1-6] in search for new polymeric materials, blending of polymers is a method for obtaining new desirable property combinations without having to synthesize novel structures. Many of such mixtures were commercialized including those based on poly (butylene terepthalate) (PBT) and poly (bisphenol A-carbonate) (PC) [7].

The PBT/PC blends are a mixture of a fast-crystallizing polymer (PBT) which is partially miscible with a second, amorphous constituent (PC). This blend is used extensively for production of automobile parts. There is a growing interest in such blends. Several semi crystalline/amorphous polymer systems that are miscible in the amorphous state have recently been reported, for example blends of PBT and polyvinyl chloride (PVC) and polyester oligomers with PVC[8-12].

From the application point of view polycarbonate (PC) is tough and stable to 573 K but has poor solvent resistance, its glass transition temperature T_g is approximately 418 K[13]. Poly (butylene terephthalate) (PBT) has relatively good solvent resistance, a low T_g (approximately 316 K) and a high melting temperature T_m (> 493 K)[13]. A blend formed with PBT and PC produces a material with good chemical resistance as well as good heat and impact resistance[13-14].

2.2   Miscibility of polymer blends

The main aim of the study of sulphonated poly (butylene terephthalate) (SPBT) and polycarbonate blends was to determine their miscibility. The way to achieve it was

through detailed structural studies and thermal properties determination. Since polymer blends are immiscible this means that their components are not intimately mixed and the blends behave as two-phase systems. There are however some polymer pairs that form a single homogeneous phase. These are termed *miscible blends* and behave as one-phase systems. If they are miscible just for limited ranges of temperature and composition they are called *partially miscible*.

The term "compatibility" is used extensively in the description of polymer blends. "Compatibility" refers to some advantageous technological properties of the blend regardless of its one or two-phase behavior. A compatible blend can be immiscible.

Several factors control the degree of miscibility of two polymers: molecular weight M_w and molecular distribution M_w / M_n where M_n is called the number average molecular weight, chemical composition which will determine the presence of interactive forces, morphology, crystal structure and processing. The equilibrium state of a blend is governed by the laws of thermodynamics. From a thermodynamic point of view $\Delta G_{mix} = \Delta H_{mix} - T \Delta S_{mix}$, mixing will occur when the Gibbs free energy G involved in that process is negative. The entropy term S is usually very small due to their huge size and thus the enthalphic term H will have to be negative, or close to zero if it is positive, for mixing to occur.

Experimentally there are several ways of studying the miscibility of blends, the most common being determination of its glass transition temperature, T_g. If the blend shows a single T_g, intermediate between the T_g's of the components, it is then considered to form a *miscible system*[15]. If it shows two T_g's instead each corresponding to the separate components transitions, the system is *immiscible*. This criterion has some limitations: for example the T_g's of the components have to differ by at least 20 K in order to be observed separately. A direct way of determining a blend's miscibility is just looking at it, either by eye or by microscope. If the sample looks cloudy it will be a two-phase system, since the light is dispersed by the different phases. If it is transparent, it will be a completely mixed system. Scattering is also a frequently used way of studying at miscibility because either light, X-rays or neutron beam going

through a sample will be scattered very differently by a mixed or by a phase-separated system.

2.3   Microstructure of semicrystalline polymer

In order to attempt a description of a semi-crystalline and amorphous miscibility of polymers on a local scale, it is useful to recall basic ideas of crystallinity. When small molecules crystallise, each granule often has the form of a crystal grown from a single nucleus. Such crystals are relatively free of defects and have well-defined crystal faces and cleavage planes. Their shapes can be related to the geometry of the unit cell of the crystal lattice. Polymers crystallised from the melt are polycrystalline. Their structures are a conglomerate of disordered material and clusters of crystallites that developed more or less simultaneously from the growth of many nuclei. Distinct crystal faces cannot be distinguished, and the ordered regions in semicrystalline polymers are generally much smaller than those in more perfectly crystallised micromolecular species. Generally maxima appearing in the X-ray patterns are broadened by small crystallite sizes and by defects in larger crystals. If the sample is polymeric then such data may be interpreted in terms of highly ordered regions in semicrystalline polymers having dimensions of the order of 10-100 nm. These domains are held together by tie "molecules" which traverse more than one crystallite. This is what gives a semicrystalline polymer its mechanical strength. (Aggregates of crystals of small molecules are held together only by secondary forces and are easily split apart). Hence the term *crystallite* is used in polymer science to imply a component of an interconnected microcrystalline structure[16].

2.3.1   Crystal lamellae

Polymer crystallisation has been intensively studied over the last few decades[16]. Once nucleated, crystallisation proceeds with the growth of a ribbonlike folded chain called *lamellae*. The arrangement of polymer chains in the lamellae has some resemblance to that in platelike single crystals which can be produced by precipitating a crystallisable polymer from its dilute solutions. In such single crystals the molecules are aligned

along the thinnest dimension of the plate. The lengths of extended macromolecules are much greater than the thickness of these crystals and it is evident that a polymer chain must fold outside the plate volume and reenter the crystallite at a different point. The dimensions of polymer single crystals are typically of the order of microns, for the length and breadth and about 0.1 μm for the thickness. The thickness remains constant for a given set of crystallisation conditions but increases with the crystallisation temperature. Perfect crystallinity is not achieved, because the portions of the chains at the surfaces and in the folds are not crystallised. Three models of chain conformations in a single crystal are illustrated in Figures 2.1(a-b) and 2.2[17-18].

[a]   [b]
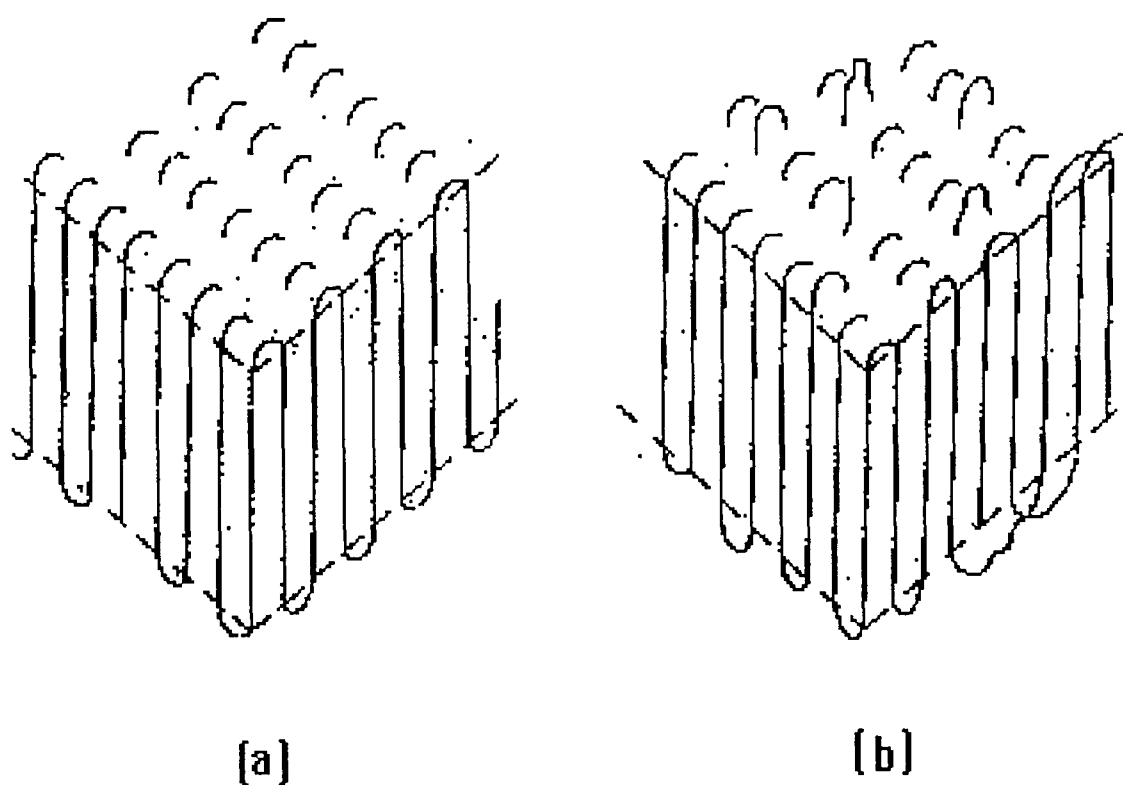
Figure 2.1 (a) Adjacent re-entry model with smooth , regular chain fold.

(b) adjacent re-entry model with rough fold surface[16]
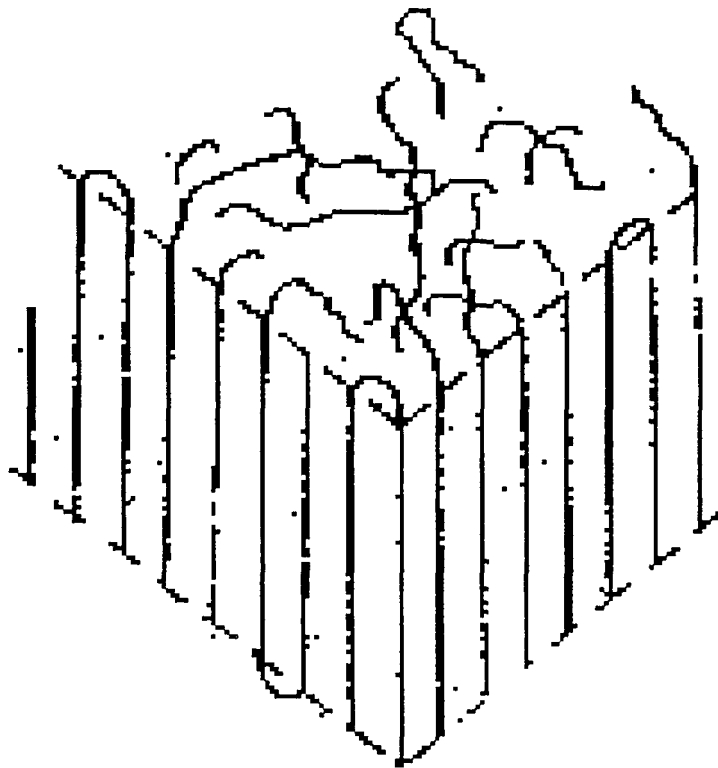
Figure 2.2 Random re-entry (switchboard) model[16].

Folded-chains crystals grow by extension of the length and breadth, but not the thickness. The supply of polymer segments is much greater in the melt than in dilute solutions, and crystallisation in the bulk produces long, ribbon like folded chain structures. These lamellae become twisted and split as a result of local depletion of crystallisable material and growth around defect structures. The regularity of chain folding and reentry is very likely much less under these conditions than in the single crystals produced by slow crystallisation from dilute solution.

Another major difference in crystallisation from melt and from dilute solution is that neighboring growing lamellae will generally be close together under the former conditions. Segments of a single molecule are thus likely to be incorporated in different crystallites in bulk crystallised polymer. These "tie molecules" bind the lamellae together and make the resulting structure tough.

2.3.2 Morphology of semicrystalline polymers

The morphology of a crystallisable polymer is a description of the forms that result from crystallisation and the aggregation of crystallites. Crystalline lamellae are the basic units in the microstructures of solid semicrystalline polymers. The lamellae are observed to be organized into two types of larger structural features depending on the conditions of the bulk solidification process.

The major feature of polymers that have been bulk crystallised under quiescent conditions are polycrystalline structures called *spherulites*. These are roughly spherical supercrystalline structures which exhibit Maltese cross-extinction patterns when examined under polarised light in an optical microscope. Spherulites are characteristic of semicrystalline polymers and are also observed in low-molecular weight materials that have been crystallised from viscous media.
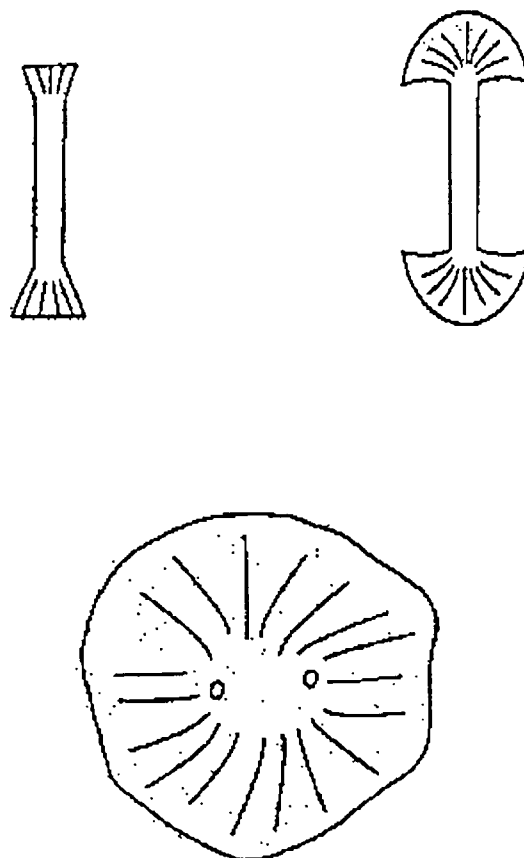
Figure 2.3 Successive stages in the development of a spherulite by fanning growth from a nucleus[19].

BRANCHED FIBRILS, WITH
POLYMER CHAIN FOLDED
AT RIGHT ANGLES TO LONG
AXIS

INTERFIBRILLAR
MATERIAL, LARGELY
AMORPHOUS

SINGLE
CRYSTAL
NUCLEUS
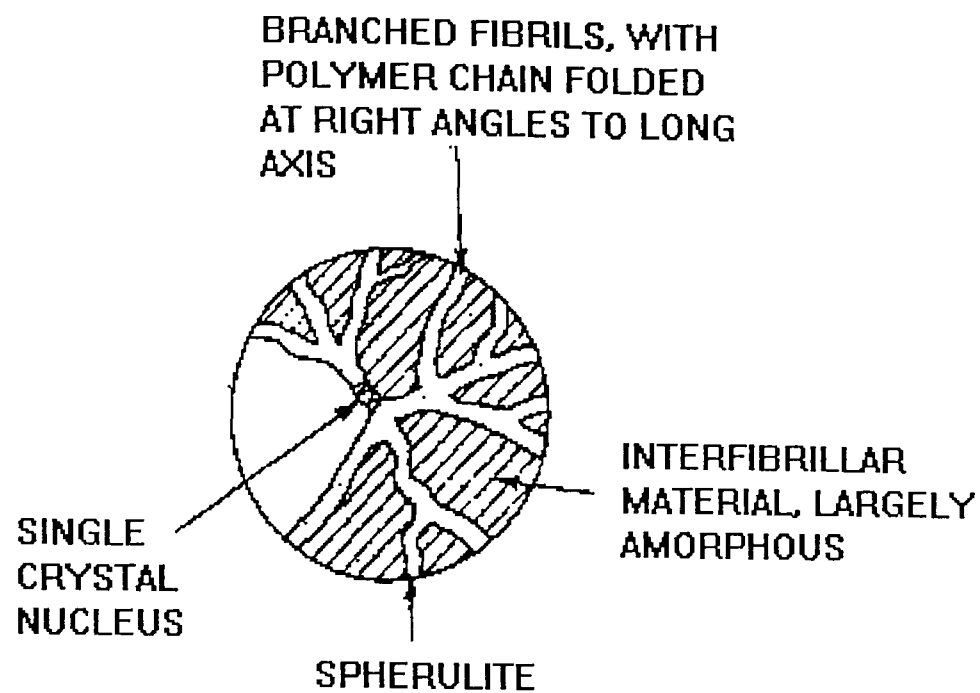
SPHERULITE

Figure 2.4 Schematic representation of basic structure of a polymer spherulite[19].

Spherulites are aggregates of lamellar crystallites. They are not single crystals and include some disordered material within their boundaries. The sizes of spherulites may vary from somewhat greater than a crystallite to dimensions visible to the naked eye.

A spherulite is built up as lamellar subunits that grow outwards from a common nucleus. As this growth advances into the uncrystallised polymer, local inhomogeneities in concentrations of crystallisable segments will be encountered. The folded chain fibril will inevitably twist and branch. At some early stage in its development the spherulite will resemble a sheaf of wheat, as shown in Figure 2.3. Branching and fanning out of the growing lamellae tends to create a spherical shape, but neighbouring spherulites will impinge on each other in bulk crystallised polymers and prevent the development of true spherical symmetry. Figure 2.4 shows the various structural units that are probably involved in formation of a spherulite[19].

The growth of polymer spherulites involves the segregation of non-crystallisable material into the regions between the lamellar ribbons. The components that are not

incorporated into the crystallites include additives like oxidation stabilisers, catalyst residues, as well as co-monomer units or branches. The spherulite structures and interspherulitic boundaries are held together primarily by polymer molecules which run between the twisted lamellar subunits and the spherulites themselves.

2.3.3 Semicrystalline ionomers: crystallisation kinetics and morphology

The polymer studied in this thesis, PBT is semicrystalline, and it is only partially miscible with the amorphous PC. Sulphonation of PBT has an effect of increasing miscibility of SPBT/PC blend, as shown in chapter 4. Clearly, a question to be asked is 'what is the influence of sulphonation on the structure of semicrystalline PBT'? In order to address this question, the effects of introduction of ionic groups into neutral polymer through the process of sulphonation are briefly described below.

It is well known[20] that the introduction of a comonomer into a crystallisable polymer chain typically decreases both crystallisation kinetics and overall degree of crystallinity because it gives rise to an imperfection in the polymer chain. In addition, the effects of intermolecular ionic interaction can strongly influence the flow characteristics of a polymer system as long as the thermal energy of the system is below that necessary to promote 'thermal dissociation' of the ionic species. As a result, the presence of ionic groups on an otherwise molecularly symmetric backbone that favours crystallisation will generally lead to a reduction in the rate of crystallisation. Furthermore, the retardation of crystallisation kinetic, the introduction of imperfections in the polymer chain, and the greater energy required to align the polymer chains, will tend to reduce the overall level of crystallinity in a typically processed sample when compared to the unfunctionalised polymer. However, the magnitude of these effects will depend upon the location of the ionic groups within the chain. Therefore, the crystallisation behaviour of ionomers of various molecular architectures, such as block, random copolymer, telechelic, etc. will not necessarily the same.

To date there has been relatively little systematic information obtained concerning the effects of ionic groups on the crystallisation behaviour and, more specifically, on the

effect of crystallinity on morphological behaviour.

It is worthwhile to recall that, in general, polymers that undergo crystallisation from the undeformed melt typically form a spherulitic morphology. Basically, this superstructure is composed of radiating fibrillar folded-chain lamellae with interlayer amorphous or more disordered regions generally connected through tie chains. Depending on the level of crystallinity, the interlayer amorphous regions may comprise minor component of the system, but one can also picture in low crystallinity systems that amorphous regions may also exist in the boundaries between spherulites as well as between the lamellae within individual spherulites. Certainly, the general features of connectivity at the boundaries of spherulites and the general continuity of the crystalline phase within a material is of importance to properties, as is whether the material is above the T_g of the amorphous phase. Of course, if the material is above the T_g and if the amorphous content is considerable, the system may be much softer or more rubbery than if the crystalline texture is continuous throughout.

2.4 Mixing of polymers (semi-crystalline and amorphous)

The study of the crystalline structure has been very important and provoked passionate discussions for many years: how could molecules of around 100 *nm* in length fit unit cells of 10 *nm* thickness. Diffraction measurements indicated that polymer chains are oriented normal or very nearly normal to the plane of the lamellae. The only plausible explanation was that polymer chains pass through many cells, in other words, each unit cell contains only a few mers, as described by Sperling [20].

Crystalline or more precisely semicrystalline polymers give regular X-ray diffraction patterns and exhibit a first order thermodynamic transition known as melting [20]. Their crystallinity usually lies in the range 40-75 %. In some highly crystalline polymers the amorphous fraction can be so small that it often become difficult to detect its transitions T_g. For example, poly (butylene terephthalate) (PBT) due to high level of crystallinity above 40 % did not show any significant glass transition during DSC measurements as discussed in chapter 4. On the other hand, amorphous polymer do

not show any distinct peaks in the X-ray diffraction pattern, but a broad feature referred to as an 'amorphous halo'. They also do not possess a clearly defined melting temperature. Hence one can expect that an X-ray pattern from the blend may be difficult to interpret, and the data analysis will be guided by the DSC results.

2.4.1 Crystalline polymer/ amorphous polymer blend

A crystalline polymer can be mixed either with an amorphous polymer or with another crystalline polymer to form a blend. These mixtures are interesting because a combination of complementary properties can be achieved. In the molten state these mixtures may exist as one or two phases which will affect the crystallisation process. If the non-crystallising component comes from one phase then it may reside as defects within the crystal of the other or it may be excluded from the crystals. The latter is the most common case. In both cases the crystallisation rate will be slowed down in comparison to the crystallisation rate of pure polymer due to the dilution of crystal and the decrease of melting temperature T_m which means a smaller degree of supercooling, $(T_m\text{-}T_c)$, where T_c denotes the critical melting temperature of crystalline homopolymer. If the T_g of the mixture is higher than the crystalline polymer's T_g this will also contribute to a slower crystallisation rate.

If the mixture in the molten state exists as two phases, the crystals will be confined to the phase containing the higher concentration of the crystallisable component, so the size of the crystallise region depends upon the size of this phase prior to crystallisation. This can also result in a slowing down of the crystallisation rate because the crystallisable domains can be too small to contain heterogeneous nuclei (often crystallisation is nucleated heterogeneously: the nuclei may be impurities or may be intentionally introduced)[19-20].

2.5   Lattice theories of polymer miscibility

2.5.1   Flory-Huggins lattice theory

The classical theory used to describe miscibility of polymers is based on the Flory-Huggins lattice theory established for polymer in solution. It was developed independently by P J Flory [21-22] and M L Huggins [23] in the early 1940's. It was adapted for polymer-polymer and polymer-solvent mixture by Scott [24] and Tompa [25] some years later. The Flory-Huggins theory is an approximate theory, over the years it has undergone various additions and modifications and has been surpassed by the Flory Equation-of-State theory. However, it does successfully predict some basic features of polymer-polymer miscibility and is relatively manageable; it is a good point to start a study of the thermodynamics of polymer blends. A brief outline of the current version of the Flory-Huggins theory is presented here. The Gibbs free energy of mixing is given by:

$$\Delta G_{mix} = \Delta H_{mix} - T\Delta S_{mix} \qquad\qquad 2.1$$

where ΔH_{mix} is the enthalpy change, ΔS_{mix} is the entropy change per given volume on mixing, and T is temperature. For non-polar polymers, ΔH_{mix} is positive and ΔS_{mix} is positive, but small owing to the relatively low molality. In order for mixing to proceed favorably it is required that the change in Gibbs energy is negative:

$$\Delta G_{mix} < 0 \qquad\qquad 2.2$$

An additional condition for the stability of the single phase is that:

$$\left[\frac{\partial^2 \Delta G_{mix}}{\partial \phi_i^2}\right]_{T,P} > 0 \qquad\qquad 2.3$$

where ϕ_i is the fraction of the i-th component. The second derivative of the free energy with respect to blend composition must be positive at a specific temperature and

pressure. The Flory-Huggins theory assumes that ΔS_{mix} is the simple combinatorial entropy of mixing[16]:

$$\Delta S_{mix} = -R\ (V_A + V_B)\left[\frac{\phi_A \ln \phi_A}{\overline{V}_A} + \frac{\phi_B \ln \phi_B}{\overline{V}_B}\right] \qquad 2.4$$

where V_A and V_B are the volumes, $\overline{V}_A$ and $\overline{V}_B$ are molar volumes, ϕ_A and ϕ_B are the volume fractions of the two components A and B. The gas constant is denoted by R .

The enthalpy of mixing is expressed by a van Laar type expression:

$$\Delta H_{mix} = (V_A + V_B)\ \phi_A\ \phi_B\ \chi_{AB}\ RT \qquad 2.5$$

where χ_{AB} is an interaction parameter (polymer-polymer interaction). Combining (2.4), (2.5) and (2.1) yields:

$$\Delta G_{mix} = (V_A + V_B)\ RT\left[\frac{\phi_A \ln \phi_A}{\overline{V}_A} + \frac{\phi_B \ln \phi_B}{\overline{V}_B} + \chi_{AB}\phi_A\phi_B\right] \qquad 2.6$$

for the free energy of mixing. Equation (2.6) may be rewritten to express free energy per unit volume. Replacing the molar volume of component i by M_i / p_i (M_i is the molar mass and p_i, density):

$$\frac{\Delta G_{mix}}{V_A + V_B} = RT\left[\frac{\rho_A\phi_A \ln \phi_A}{M_A} + \frac{\rho_B\phi_B \ln \phi_B}{M_B} + \chi_{AB}\phi_A\phi_B\right] \qquad 2.7$$

The strength of the Flory-Huggins theory is its ability to quantitatively represent the basic thermodynamics of polymer blends, i.e. indicating the dependence of miscibility on composition, molecular weight and temperature.

2.6   Ion aggregation and its effect on ionomer properties

In addition to the consideration of crystalline properties and thermodynamic governing polymer-polymer miscibility, the effect of sulphonation and polymerisation of PBT has to be considered. In what follows several properties of ion-containing polymers are briefly described, and three of the models describing their aggregates are presented.

2.6.1   Definition of ionomers

Ionomers are defined as ion-containing polymers with a maximum ionic group content of about 15 mole % [26]. The percentage of ionic groups (usually quoted as mole %) is calculated from the number of backbone atoms or repeat units to which ionic groups are attached [27]. The following alternative definition is based on the distribution of ionic groups in the material: Ionomers are ion-containing polymers in which the bulk properties are governed by ionic interactions in discrete regions of material termed "the ionic aggregates"[28]. The size of the aggregate depends on a delicate balance between the entropy loss of the chains and the energy gain when charges "avoid" the amorphous domains [29].

2.6.2   Ionomer architecture

The above definition needs further clarification, hence ionomers have been classified in several types as follows: simple ionic, ampholytes, betines, ionenes, and telechelic [30]. In random ionomers, the pendant ionic groups are
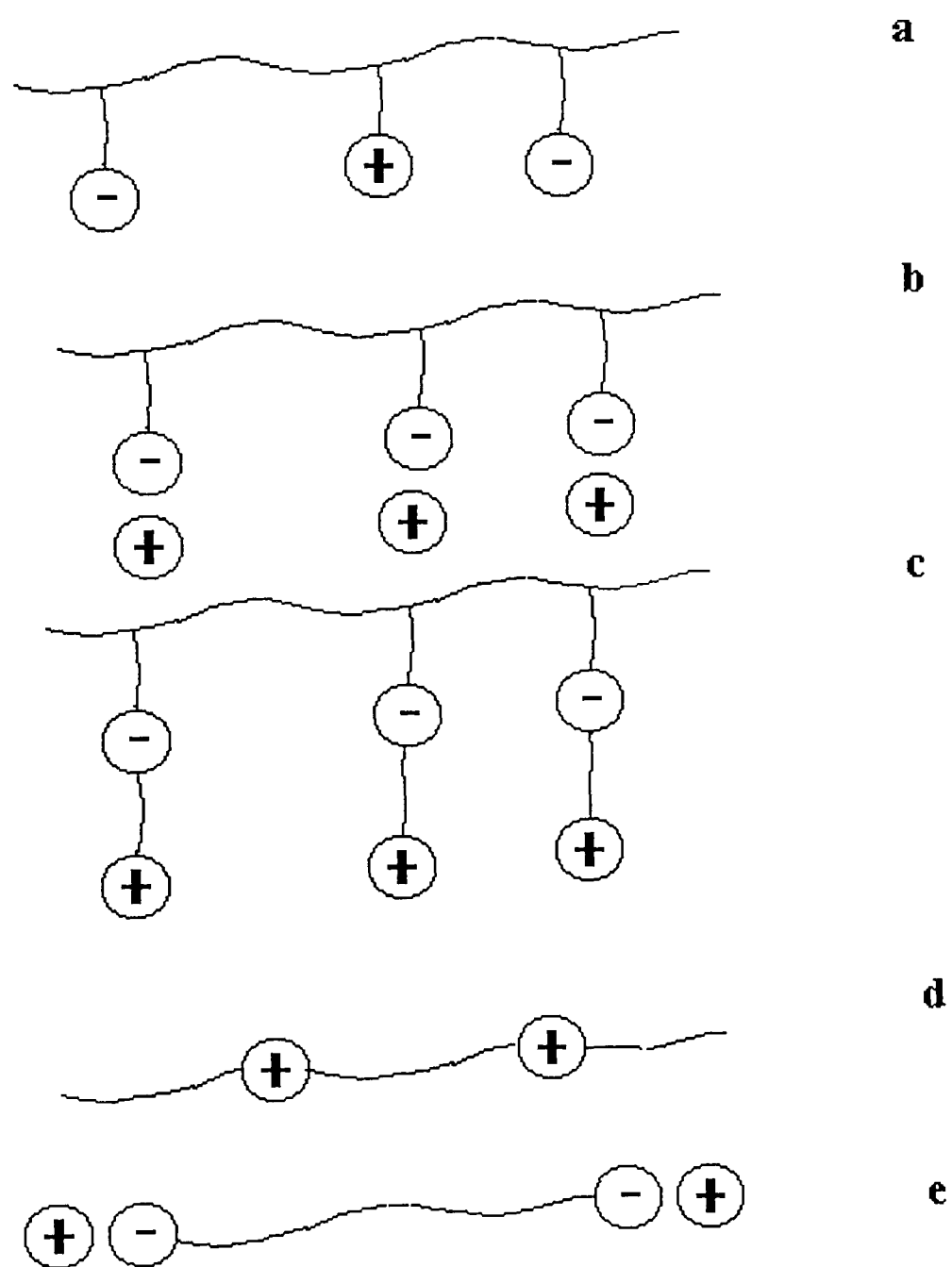
Figure 2.5 Ionomer Architecture: (a) Simple ionic (b) Ampholytes (c) Betaines (d) Ionenes (e) Telechelic[31].

randomly attached to backbone atoms; the telechelic ionomers, however, contain ionic groups only at the chain ends as shown in Figure 2.5(e). Many structural variations are possible due to variations of the backbone (homopolymer, random, or block

copolymer), of the ionic group (sulphonic, carboxylic, or phosphoric acids, for example), and of the counterions (protons, monovalent or multivalent ions).

2.6.3 Effect of solvents on ionic polymers

Although this thesis is concerned with ionomers in the bulk, the effect of solvent is important due to the solvent casting of blends. In terms of ionic content, ionomers form an intermediate class between organic ("ion-less") polymers and polyelectrolytes. Unlike polyelectrolytes, ionomers are insoluble in highly polar solvents, especially water, because of the relatively small number of ions. Ionic groups can be neutralized by various ions to obtain the corresponding salts. Some ionomers such as telechelic ionomers and other systems containing a small amount of ions, dissolve in nonpolar solvents. Although ionomers do not dissolve in polar solvents under normal temperature and pressure conditions, they can retain large quantities of such solvents. The absorption of solvents is further complicated by the different affinity for solvents of the organic and inorganic parts of the ionomers. Polar organic solvents such as methanol and ethanol penetrate in the organic parts and plasticize the chains [32-34] (which may aid the process of blending of two polymers).

By contrast, the presence of water leads to the formation of nonpolar domains where the polymer chains behave as in the bulk dry ionomer, and a polar domain where the counterions and the polar heads are located [34].

2.6.4 Morphology of ionomers

The appearance of the so-called "ionomer peak" in the small angle X-ray scattering (SAXS) profile of ionic polymers [35-36] resulted in several models which interpret the origin of this peak. Different models have been proposed such as Hard Sphere, Core-Shell and the most recent one, the so-called Eisenberg-Hird-Moore (EHM) model [29]. All of these models assume the aggregation of ionic species and differ only in the interpretation of the scattering peak. A brief description for each model is given below.

A.   Hard-sphere model

One family of models interprets the ionomer peak as being due to the distance between ionic aggregates. In the first of these models Marx et al. [37] ascribed the ionic peak to the distance between ionic aggregates, with the contrast provided by the difference in electron density between the aggregates and the hydrocarbon phase. They treated the scattering moieties as points on a paracrystalline lattice. This model was refined in 1983 in the hard-sphere model of Yarusso and Cooper,[38] who proposed that the aggregates have liquid-like order and the distance of closest approach is determined by the thickness of a layer of attached polymer chains on the surface of each aggregate.

B.   Core-shell model

A completely different approach was taken in 1974 by MacKnight et al.,[39] who interpreted the peak as being due to the characteristic *intra*-particle distances. Their core-shell model is based on the idea that an ionic core of ~ 10 Å radius is surrounded by a shell of polymer which contains no ionic groups and is, in turn, surrounded by a shell of polymer of somewhat higher ion density. In contrast to the hard-sphere model, the distance between the two ion-rich regions, i.e., the core and the outer shell, provides the characteristic distance which gives rise to the SAXS peak. This model was subsequently refined in 1980 by Roche et al.,[40] who found that SAXS pattern of ionomers is dependent on sample elongation and it was postulated that the central ionic core may be lamellar rather than spherical.
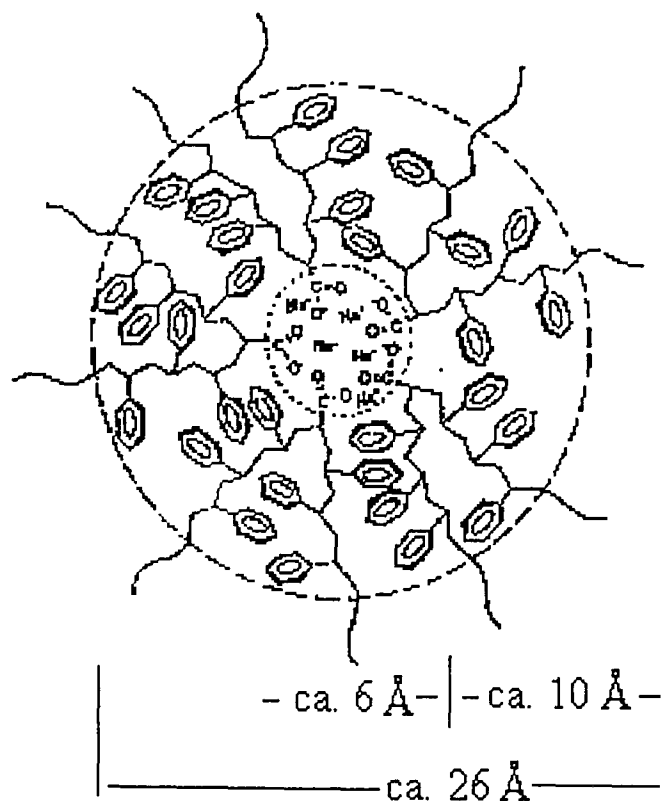
Figure 2.6 Schematic representation of a multiplet and of the region of restricted mobility surrounding it in a poly styrene co polymer ionomer [29].

C.   EHM model

The EHM model assumes on the existence of ionic aggregates and ionomer peak comes from the ionic aggregates[29]. In 1970 Eisenberg suggested that these primary aggregates, the multiplets, consist of several ion pairs [41] as shown in Figure 2.6. The total number of ion pairs is limited by the size of the ion pair and by the steric effects of the polymer chain segment adjoining this pair, which "can not get out of the way" when the aggregates are formed. Thus, small ion pairs attached to a very flexible backbone are expected to lead to very small multiplets. The size of multiplets is expected to be influenced by the dielectric constant of the polymer backbone; if the dielectric constant is high enough, no multiplets are formed, because the ions are solvated[42].

In this thesis the assumption of ionic aggregation of ionic aggregate is upheld. However due to the fact that it is wide angle X-ray scattering patterns studied here, no direct interpretation in terms of any model was possible.

References

1   J M G Cowie, in "Polymers: Chemistry and Physics of Modern Materials" 2nd edition, Chapman & Hall, New York (1990).

2   J P Runt and P B Rim, *Macromolecules*, **15** 1018 (1982).

3   S C Chik and T G Smith, *J. Appl. Polym. Sci*, **29** 1781 (1984).

4   E M Woo, J W Barlow and D R Paul, *Polymer*, **26** 763 (1982).

5   L A Utracki, in "Polymer Alloys and Blends", Hanser Publishers, Munich Vienna New York (1991).

6   J A Manson and L H Sperling, in "Polymer Blends and Compositions", Plenum, New York (1976).

7   G Pompe, L Haubler and W Winter, *J. Polym. Sci.: Part B: Polym. Phys*, **34** 211 (1996).

8   G C Alfonso, A Turturro, M Pizzoli, M Scandola and G Geccorulli, *J. Polym. Sci. Polym. Phys. Edn*, **27** 1195 (1989).

9   R L Imken, D R Paul and J W Barlow, *Polym. Phys. Edn*, **16** 593 (1976).

10   B S Morra and R S Stein, *J. Polym. Sci, Polym. Phys. Edn*, **20** 2243 (1982).

11   M Galin, *Makromol. Chem*, **188** 1391 (1987).

12   R M Briber and F Khoury, *Polymer*, **28** 38 (1987).

13   M P Jarman and M Hetem, *Plastics, Rubber and Composites Processing and Applications*, **23** 31 (1995).

14   D E Bergbreiter and C R Martin, in "Functional Polymers", Plenum Press, London and New York (1991).

15   D R Paul, J W Barlow and H Keskkula, in "Polymer Blends, Concise Encyclopedia of Polymer Science and Engineering", J I Kroschwitz, John Wiley & Sons, New York (1990).

16   A Ruddin, in "The Elements of Polymer Science and Engineering", Academic Press London (1982).

17   D M Sadler and A Keller, *Polymer*, **17** 37 (1976).

18   M Dettenmaier, E W Fischer and M Stamm, *Colloid & Polymer Sci*, **258** 343 (1980).

19   R J Young, in "Introduction to Polymers", Chapman and Hall, New York (1981).

20   L H Sperling, in "Introduction to Physical Polymer Science", John Wiley & Sons, New York (1992).

21   P J Flory, *J. Chem. Physics*, **9** 660 (1941).

22   P J Flory, *J. Chem. Physics*, **10** 51 (1942).

23   M L Huggins, *J. Chem. Physics*, **9** 440 (1941).

24   R L Scott, , *J. Chem. Physics*, **17** 279 (1949).

25   H Tompa, *Transactions of the Faraday Society*, **45** 1142 (1949).

26   M R Tant and G L Wilkes, in "Structure and Properties of Ionomers", M Pineri, A Eisenberg, NATO ASI Series, Reidel, Dordrecht, (1987).

27   W J MacKnight and T R Earnest, *J. Polym. Sci. Macromol. Rev*, **61** 41 (1981).

28   A Eisenberg and M Ridnaudo, *Polym. Bull*, **24** 671 (1990).

29   A Eisenberg, B Hird and R B Moor, *Macromolecules*, **23** 4098 (1990).

30   W J MacKnight, in "Structure and Properties of Ionomers", M Pineri, A Eisenberg, NATO ASI Series, Reidel, Dordrecht (1987).

31   S Schlick, in "Ionomers Characterization, Theory And Applications", CRC Press Inc, New York (1996).

32   S Schlick, G Gebel, M Pineri and F Volino, *Macromolecules*, **24** 3517 (1991).

33   H Li and S Schlick, *Polymer* **36** 1141 (1995).

34   H R Zelsmann, M Pineri, M Thomas, and M Escoubes, *J. Appli. Polym. Sci,* **41** 1673 (1990).

35   R W Rees and D Vaughan, *J. Polym. Prepr.*(*Am. Chem. Soc. Div. Polym. Chem.*), **6** 287 (1965).

36   F C Wilson, R Longworth, D Vaughan, *J. Polym. Prepr.*(*Am. Chem. Soc. Div. Polym. Chem.*), **9** 505 (1968).

37   C L Marx, D F Caulfield, and S L Cooper, *Macromolecules*, **6** 344 (1973).

38   D J Yarusso and S L Cooper, *Macromolecules*, **16** 1871 (1983).

39   W J MacKnight, W P Taggart and R S Stein, *J. Polym. Sci. Symp*, 45 113 (1974).

40   J E Roche, R S Stein, T P Russel and W J MacKnight, *J. Polym.Sci. Polym. Phys. Edn*, **18** 1497 (1980).

41   A Eisenberg, *Macromolecules*, **3** 147 (1970).

42   A Eisenberg and T Sasada, in "Physics of Non-crystalline Solids", J A Pins, Amsterdam (1965).

CHAPTER 3

EXPERIMENTAL TECHNIQUES

3.1   Materials

Experimental work was carried out on poly (butylene terepthalate) (PBT), sulphonated poly (butylene terepthalate) (SPBT) and the blends of SPBT and polycarbonate (PC) with different wt. %. Details of samples used in the present study are given in chapters four and five. Different techniques were used to investigate these materials: Differential Scanning Calorimetry (DSC), Thermo-gravimetry Analysis (TGA), Wide Angle X-ray Diffraction (WAXD) and Optical Microscopy. A brief description of these techniques is given in this chapter. The quantities investigated are percentage of crystallinity, glass transition temperature, miscibility, the effect of sulphonation on the structure of the material, and microstructure-related properties such as spherulite size, respectively.

3.2   Wide angle X-ray diffraction (WAXD)

3.2.1   Introduction

Wide angle X-ray scattering is an established technique for studying the internal structure of materials, since X-ray wavelength is of the order of the atomic and intermolecular spacing. Scattering patterns provide information about the relative molecular positions in the cell, the geometry and perfection of the crystallites, the crystallinity and the quality of preferred orientation with respect to an external axis. More detailed information can be obtained from the relative intensity, position and line width of the diffraction peaks. It is usually assumed that the wide angle diffraction pattern of a semicrystalline polymer is additively composed of the diffraction diagrams of the amorphous and crystalline regions[1].

X-ray scattering (or diffraction) techniques are usually categorised into wide-angle X-ray scattering (WAXD) and small angle X-ray scattering (SAXS). In the former, the desired information on the polymer structure is obtained from the scattered intensities at large scattering angles, and in the latter, at small scattering angles. In general terms,

WAXD is used to obtain structural information on a scale of 0.1-2 nm or smaller, and SAXS on a scale of 1-100 nm.

3.2.2 Principles of X-ray diffraction

The diffraction of X-rays by liquids or gases gives rise to diffuse haloes; the diffraction of X-rays from crystalline substances gives rise to sharp circles or spots if a film is used to collect the data. In the case of semi-crystalline polymers, X-ray analysis may give information about the crystallinity and texture of the polymeric material: they may be studied as a function of the thermal and mechanical treatments that the material has undergone[2-3].

When irradiated by X-rays, all crystalline polymers give patterns containing both relatively sharp lines and diffuse haloes which may be interpreted in terms of distances within the sample. The distance d is related to the scattering θ by the Bragg's law $n\lambda = 2d \sin \theta$ with λ the X-ray wavelength and n is the number of plans. It is now generally agreed[1] that in polymeric materials of high crystallinity the major part of the material is made up of crystals, in the form of thin platelets, in which chains run perpendicularly, folding many times within the crystal. The presence of dislocations, chain folds and chain ends in the crystals could explain the presence of amorphous haloes.

In the spectrum of electromagnetic radiation, X-rays lie between the ultraviolet and γ-radiation. The X-rays used for structure analysis have wavelengths λ in the range 0.05-0.25 nm. Most work on polymers is done with the Cu K_α emission line, a doublet with an average wavelength equal to 0.154 nm. Energy of X-rays equals to $h\nu$, where h is Planck's constant and the frequency ν is given by c/λ (c = velocity of light). Thus, the Cu K_α line consists of photons of energy of 8.04 keV.

Normally the sample is irradiated with a collimated beam of X-rays and the intensity of the scattered X-rays is measured as a function of scattering direction. The scattering angle, (the angle between the direction of the scattered and the incident beam) is

customarily denoted by 2θ (Figure. 3.1). If $\underline{S}_0$ is defined as the unit vector in the incident beam direction and $\underline{S}$ as the unit vector in the scattered beam direction, the relation between incident and scattered beams of the scattering vectors $\underline{S}$ given by:

$$\underline{S} = (\underline{S} - \underline{S}_0)/\lambda \qquad\qquad 3.1$$

The magnitude of $\underline{S}$ is related to the scattering angle θ by

$$S = 2(\sin\theta)/\lambda \qquad\qquad 3.2$$
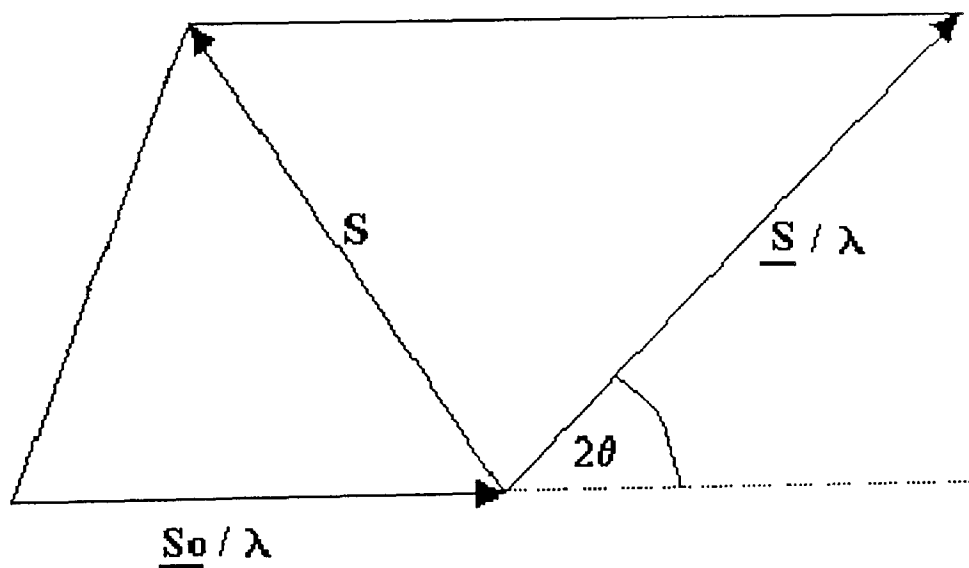
Figure 3.1 Definition of the scattering vector $\underline{S}$.

If an (unpolarised) X-ray beam of intensity I_0 irradiates a free electron, the intensity I scattered at angle 2θ and measured at distance r from the electron is given, according to the classical theory[4], by the equation

$$I = I_0 \frac{K}{r^2} \left(\frac{1 + \cos^2 2\theta}{2} \right)$$

3.3

which is called the Thomson formula. Here the constant K is defined as

$$K = e^4 / m^2 c^4$$

3.4

where e and m are the charge and mass of an electron and c is the velocity of light. The square root of K is often referred to as the classic electron radius and is equal to 2.82 x 10^{-13} cm.

3.2.3 Instrumentation

WAXD scans were carried out on samples (described in chapter 5) in order to investigate the level of crystallinity and any modification in the crystal structure itself due to sulphonation. A Philips XRG-3000 generator with Ni filtered CuK_α radiation source ($\lambda=1.5418$ Å), in the Department of Materials Engineering at Brunel University, was operated at 36 kV and 25 mA. The samples were mounted on the spinning stage of diffractometer. Diffraction patterns were recorded at a scanning rate of 0.021° 2θ/s over an angular range 7° < 2θ < 50°. After background subtraction and the necessary instrumental correction, the data were transferred to a PC where they were plotted out. Maximum scattering intensities obtained were mainly in the range of 200-400 counts/s. An attempt was made to ensure a constant mass of sample in the X-ray beam. All other physical conditions were kept the same for all the samples.

3.3   Thermal analysis

Thermoanalytical techniques have been used for analysing the thermal stability and morphology of PBT/PC blends[5-8]. "Thermal analysis" refers to the group of methods in which some physical property of the sample is continuously measured as a function of temperature, whilst the sample is subjected to a controlled temperature change[9]. A brief description of thermal techniques employed to characterise the samples is given

below.

3.3.1 Thermogravimetry analysis (TGA)

Thermo-gravimetry Analysis (TGA) is a technique whereby the weight loss of a sample is continuously measured as a function of temperature or time during heating. The resulting weight change with temperature or time curve is called the TGA curve, while the rate of weight change as a function of temperature or time is called the DTG curve. These curves can give information concerning the thermal stability and composition of the original sample, the composition and the thermal stability of intermediate compounds, and the composition of the residue.

In this study, DSC and TGA were carried out using a Perkin-Elmer model TGS-2 thermogravimetry apparatus in the Department of Materials Engineering Brunel University. The experiments were performed both in nitrogen and air atmosphere. The sample weight was kept at about 5 mg. TGA study was carried out on the poly (butylene terepthalate) powder samples listed in chapter 4.

3.3.2 Differential scanning calorimetry (DSC)

Differential Scanning Calorimetry (DSC) is a modification of differential thermal analysis (DTA). The methods of DTA/DSC detect the enthalpy changes which occur in a sample as it is heated or cooled under fixed conditions and also offer a basis for quantitative and qualitative measurements. The enthalpy of a sample refers to its heat content. In this method the instrument keeps the sample and reference at the same temperature. The amount of heat that has to be applied to the sample or reference to achieve this thermal equilibrium is constantly measured over the temperature range employed. The recorded heat flow gives a measure of the amount of energy absorbed or evolved in a particular transition, and hence gives calorimetric measurements directly. In practice, the base shift is measured with reference to a base line obtained
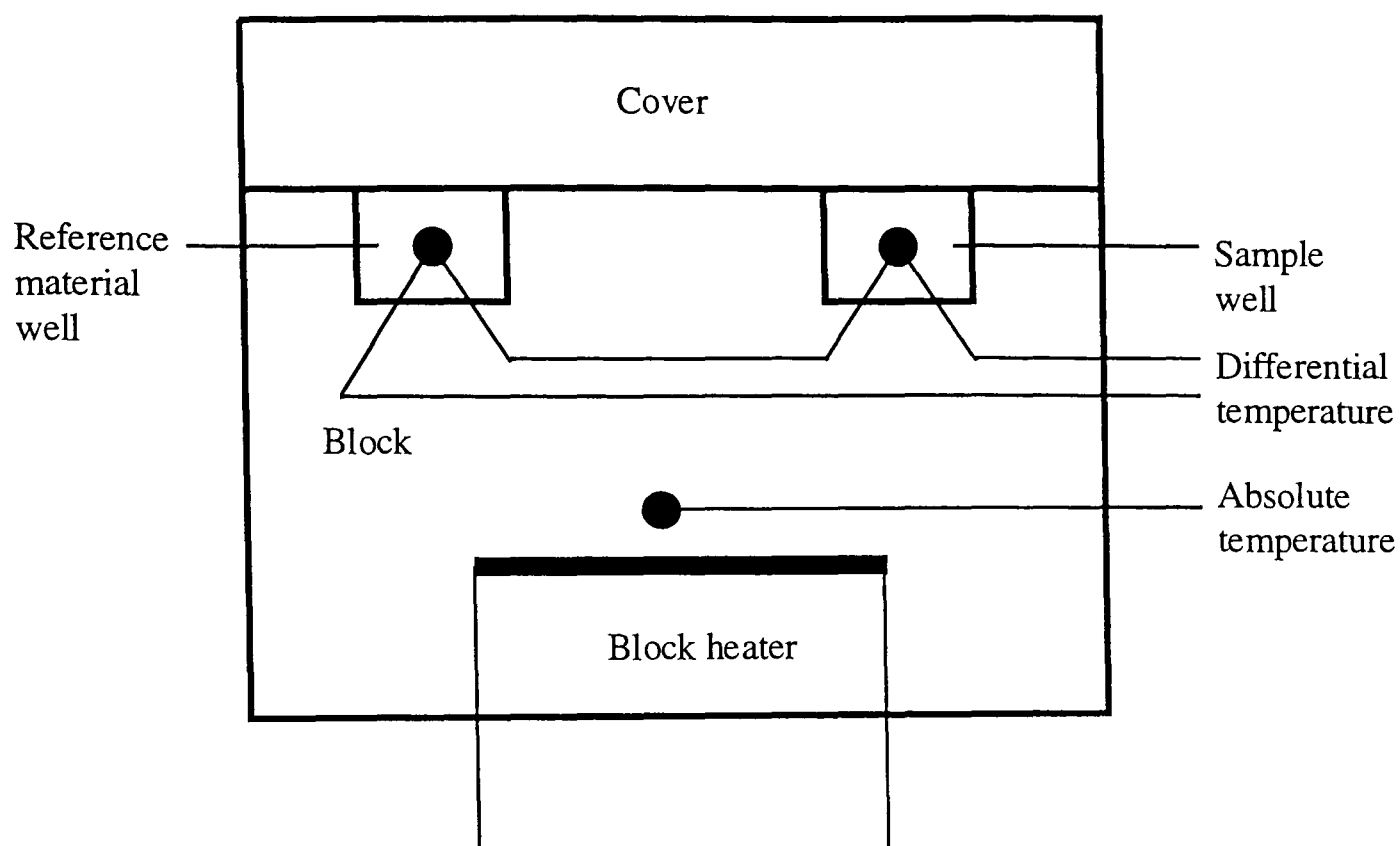
Figure 3.2 Schematic diagram of a differential thermal analysis device.

for empty sample and reference pans. The point at which the sample undergoes an exothermic effect and the curve begins to deviate from the base line corresponds to the onset temperature. The schematic diagram of a DSC apparatus is shown in Figure 3.2. The sample well is packed with the material to be tested. Once assembled, the block is heated at a constant temperature rate. The absolute temperature of the system and the differential temperature between the sample and empty reference pan are recorded continuously. The differential temperature between the sample and empty reference pan shows a slight upward or downward drift. However, if the sample undergoes a transition at some temperature, a characteristic change in differential temperature is observed. The nature of this change depends on whether the transition is a first-order thermodynamic transition, such as the melting of the crystalline portions of a partly crystalline glass or a quasi thermodynamic transition, such as the glass transition. The DSC method can be used to measure specific heat capacity, transitional phenomena, heats of transitional reaction, and rates of crystallisation reaction, melting and peak area.

There are several criteria for choosing the melting and glass transition T_g temperatures. For the melting point temperature T_m, the DSC curve shows a peak and T_m can be

taken either as the maximum of the peak or the onset (intersection of the tangent of the upgoing curve with the base line) as shown in Figure 3.3. The curve shows a change in the slope and T_g can be taken as the halfway point of the transition, the onset or the inflexion point.

DSC can also be used to calculate the percentage of crystallinity of a polymer. The area under a melting peak is a direct measure of the heat absorbed during the melting process. The instrument is calibrated with a low M_w material, usually indium, of known heat of fusion, ΔH_m . Knowing the heat of ΔH_m of the 100 % crystalline polymer (which can be found in the literature) the crystallinity percentage can easily be calculated. ΔH_m for 100% crystalline PBT is 142 J/g[10].

3.3.3 Effect of copolymerization on T_g

Addition of a second component may take the form of copolymerization or polymer blending. Experimentally, two general cases may be distinguished: i) one phase is retained and ii) two or more phases exist. Determining the T_g of a polymer blend is the most common way of determining its miscibility. A single T_g for a perfectly miscible blend would be an intermediate between those of the constituent polymers and would dependent on blend composition. On the other hand, the presence of two T_g's, independent of composition, means that aggregates of each polymer exist.

How does the T_g of a miscible blend change with composition ? Several equations relating T_g with blend composition have been formulated: the Couchman equation[10], the Gordon-Taylor equation[11], the Fox equation[11-12] and others. The Fox equation, which has been proved valid for several blends is given by[12].

$$\frac{1}{T_g} = \frac{W_1}{T_{g_1}} + \frac{W_2}{T_{g_2}}$$

            3.5

a
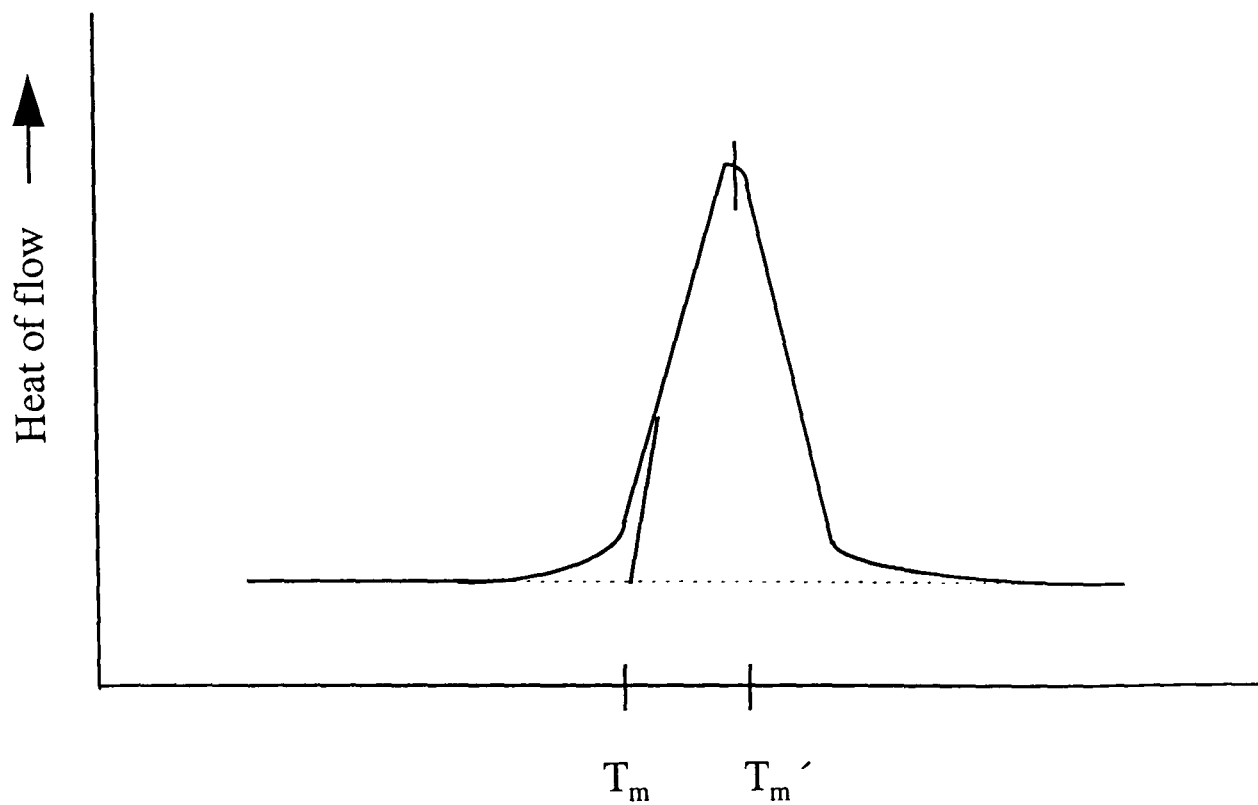
T_m = onset $T_m{}'$ = maximum

b
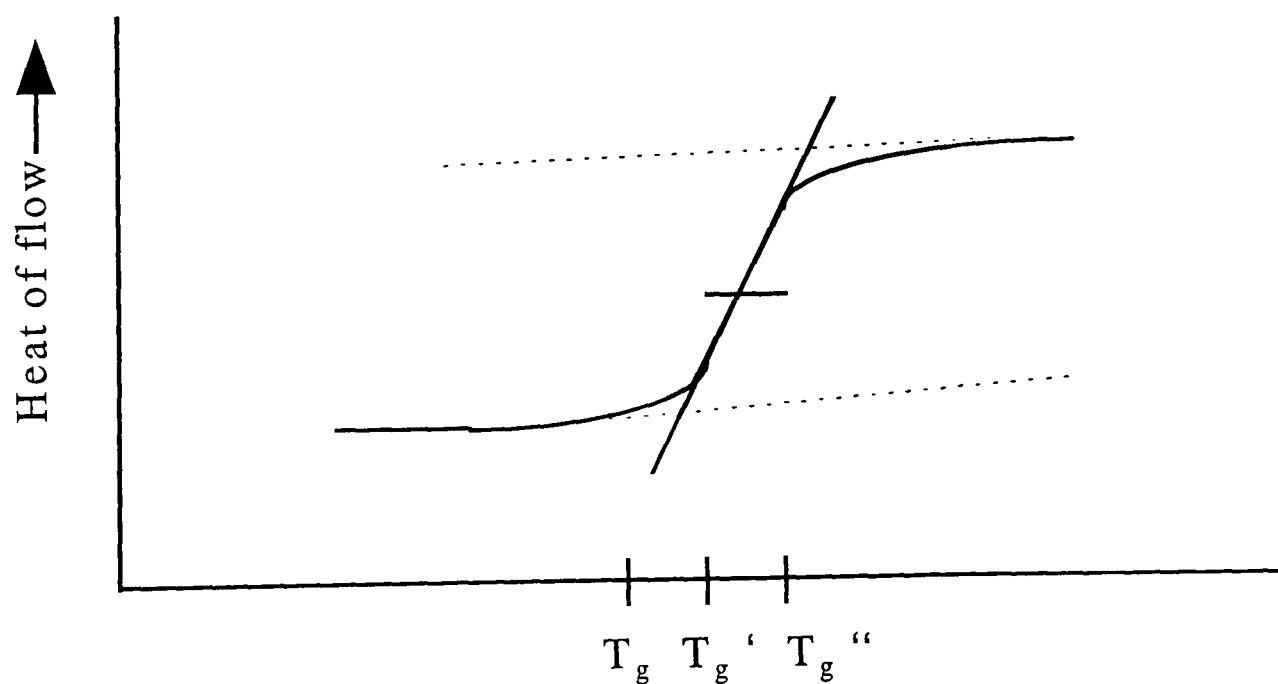
T_g = onset $T_g{}'$ = 1/2 (ΔC_p) $T_g{}''$ = inflexion point

Figure 3.3 Schematic DSC curves : (a) Main melting temperature

(b) Glass transition temperature.

where W_1 is the weight fraction of component one and T_{g1} the glass transition temperature of polymer one. There is no universal equation for predicting T_g as a function of composition for all the miscible blends, and other equations can better predict the results obtained on blends.

DSC can also be used to study the miscibility of crystalline or semi-crystalline polymers in three ways:

i)   for a miscible crystalline/amorphous blend a melting point depression is expected. From this measurement the interaction parameter χ can be calculated[13].

ii)   by measuring how the crystallinity percentage of a polymer changes with blending. In general terms, the more mixing occurs, the less crystalline the polymer blend will be.

iii)   by looking at the crystallisation rate of a polymer the kinetics of crystallisation of a polymer will be altered by the presence of a second polymer. The effect produced is a sign of the degree of mixing between the two.

3.3.4   SPBT/PC blend preparation

Two basic techniques have been employed to prepare SPBT/PC blends, namely solvent casting and precipitation from solution. 2% solutions of the start polymers (SPBT and PC) in the common solvent phenol/tetrachloroethane (40:60 by weight) were prepared and stirred continuously for at least 60 hours at room temperature prior to accurately mixing them in the appropriate ratios by volume. When mixed the solutions were stirred for a further 60 hours at room temperature.

i)   Precipitation methods

To extract the polymers by precipitation the mixed solution was added dropwise to an excess, at least 10 times by volume, of methanol. Subsequently the samples were

centrifuged to extract the (very fine) precipitate. Fresh methanol was added the precipitate, stirred thoroughly and centrifuged again. This washing process was repeated at least ten times to ensure removal of the original solvent. UV spectra of the methanol removed from the later washings were taken to check the level of phenol remaining. The results were compared to those from a standard phenol solution. The precipitated blend was then baked at 353 K under vacuum for at least 8 hours prior to analysis.

ii) Solvent casting

The mixed solutions were decanted and left to evaporate slowly prior to baking at 80 °C under vacuum for at least 8 hours. The solution casting method is the most efficient and has been chosen as the preferred preparation technique. Using this method SPBT/PC blends have been prepared. Control samples of each of the start polymers (PC and 0, 3.5, 7.9, & 11.1 % SPBT) have been processed by the same method.

Thermal Analysis of samples was carried out using a Perkin-Elmer DSC-7 instrument, in the Department of Materials Engineering at Brunel University. The equipment was calibrated against indium and lead standards. Samples of 5 mg weight were scanned at 20 K/min to avoid a over-heating effect. The following scanning procedure was then used for polystyrene samples and PBT blends:

a) (i) Without baking

Samples were preheated from 298 K to 393 K in the DSC cell, and then cooled rapidly to 320 K at a rate of 320 K/min. Samples were then heated from 320 K to 560 K at a rate of 20 K/min. Samples were cooled at a rate of 320 K/min to 320 K, and the run was repeated under the same experimental conditions as used during the first scan. Nitrogen gas was used as inert atmosphere to prevent any possible oxidation of the samples. The degree of the crystallinity of the material was calculated using the heat of melting of the crystalline regions PS ΔH = 105 J/g, for both 100 % crystalline isotactic

PS and isotactic SPS.

(ii)   With baking

Samples were baked for 36 hours at 333 K under vacuum to dehydrate the samples. Samples were a) preheated from 298 K to 393 K in the DSC cell, and kept at this temperature for 5 min; cooled to 320 K at a rate of 320 K/min, kept the sample at this temperature for 5 min; and b) Heating the sample from 320 K to 560 K in (N_2) at a rate of 20 K/min, held temperature for 5 min followed by cooling at a rate of 320 K/min. c) Heating the sample from 320 K to 560 K at a rate 20 K/min.

b)   In case of PBT samples DSC investigations were carried out on, I) powder samples, II) melt pressed film samples and III) SPBT/PC blends. Samples 5 mg (same mass for all the samples) were scanned with the following heating programme. "Pretreatment" (to remove any water): samples heated to 393 K at a rate of 20 K/min, maintained at 393 K for 5 minutes, rapidly cooled (320 K/min) to room temperature (RT) in situ. "First Scan": samples heated to 553 K at a rate of 20 K/min, maintained at 553 K for 5 minutes, rapidly cooled to RT (320 K/min) in situ.

"Second Scan": heated to 553 K at a rate of 20 K/min, maintained at 553 K for 5 minutes, quenched in liquid Nitrogen. "Post Quench Scan": heated from RT to 553 K at a rate of 20 K/min. The degree of the crystallinity of the material was calculated using the value of heat of melting of the crystalline regions PBT of $\Delta H = 142$ J/g[10].

3.4   OPTICAL MICROSCOPY

3.4.1   Polarised light microscopy

Optical microscopy plays an important role in investigating the microstructure of the polymer blends, especially the nature and the distribution of the dispersed phase. It provides an overview of structure larger than a micrometre in size. The crystalline superstructures such as dendrites and spherulites, are easily detected by polarising

microscope. Polarising light microscopy has been used in the investigation of spherulites in poly (butylene terephthalate) PBT[14] and polystyrene PS[15-17].

3.4.2 Instrumentation

Glass slides containing thin films of the samples were examined under a Reichart - Jung Microstart 110 microscope in the Department of Materials Engineering at Brunel, using crossed - polars at magnifications 200, 100, and 40 times. To allow the spherulites, and other details of the microstructure to be seen the specimens were rotated until the polarised light showed up the desired microstructure. Photographs were taken using an automatic Nikon photography system.

References

1   J Baruchel, J L Hodeau, M S Lehmann, J R Regnard and C Schlenker, "Neutron and Synchrotron Radiation for Condensed Matter Studies", Vol. 1, Jose Baruchel, Springer-Verlag Berlin Germany (1994).

2   J I Kroschwitz, in "Concise Encyclopedia of Polymer Scienceand Engineering", J Wiley & Sons, New York (1990).

3   R G Griskey, in "Polymer Process Engineering", Chapman & Hall London, New York (1995).

4   V A Drits and C Tchoubar, in "X-Ray Diffraction by Disorder Lamellar Structures", Springer-Verlag, Berlin Germany (1994).

5   D C Wahrmund, C J Paul and J M Barlow, _J. Appl. Polym. Sci_, **22** 2155 (1978).

6   J S Trent, J I Scheinbeim and P R Couchman, _Macromolecules_, **16** 589 (1983).

7   W W Wendlandt, in "Thermal Analysis", 3rd edition, (Chemical Analysis Vol 19), John Wiley and Sons, New York (1986).

8   J M Richardson, _Polymer Testing_, **4** 101 (1984).

9   J W Dodd and K H Tonge, in "Thermal Methods", (1987).

10   K H Illers, _Coll. Polym. Sci_, **258** 117 (1980).

11   L A Utracki, in "Polymer Alloys and blends: Thermodynamics and Rheology", Hanser Publishers, New York (1989).

12   O Olabisi, L M Robeson and M T Shaw in "Polymer-Polymer Miscibility", Academic Press, London (1984).

13   S K Kumar, _Macromolecules_, **27** 260 (1994).

14   L Bartosiewicz and C J Kelly, in _"Advances in Polymer Technology"_, **6(2)** 185 (1986).

15   D C Bassett and A S Vaughan, _Polymer_, **26** 717 (1985).

16   D C Bassett; in "Principles of Polymer Morphology", Cambridge University Press, UK (1981).

17   D V Rees and D C Bassett, _J. of Mat. Sci._ **6** 1021 (1971).

CHAPTER 4

THERMAL ANALYSIS

4.0   Introduction

In this chapter thermal properties of PBT, SPBT, and their blends with PC are characterised. Interactions between ionic groups located within, or pendant to, polymer chains influence the morphological structure and for instance phase behaviour of a blend. This is turn has an impact on mechanical properties. "Phases" in the system of interest may be the glassy state, the glass transition region, or the rubbery region. If crystallinity is present in the sample, the level of crystallinity and the crystalline morphology will also affect glass transition temperature T_g. The ionic aggregates may reside preferentially in a particular phase, and how they are distributed among the various phases is a critical factor affecting blend miscibility and its optical properties. Finally, ionic interactions can influence properties of crystalliseable PBT ionomers through the large effect they can have on both crystallisation kinetics as well as final semicrystalline morphological structure that develops. The results obtained from DSC studies are discussed at each stage to put them in context with the rest of the work.

4.1   Results and discussion for PBT and SPTB samples

The differential scanning calorimetry (DSC) was employed in the thermal analysis of PBT, SPBT, and their blends with PC in order to investigate melting behaviour, crystallinity and blend miscibility. Furthermore thermogravimetry analysis (TGA) was used to investigate the thermal stability as a function of level of ionic content on the PBT ionomers. Results obtained are described in the following section.

4.1.1   Melting behaviour of PBT and SPBT samples

DSC thermograms of Figures 4.1-4.4 show typical examples of cyclic heating experiments for PBT and SPBT powder samples with 0.0, 3.5, 7.9 and 11.1 mole % sulphonation. Figures 4.5-4.8 display DSC thermograms for PBT and SPBT hot

pressed film samples with 0.0, 4.9, 8.4 and 13.5 mole % sulphonation. All the samples exhibited main melting endotherms appearing in the range 487-499 K. The melting temperature, T_m will be taken to be the temperature at the maximum of this main endotherm. The melt temperature was found to decrease with increasing sulphonation level and with thermal cycling, as will be demonstrated in a later section.

4.1.2   Main melting endotherms

a)   **Powder samples**

Figure 4.1(a) shows DSC melting curve for a sample undergoing different heat treatment. During the first heating of PBT 0.0 mole % (pure PBT) sample showed one melting maximum at 498 K. A small shoulder at 486 K followed by a main melting peak at 497 K during the second scan is seen in Figure 4.1(b). Curve (c) in this figure is the melting endotherm during the post quench heating cycle, showing a single main endotherm at 496 K.
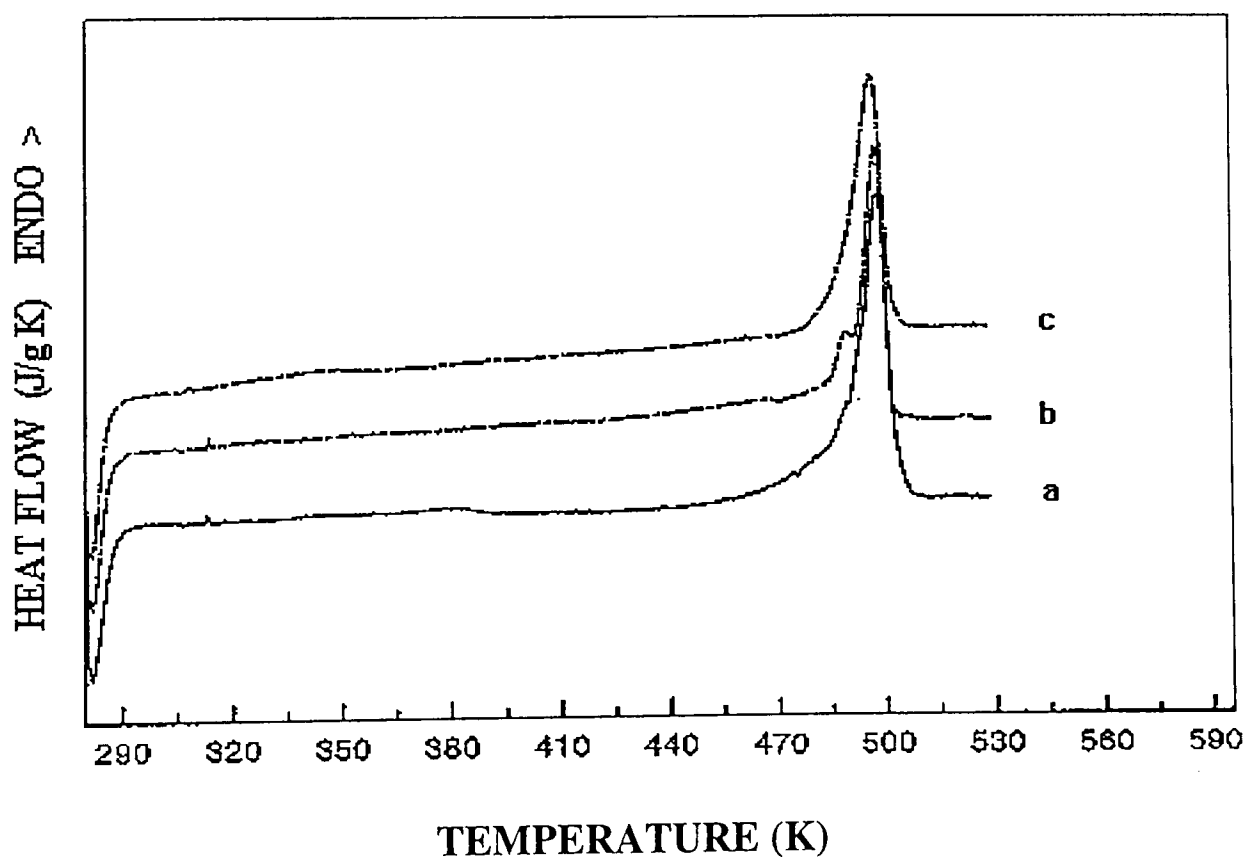
Figure 4.1 PBT 0.0 mole % powder sample a) first scan,

b) second scan, c) post quench.
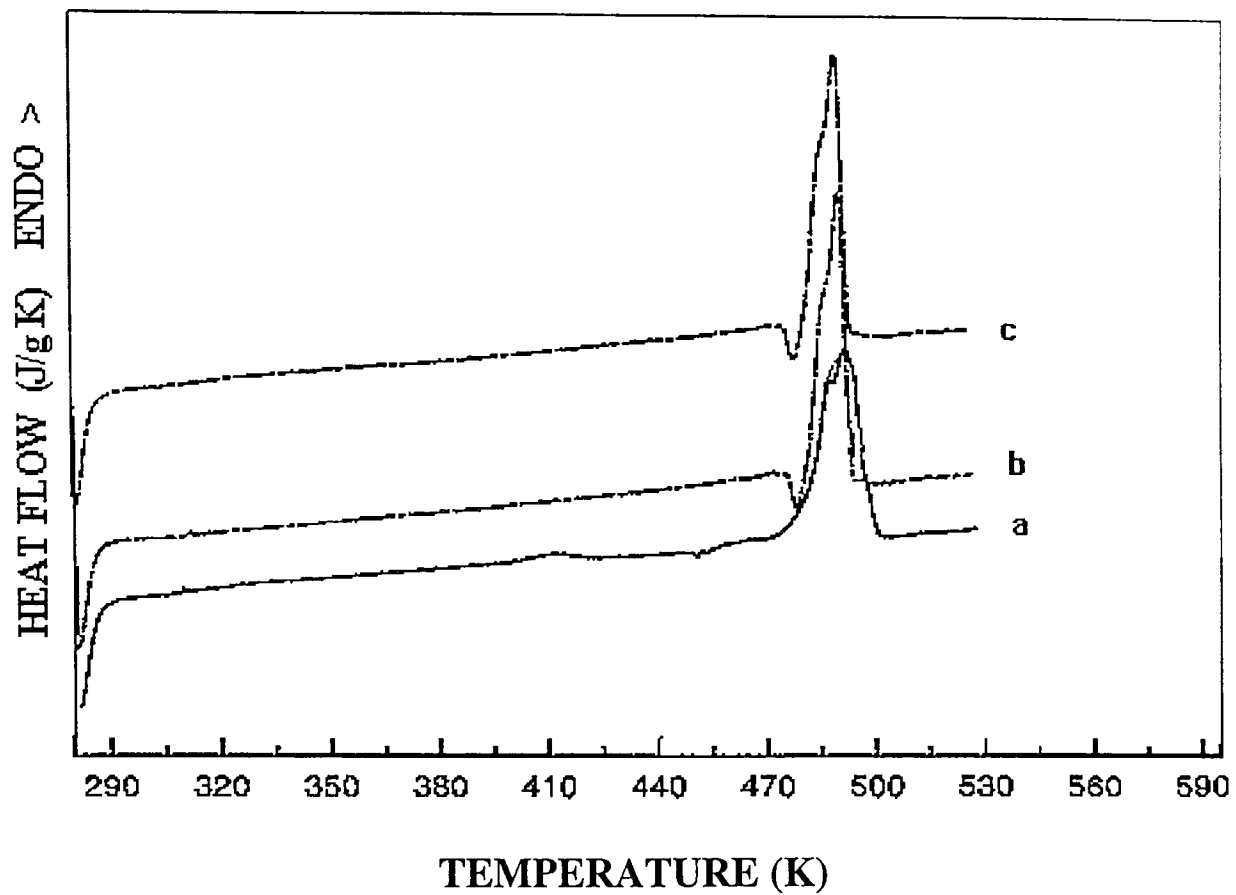
Figure 4.2 SPBT 3.5 mole % powder sample a) first scan,

b) second scan, c) post quench.
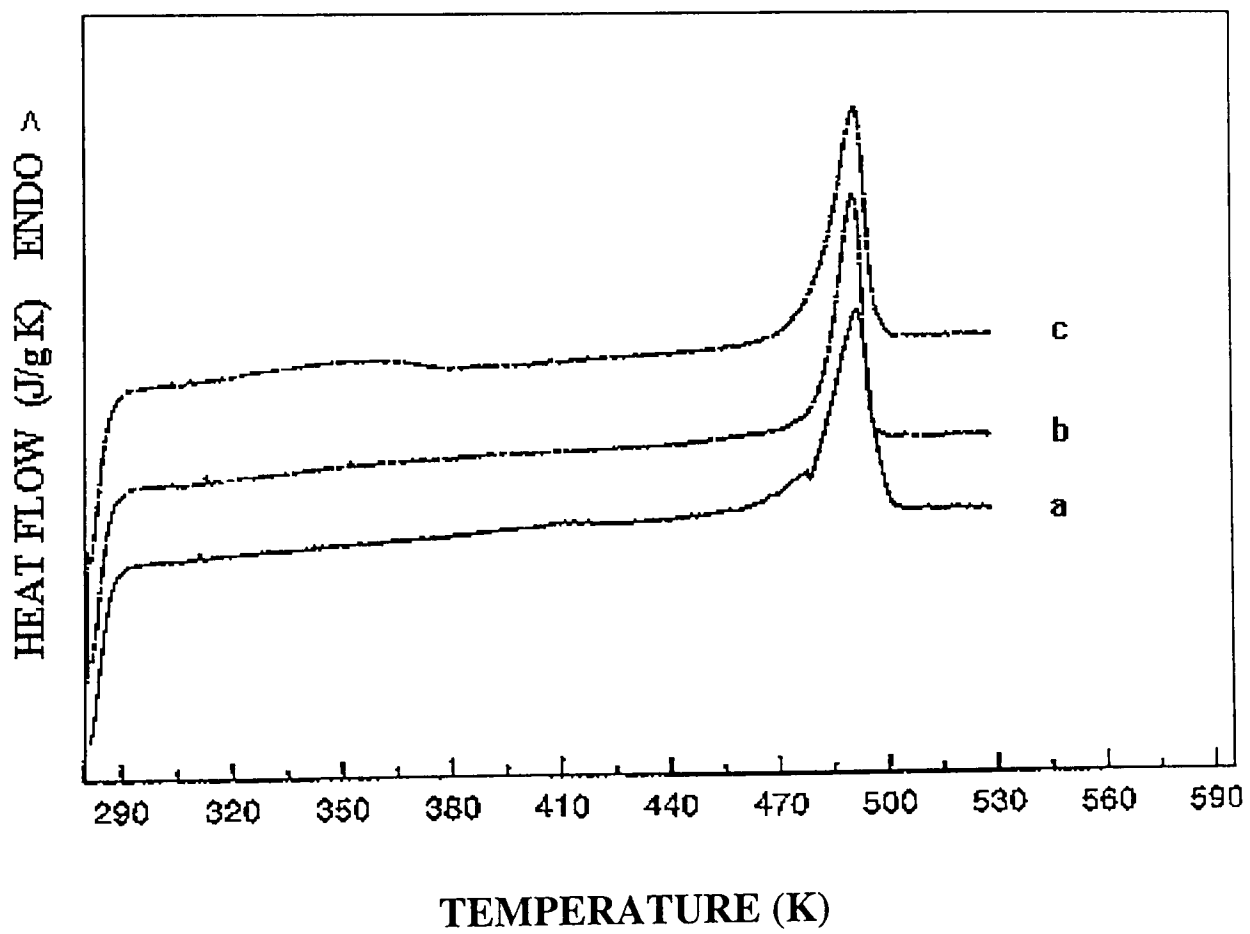
Figure 4.3 SPBT 7.9 mole % powder sample a) first scan,

b) second scan, c) post quench.
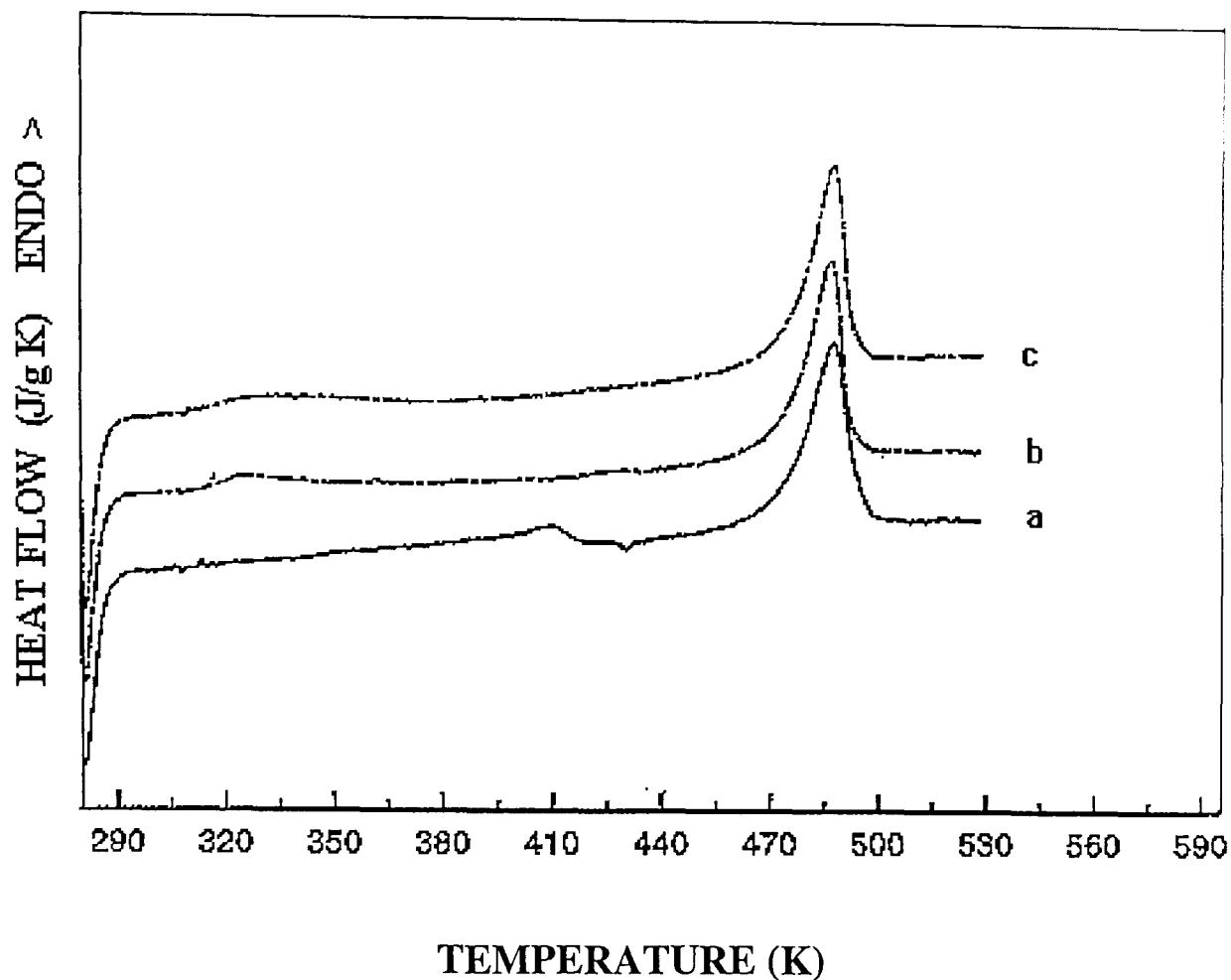
Figure 4.4 SPBT 11.1 mole % powder sample a) first scan,

b) second scan, c) post quench.

For the 3.5 mole % sample evidence of a second peak was only seen during the first scan at 485 K as illustrated in the Figure 4.2(a). During the second scans (i.e. after rapid cooling in situ) of the 3.5 mole % samples a small exotherm (presumably indicative of recrystallisation) was routinely observed just prior to the onset of the melting endotherm.

Figures 4.3(a-c) and 4.4(a-c) display DSC thermograms for SPBT 7.9 mole % and SPBT 11.1 mole %. Single main melting endotherms for these samples were obtained.
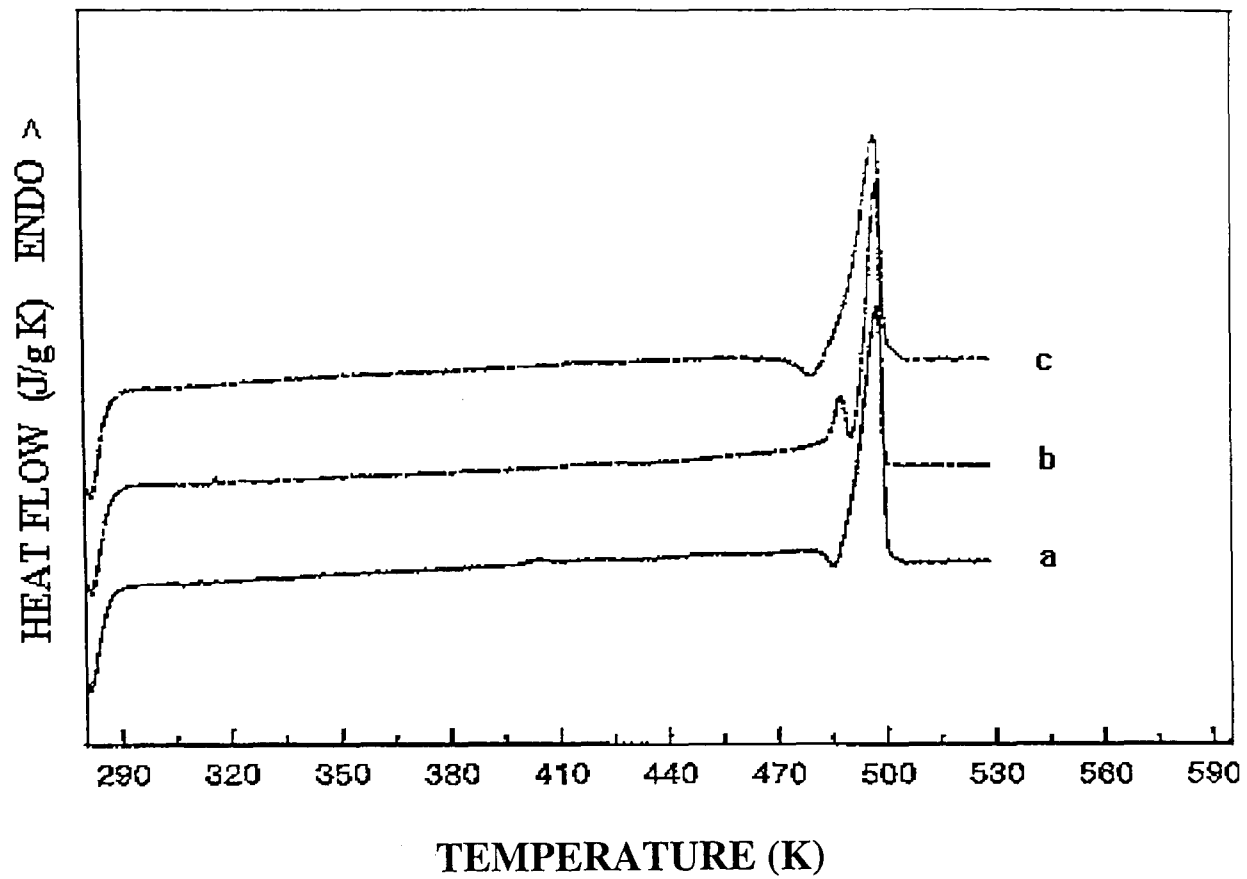
Figure 4.5 PBT 0.0 mole % film sample a) first scan,

b) second scan, c) post quench.
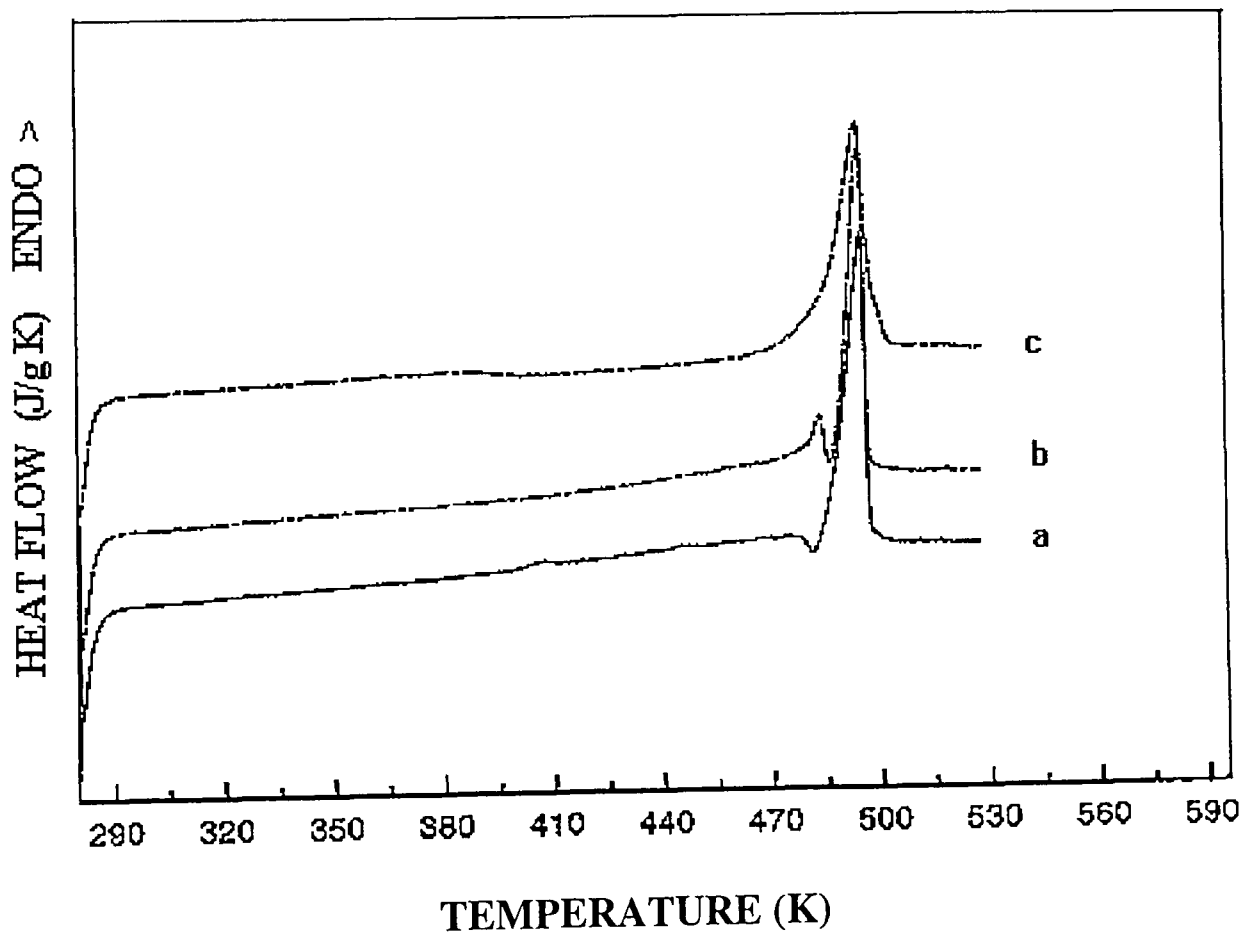
Figure 4.6 SPBT 4.9 mole % film sample a) first scan,

b) second scan, c) post quench.

b)   PBT/SPBT film samples

The hot pressed film samples of PBT/SPBT with mole % sulphonation less than 5 % exhibited similar exotherms as seen in 3.5 mole % powder sample. Figure 4.5(a) shows the DSC trace for PBT(F) film sample during the first scan. The exotherm at 483 K is clearly seen, also a sharp single main melting peak at 498 K. Two high temperature endotherms appeared at 485 K and at 497 K (main melting peak) during
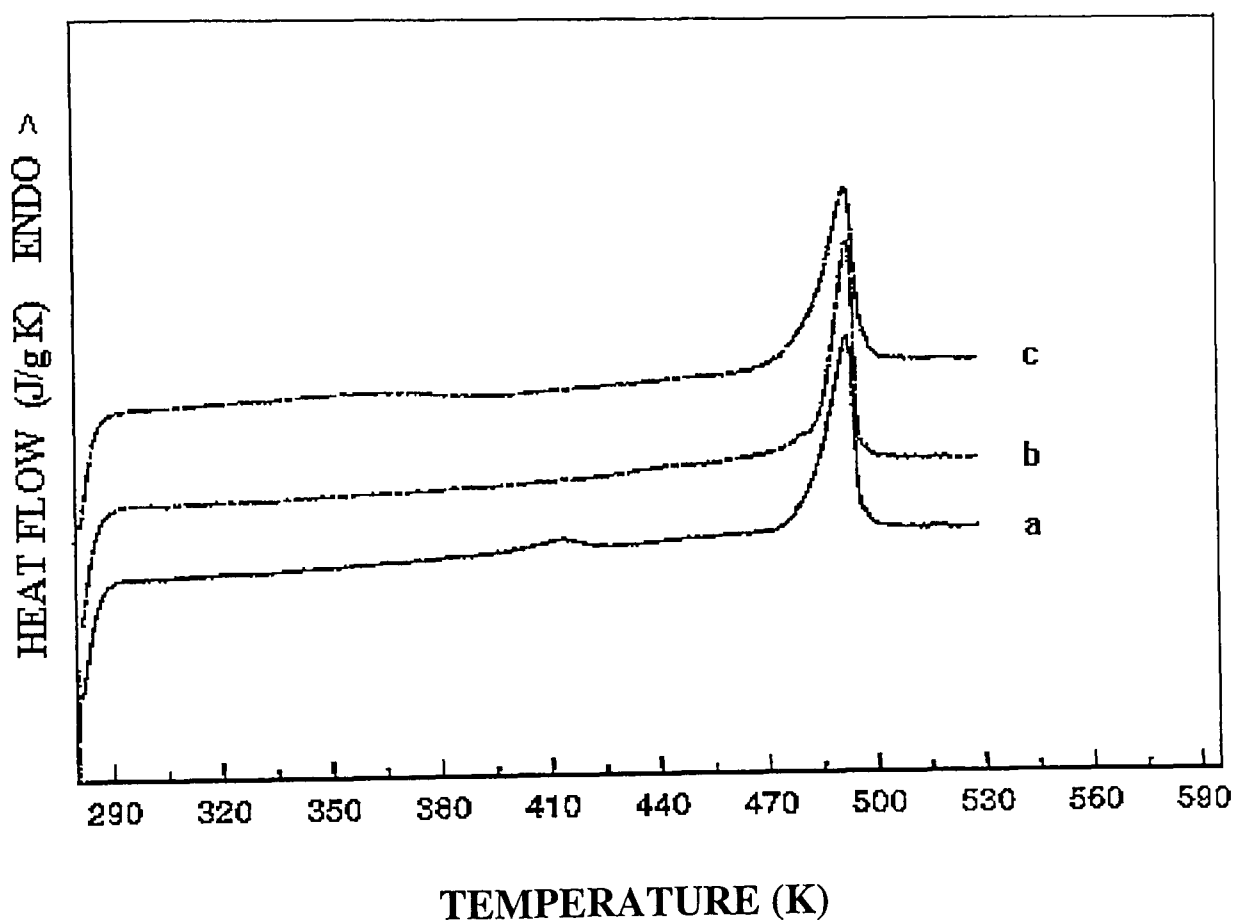
**Figure 4.7 SPBT 8.4 mole % film sample a) first scan,
b) second scan, c) post quench.**
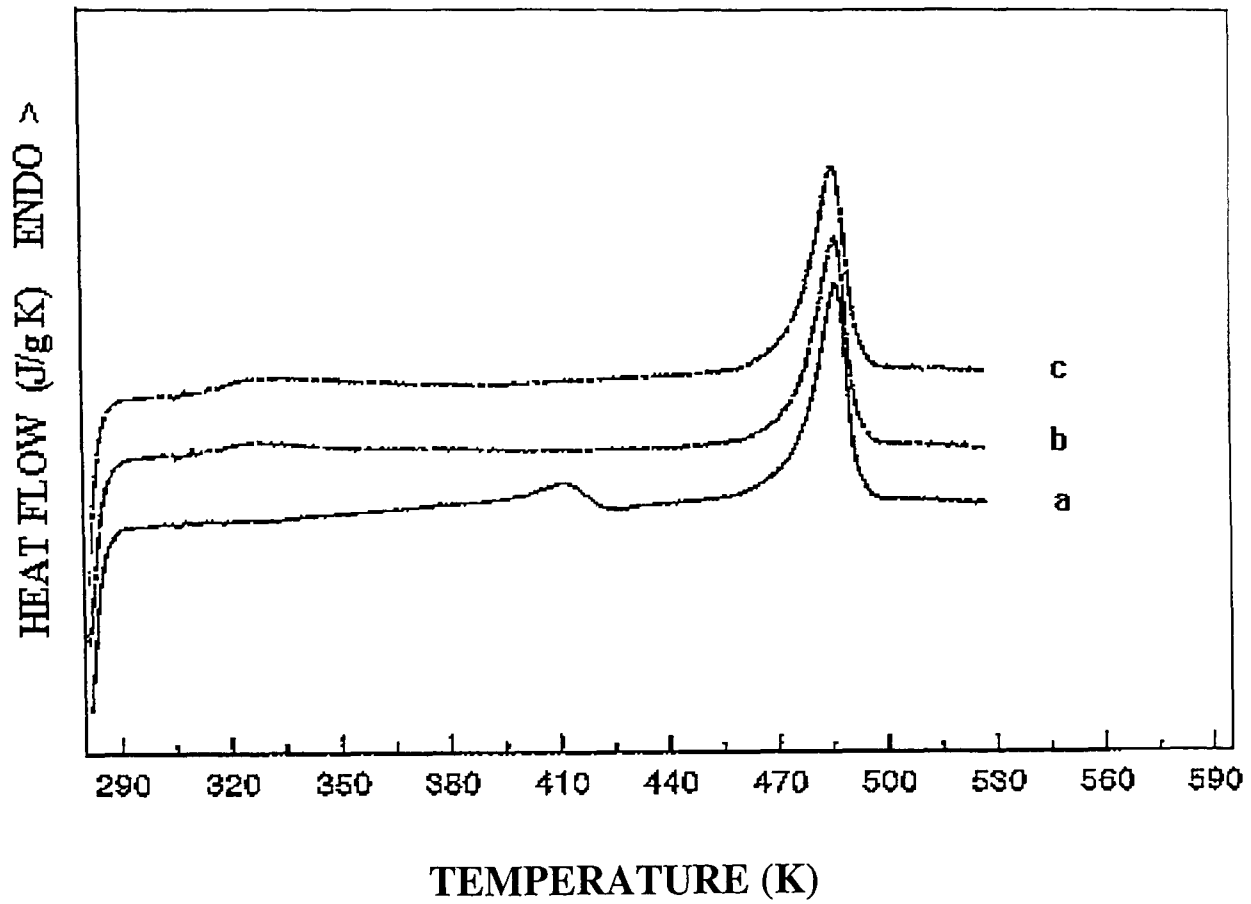
Figure 4.8 SPBT 13.5 mole % film sample a) first scan,

b) second scan, c) post quench.
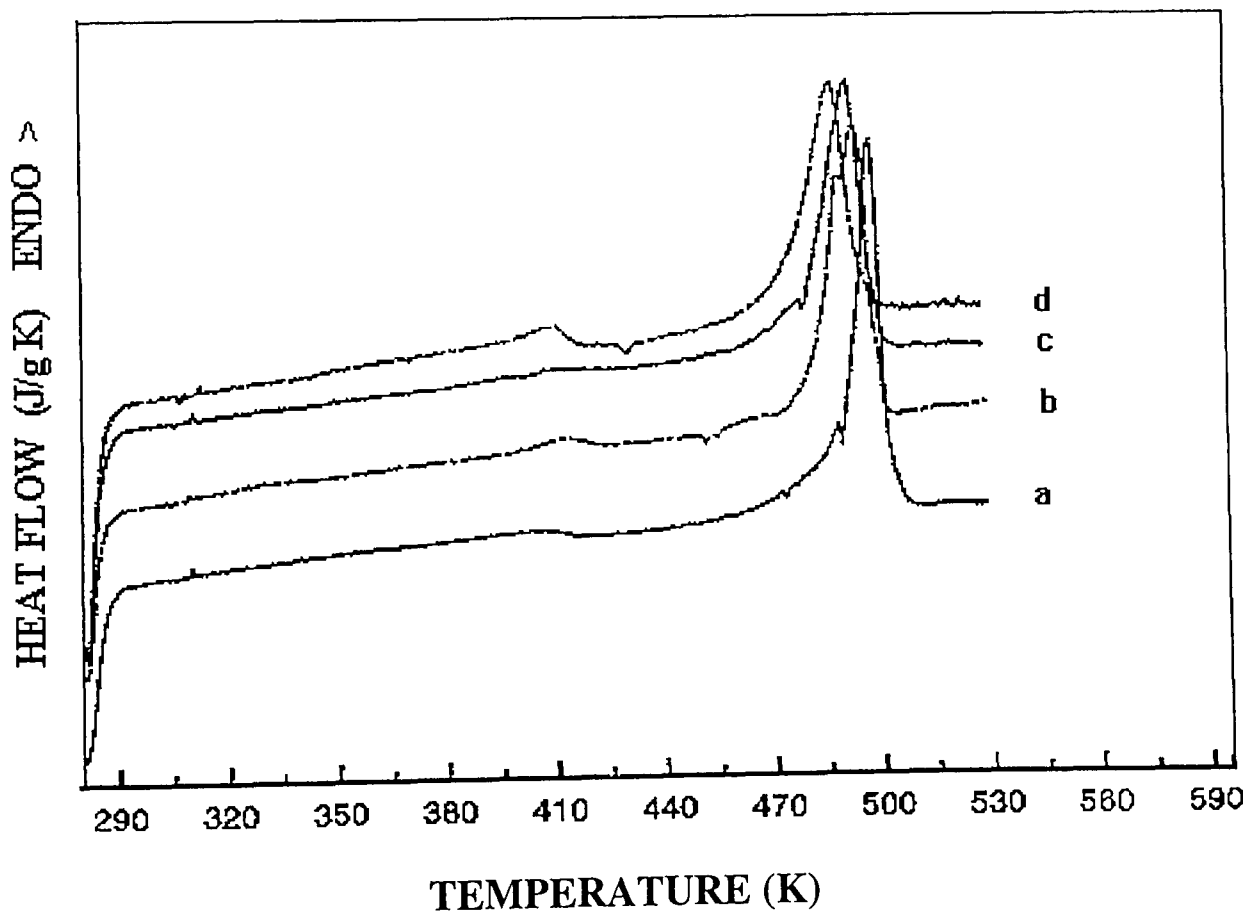
Figure 4.9 First scans of a) PBT 0.0 mole %, b) SPBT 3.5 mole %,

c) SPBT 7.9 mole %, d) SPBT 11.1 mole %.
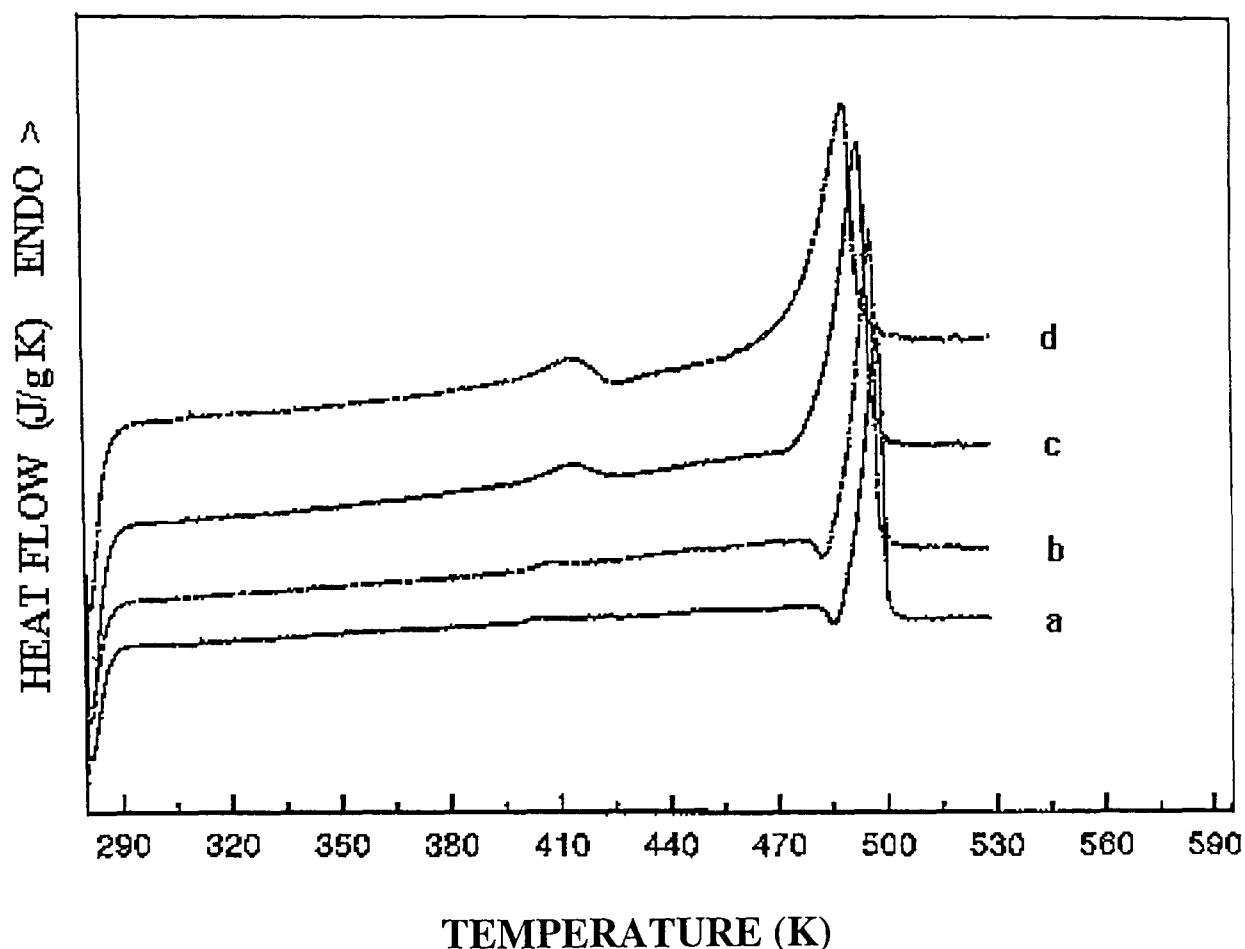
Figure 4.10   **First scans of a) PBT(F) 0.0 mole %, b) SPBT(F) 4.9 mole %,**

c) SPBT(F) 8.4 mole %, d) SPBT(F) 13.5 mole %.

the second scan. The peak at 485 K may be due to melting of unusual crystallites[1]. The post quench trace exhibited wide exotherm at lower temperature.

Figure 4.6(a-c) shows DSC scans of SPBT 4.9 mole %. This sample exhibited exotherms during the first and second scans, no evidence of exotherms was found during the post quench scan. Figure 4.6(b) reveals high temperature endotherm followed by exotherm and a main melting endotherm at 487 K. The samples of SPBT 8.4 and 13.5 mole % showed evidence of melting. The location of this melting endotherm remained 10 K lower than the pure PBT melting point. This decrease in T_m on increase of ionic content could be attributed to the increasing disorder in the sample, and T_m moving closer to T_g which is characteristic of amorphous phase. The corresponding DSC curves are plotted in the Figures 4.7-4.8 (a-c).

4.1.3 Low temperature endotherms

During the first scan as shown for all samples in cumulative graphs in Figures 4.9(powder) - 4.10(film) (a-d), a low temperature endotherm was observed with its onset slightly above the pretreatment temperature of 393 K. The magnitude of this peak was typically from 5 - 10 % of the main peak, representing 2 -5 % in terms of crystallinity. Following rapid cooling to room temperature (593 K/min) this peak disappeared in the 0.0, 3.5 and 4.9 mole % samples (this effect is visible in Figures 4.1(b), 4.2(b) and 4.6(b) respectively). It apparently reappeared at a lower temperature with the onset typically at 308 K, following the liquid nitrogen quench. The SPBT 7.9 mole % sample showed a rather broad feature during the second scan, from approximately 308 K to 413 K, and as described below exhibited a T_g during the post quench scan.

For samples with the highest sulphonation levels (11.1 & 13.5 mole %) small peak was found in the three scans [see Figures 4.4 and 4.8 (a-c)]. Initially located slightly above the pretreatment temperature, the small endotherm appeared around 308 K and peaked at about 323 K during both the second and post quench runs. The lower melting endotherms moved progressively to higher temperatures as the level of sulphonation increased (see figure 4.10 (a-d) during the first scan). This is thought to be the ability of ionic interactions to reduce the segmental mobility of crystalline and ionic domains, as discussed further in conclusions.

4.1.4 Glass transition temperature

A small change in heat capacity C_p was measured during second scans for the 7.9 mole % sample indicating a T_g of 323 K as illustrated in Figure 4.3(b). The heat capacity change equivalent to 0.2 J/g K was low compared to that reported[2] for pure PBT (0.5 J/gK), whereas T_g of 323 K measured for the 7.9 mole % sample is slightly higher than those reported for pure PBT in the literature, which range from 296 K [2] to 316 K [2].

In ionomers, the matrix glass transition is thought to arise from the amorphous regions of a polymer. From a molecular viewpoint, the matrix transition temperature may be defined as the lowest temperature at which polymer chain segments undergo rotational and translational motions. Below this glass temperature it is believed that the, segmental mobility of the chains does not occur[3].

For SPBT 7.9 mole % sample the higher glass transition temperature T_g than that of a pure PBT is due to the level and nature of crystallinity[4], ion content and perhaps molecular orientation. Semicrystalline polymers such as PBT may be partially oriented, that is, their chains have an overall alignment that may impart to the bulk polymer certain advantageous properties, such as increased mechanical strength and thermal stability.

It is possible that due to the strong ionic interactions resulting from the incorporation of ions into polymer, and intermolecular force, such as hydrogen bonding limiting the mobility of the polymer chains for highest level of sulphonation, T_g did not occur in the first scan. SPBT 11.1 mole % exhibited T_g' s during second and post quench scans (see Table 4.1).

In other cases the appearance of the low temperature peak just above room temperature made positive identification of a T_g impossible. When this peak occurs near room temperature may be connected with the glass transition[5].

Table (4.1) Percentage crystallinity and melting temperature for PBT/SPBT powder samples determined from DSC scans as described in the text.

Mole % S	Thermal Scan	% Crystallinity	T_m (K)	T_g (K)
0.0	First	38.9	498	-
0.0	Second	31.5	497	-
0.0	Post Quench	30.1	496	-
3.5	First	44.0	496	-
3.5	Second	30.7	493	-
3.5	Post Quench	40.0	491	-
7.9	First	28.6	493	-
7.9	Second	25.7	492	323
7.9	Post Quench	25.8	492	-
11.1	First	27.0	489	-
11.1	Second	25.9	488	315
11.1	Post Quench	25.9	487	307

4.1.5 Crystallinity and melting point depression

Typical DSC results for the melting temperature and percentage crystallinity as a function of degree of sulphonation (for the powder or "as received" samples) and for film samples are gathered in Table (4.1) and Table (4.2), respectively, for each of the above thermal scans. Figure 4.11. shows typical data for the percentage crystallinity as a function of mole % sulphonation for the three thermal scans. Decreasing crystallinity with increased sulphonation was found together with a decrease in the crystallinity

after the first thermal scan. The latter is attributed to the rapid cool following the first melt. Crystallinity of 44 % measured for the pure PBT and the 3.5 mole % samples is slightly higher than previously reported values found in the literature for pure PBT, (e.g. 40 % and 39 %)[7,11]. For both samples crystallinity was reduced to about 30 % following rapid cooling (second scan).

Table (4.2) Percentage crystallinity and melting temperature for PBT/SPBT film samples determined from DSC scans as described in the text.

Mole % S	Thermal Scan	% Crystallinity	T_m (K)	T_g (K)
0.0	First	27.4	498	-
0.0	Second	35.5	497	-
0.0	Post Quench	28.45	496	-
4.9	First	30.0	495	-
4.9	Second	35.4	494	-
4.9	Post Quench	38.7	494	-
8.4	First	30.1	492	-
8.4	Second	29.0	492	-
8.4	Post Quench	32.5	491	-
13.5	First	31.0	488	-
13.5	Second	27.0	487	-
13.5	Post Quench	28.0	487	-
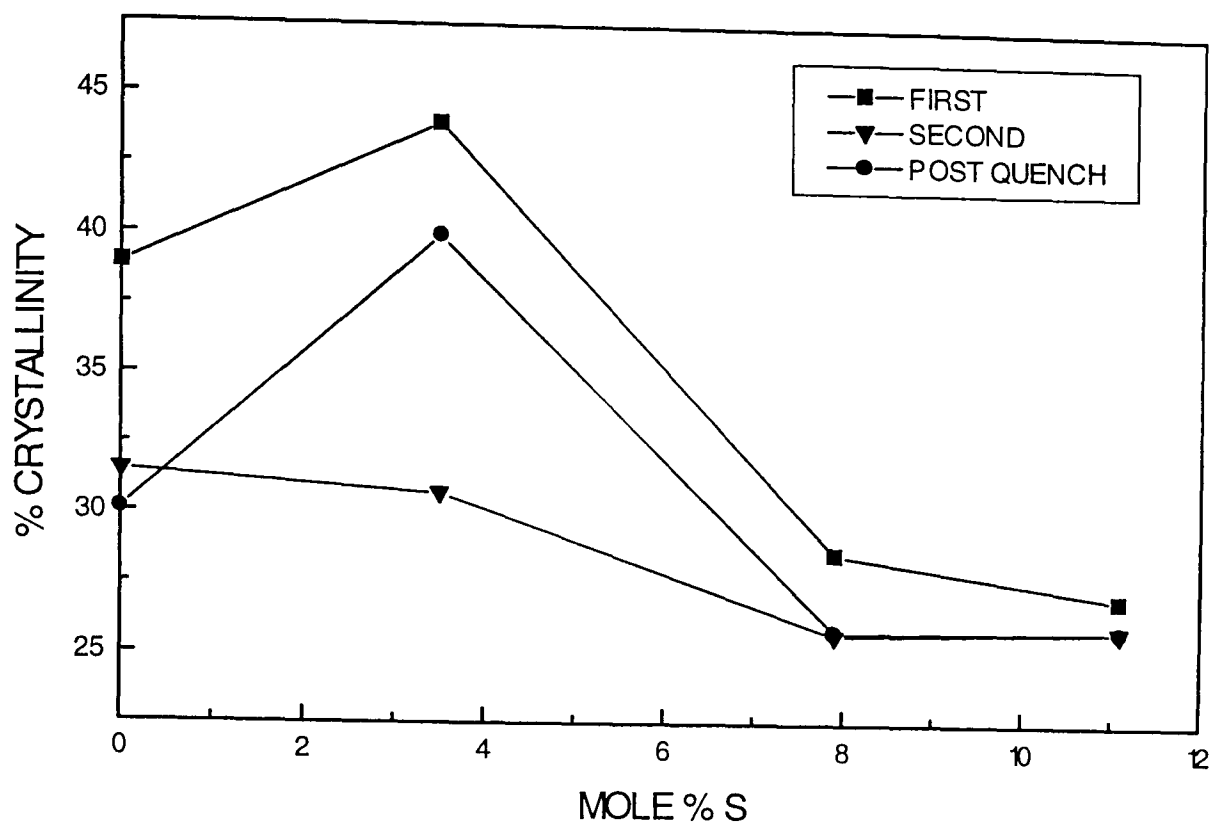
Figure 4.11 % Crystallinity as a function of the mole % sulphonation for PBT and SPBT powder samples.

The 0.0 % sample showed a further slight reduction of crystallinity post quench whereas for the 3.5 % sample an increase in crystallinity was apparent post quench. The determined value of 40 % crystallinity during the third thermal scan for this sample together with a further depression in T_m remains unexplained.

Markedly lower crystallinity of just under 30 % was found in the samples with higher levels of sulphonation. Only a small reduction in crystallinity is apparent following the rapid cooling cycles. The crystalline structure, observable melting temperature and crystallisation behaviour of a semi-crystalline polymer usually remain intact when it is blended with an amorphous polymer to form an immiscible blend. On the other hand, the addition of an amorphous polymer to a semi-crystalline one, which forms a thermodynamically miscible blend, dramatically affects the crystallisation behaviour of the latter.

The melting point also showed a decrease with increased functionality. The data obtained for the first runs exhibited smooth trends whilst values obtained followed the rapid cooling cycles were often scattered, although still showing the initially observed trend of melting point depression (Figure 4.12). It is apparent from Table 4.1 and Figure 4.9 (a-d) that there is a drop in T_m upon increase of ionic content. This effect becomes more prominent and a substantial depression in the melting temperature is observed with the highest level of sulphonation (Table 4.2). The reduction in the T_m due to ionic content can be explained as follows: in polymers with crystallisable backbones ionic groups reduce the fractional crystallinity because the ionic groups do not become the part of the crystalline lattice. Hence T_m is lowered.

4.1.6 Multiple melting endotherms in PBT and SPBT

The melting behaviour of PBT is highly dependent on its thermal history, with multiple melting peaks being reported by many workers[6-9] who have carried out thermal analysis studies using predominantly DSC to investigate the effects of cooling rates from the melt, heating rate during DSC scans and annealing temperatures. It is in order to review briefly a number of possible explanations which have been put forward to explain the observation of up to three endotherms. Hobbs and Pratt[7] first reported the appearance of multiple melting in PBT. Their investigations indicated the double peaks to arise from reorganisation processes during heating in the DSC cell. Subsequent crystallisation studies by Stein and Misra[8] indicated two optical melting points which they attributed to a combination of usual and unusual spherulites, the latter melting at the lower temperature. Luding and Eyerer[9] produced various spherulitic structures by cooling at different rates from the melt, the specific crystallisation condition being the main factor determing the spherulitic morphology obtained. Double melting endotherms at the main peak were therefore attributed to the melting of different spherulites within the sample. DSC investigations of annealed PBT by Yeh and Runt[5] showed up to three melting endotherms the lowest peak arising a few degrees above the annealing temperature and eventually merging with the main melting peak at annealing temperatures, (T approaching 473 K). For T >473 K a single melting peak

was observed which moved to a higher melting temperature as the annealing temperature was increased. It was concluded that the low melting peak was associated with crystals already present in the room temperature samples. The main peak, composed of two endotherms was attributed to crystals already present in the sample and their reorganisation during the thermal scan. Both the low temperature peak and the main melting peak were attributed to the melting of the usual spherulitic crystal form. It was thus proposed that the multiple melting may be unconnected with distinct crystal structures.

A model was put forward (Nichols and Robertson[6]) for the melting behaviour of PBT cooled at different rates from the melt. The model was based on the melting and recrystallisation of an initial distribution of melting temperatures containing one maximum and two inflection points. The occurrences of one and three endotherms was well reproduced by the simulation without considering additional crystallisation from the amorphous regions during the scanning process.

In the original work on SPBT by Gorda and Peiffer[10], detailed examination using polarised light microscopy indicated that at the lower ion contents (less than 5 mole % sulphonation) the so-called unusual spherulitic morphology is observed. The findings indicated that the PBT copolymers change from abnormal to normal spherulitic structure in the range of 5-8 mole % functionalisation. It is of interest that in this current work no double melting endotherms were observed for sulphonation levels over 3.5 mole % which may be indicative of the presence of only one spherulitic form at the higher levels of sulphonation.

Gorda and Peiffer found the optical melting of the normal spherulites to be approximately 278 K. This was higher than that observed for the abnormal spherulites. The overall reduction in the melting temperature with increased sulphonation level in the current work therefore can not be attributed to the spherulitic form. In our investigations into SPBT the presence of a small low temperature endotherm just above the "pretreatment" temperature of 393 K is similar to the observations of peaks just above the annealing temperature in the studies reported above. The appearance of

a similar peak at much lower temperatures following rapid cooling to room temperature (i.e. second scans) and after quenching in liquid nitrogen suggests similar effects. When this low endotherm is present, heat of fusion C_p for low endotherms has been detected, therefore it is not taken to be an "overshot" peak at the glass transition that is often observed on heating scans.

4.1.7   Melting point depression (Flory's expression)

The reduction in crystallinity with increasing functionality of SPBT is in general agreement with previous work[10]. However, earlier work indicated a complete suppression of crystallinity by the highest level of functionality measured (13.5 mole %). The current work indicates about 30 % crystallinity in the "as received" powder samples. Initial DSC scans on the 13.5 mole % pressed film used indicated at least 20 % crystallinity to be present.

As reported the melting temperature of the samples decreased with increasing functionalisation. Flory's expression (4.1) for the melting of random copolymers has been used to examine the data. The theory assumes the minor component (SPBT units in our study) to be randomly dispersed within the copolymer and that this component does not enter the crystal lattice.
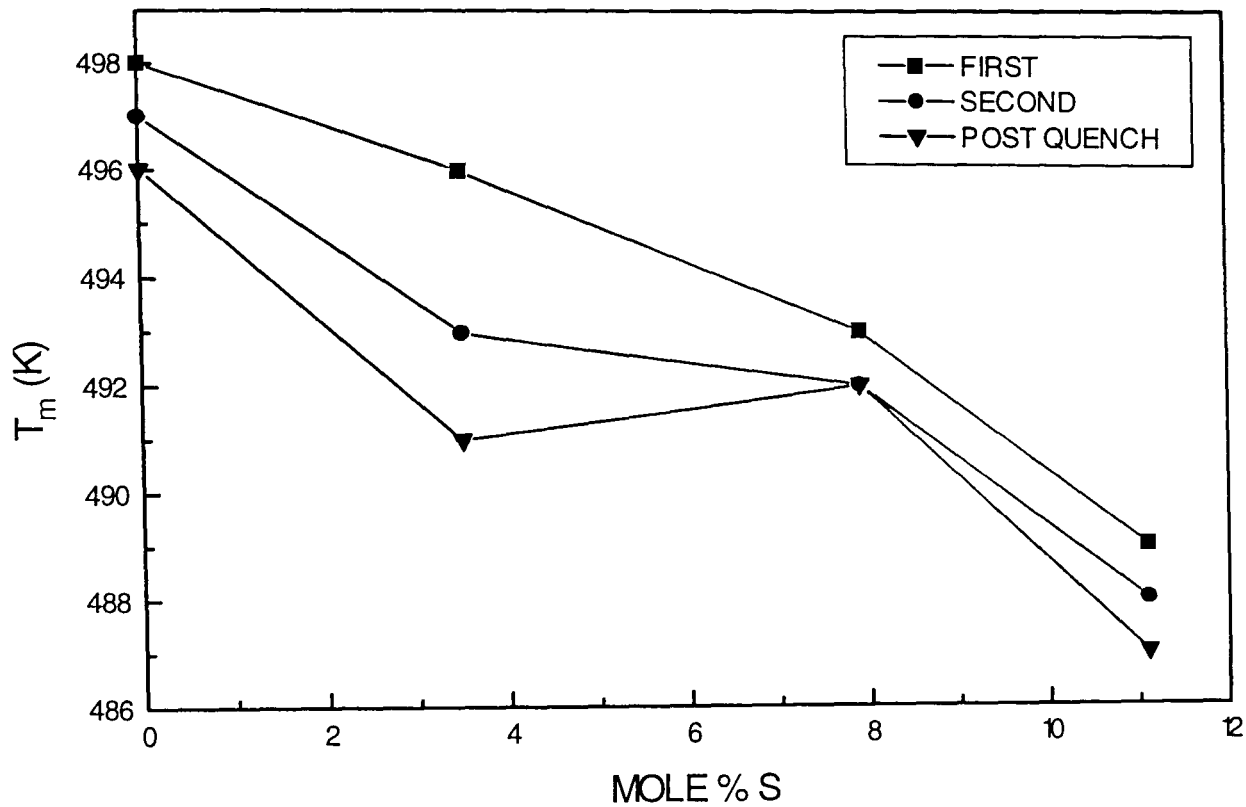
Figure 4.12 Melting point depression as a function of the mole %

sulphonation for PBT/SPBT powder samples.

According to this equilibrium theory the melting temperature of the homopolymer, T_o, is related to that for the copolymer, T_m, by the following expression:

$$\frac{1}{T_m} - \frac{1}{T_o} = -\left(\frac{R}{H_u}\right)\ln N \qquad\qquad 4.1$$

where N is the fraction of crystallisable units, H_u is the molar heat of fusion of the homopolymer crystals, and R is the gas constant.

The theory is only strictly valid under certain conditions:

i)   The crystals are in equilibrium

ii)   melting is conducted under close to equilibrium conditions

iii)   no change in the crystal system is induced by the presence of the second

          component

iv)   the second component does not undergo a phase transition within the

          investigated range.
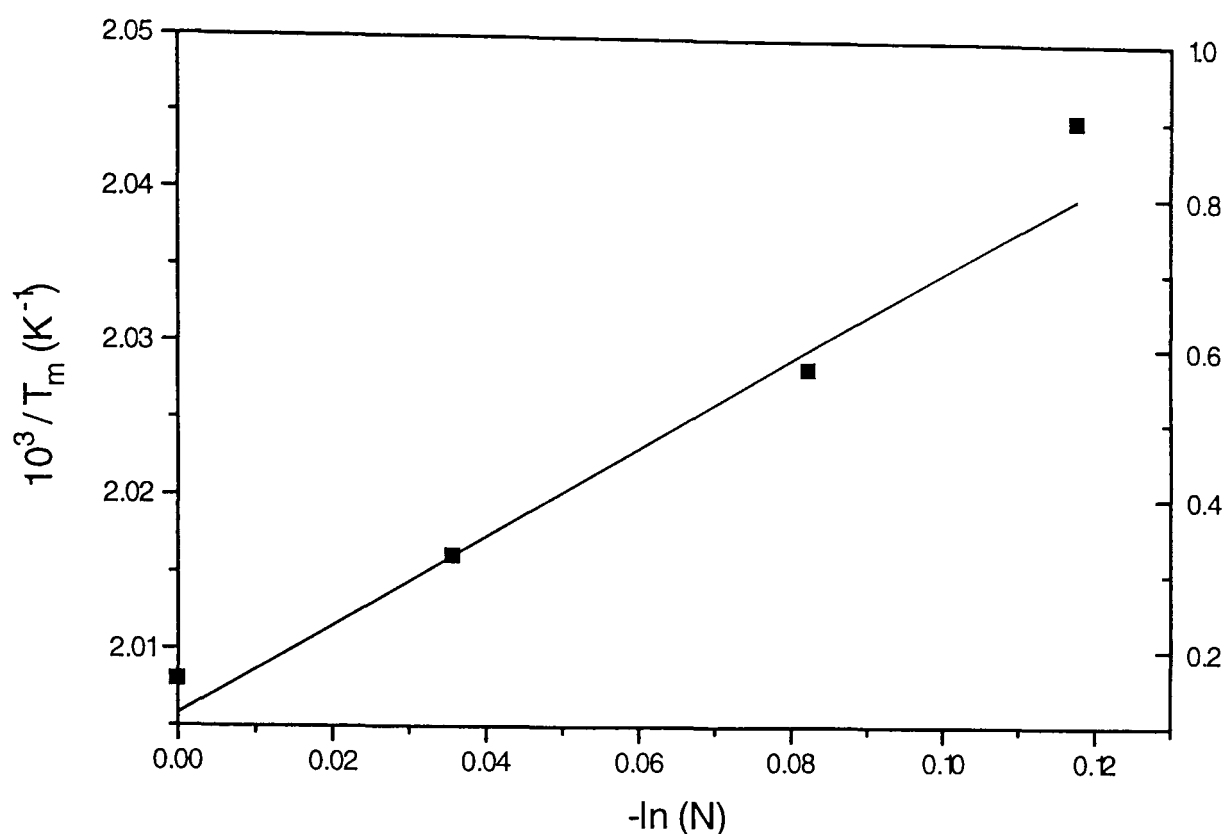
Figure 4.13 Flory copolymer plot of 10^3/T (K^{-1}) versus (-ln N).

These conditions are rarely met and at best may only be partially met in this case. Data for the first scan from Figure 4.12 is shown in Figure 4.13. presented as a Flory copolymer plot of $10^3/T$ (K^{-1}) versus (-ln$N$). The straight line represents the theoretical line for equation (1) using the measured values for T_o and the accepted value of 142 J/g for H_u. Although it is appreciated that the value used for T_o does not represent the true equilibrium melting temperature[11] the fit in terms of the slope and therefore H_u is remarkably close to the data for all except the highest level of functionality. These results additionally point to the randomness of distribution of sulphonate groups within the copolymer.

Slight deviation from Flory's theoretical curve were taken to be indicative of polymer-polymer interaction. This possibility was further investigated, as outlined below.

The thermodynamic effects of mixing two polymers was considered by Scott[12] using the Flory-Huggins approximation[13]. Using Scott's expression for crystalline polymer diluent systems Nishi and Wang[14] derived an expression for the mixing of a crystalline polymer and an amorphous polymer. Again the expression is only valid under the equilibrium conditions stated in this chapter. The expression below describes the melting point depression of a crystalline/amorphous polymer pair in terms of the volume fraction of the amorphous polymer, v, the melting temperatures of the homopolymer, T_0 and T_m and the polymer-polymer interaction χ_{12}.

$$T_m / T_o = 1 + (\chi_{12} RTV_{2u}/V_{1u}H_u) \, v^2 \qquad\qquad 4.2$$

where χ_{12} is the interaction parameter for the polymer pair at $T = T_m$

V_{1u} is the molar volume of the pure polymer (PBT)

V_{2u} is the molar volume of the 'diluent' (SPBT)

T_m is the copolymer melting temperature

T_o is the pure PBT melting temperature

Assuming $V_{1u} \sim V_{2u}$ gives:

$$T_m / T_o = 1 + \chi_{12} (RT / H_u) \, v^2 \qquad\qquad 4.3$$

To investigate the possibility of significant interaction in the functionalised PBT samples the melting point data were plotted as v^2 against T_m. From the Nishi and Wang expression this should give a straight line of negative gradient, given by $\chi_{12}(RT / H_u)$ T_o, from which the interaction χ_{12} may be obtained provided H_u is known (or independently established). Negative gradients were obtained for two sets of data, hence χ_{12} was determined to be 0.01.

Table (4.3)   DSC data 0.0 % PBT/PC blends & associated runs.

Sample	% SPBT	Thermal scan	T_g (K)	T_m (K)	H (J/g)	(100H)/ 142	% Crystallinity
PC sol cast	0	1st	415			0	
		2nd	417			0	
		post qnch	419			0	
0.0/25	25	1st		496.3	23.2	16.34	64
		2nd	401	494.4	9.9	6.97	28
		post qnch	403	489.8	9.6	6.76	28
0.0/50	50	1st		497.8	28.7	20.21	40
		2nd		489.6	21.1	14.86	30
		pqch		485	20.8	14.65	30
0.0/75	75	1st		497.8	43.7	30.77	41
		2nd		496.1	36.5	25.70	34
		post qch		493.3	36.3	25.56	34
0.0 PBT sol cast	100	1st		495.2	59.8	42	
		2nd		495.5	39	27	
		post qnch		495.3	38.3	27	

4.2   Results and discussion for SPBT/PC and SPBT/PC blends

Polymer-polymer mixtures or blends are commonly incompatible. However, if ionic groups are is incorporated into one of the polymers, the miscibility between the two polymers is enhanced. In the present study, miscibility behaviour is explored in the blend system containing a high T_g temperature PC and a low T_g temperature SPBT.

The unfunctionalized blends are explored first, followed by an investigation in which SPBT are mixed with PC. Blends prepared by the procedure (solvent casting technique) described in section 3.3.4 chapter 3 were examined by differential thermal analysis (DSC) in order to establish their glass transitions, melting, crystallisation

behaviour and miscibility. Pure PC showed a T_g at 414 K (Figure 4.14). All solvent cast samples, both blends and control samples, were examined following the same procedure as was used for the homopolymers described in chapter 3, section 3.4.4.

4.2.1 Crystallinity

The degree of crystallinity of the SPBT portion of the blends made from 0.0 and 3.5 % SPBT remains at the same level as found in the homopolymers (40 % as prepared, reducing to 30 % following melting). However, for blends produced from the higher levels of sulphonation (7.9 mole % and 11.1 mole %) overall crystallinity content of the SPBT is lowered to 20-25 % following melting. A substantial reduction in the crystallinity relative to PBT 0.0 and 3.5 % points to increased miscibility. Relevant experimental data is summarised in Tables 4.3-4.6.
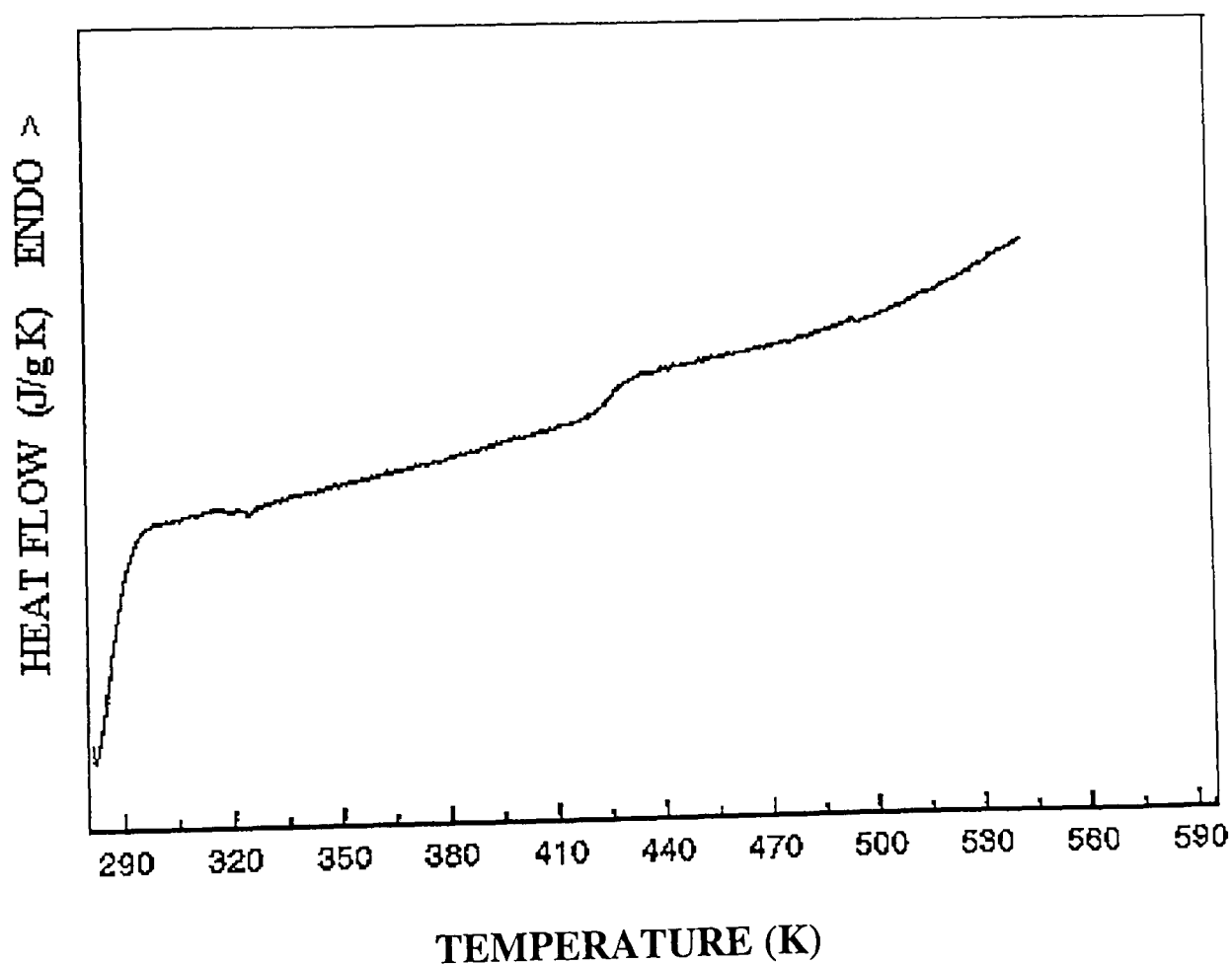
Figure 4.14. DSC thermogram of pure PC.

4.2.2   Melting behaviour

The melting temperatures (defined as the maximum of the main melting endotherm) of the blends were investigated as a function of blend composition for each of the SPBT samples (i.e for sulphonation levels of 0, 3.5, 7.9 & 11.1 mole %).

Figure 4.15(a-c) shows DSC melting curves during the first, second and post quench heating of PBT/PC 0.0 mole % 25/75 blend. The DSC melting curve on reheating displays a low temperature endotherm at 350 K and a main melting peak with a shoulder at temperatures between 470-498 K as shown in Figure 4.15(b).
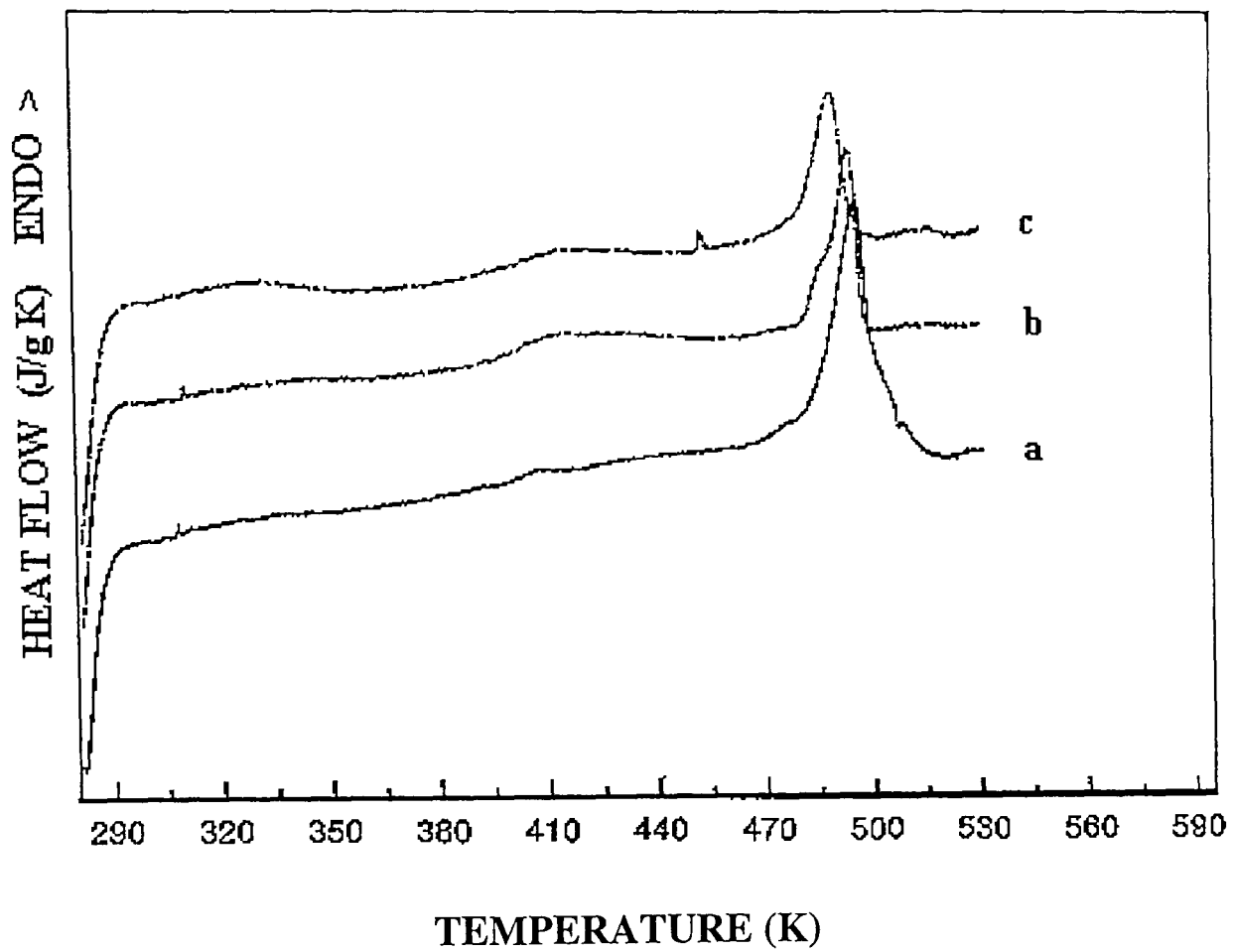
Figure 4.15 0.0 mole% PBT/PC 25/75 a) first scan,

b) second scan, c) post quench.
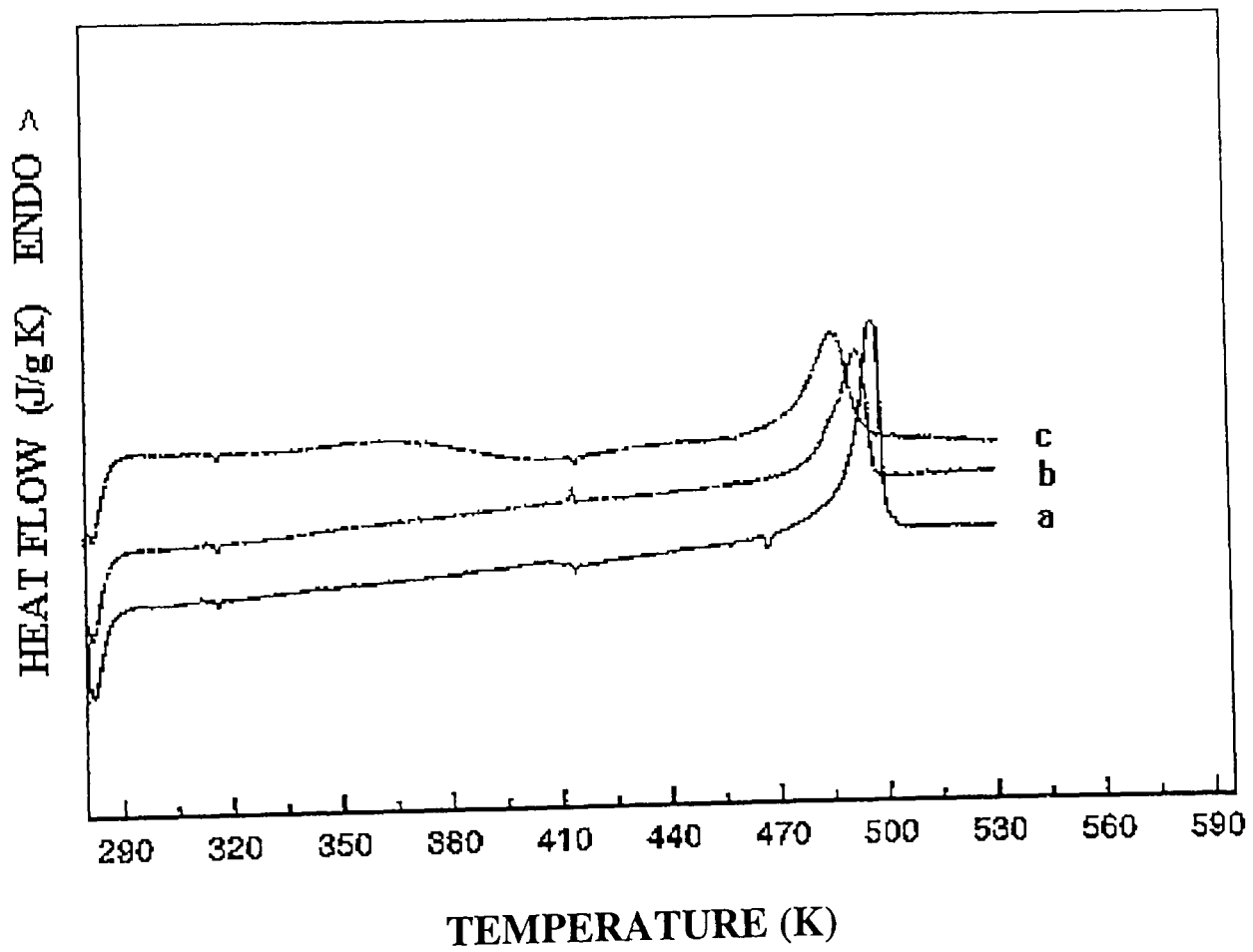
Figure 4.16 0.0 mole% PBT/PC 50/50 a) first scan,

b) second scan, c) post quench.

Table (4.4)   DSC data 3.5 % SPBT/PC blends & associated runs.

Sample	% SPBT	Thermal scan	T_g (K)	T_m (K)	H (J/g)	(100H)/ 142	% Crystallinity
PC sol cast	0	1st	415			0	
		2nd	417			0	
		post qnch	419			0	
3.5/25	25	1st	394	493.6	14.34	10	40
		2nd	401	492.6	13.2	9	33
		post qnch	398	491.2	14.1	10	40
3.5/50	50	1st		492.9	29.1	20	40
		2nd	392	492.7	26.5	19	38
		post qnch		490.9	29	20	40
3.5/75	75	1st	396	493.5	43.1	30	40
		2nd	391	493.3	42.4	30	40
		post qnch	388	491.6	45.4	32	43
3.5 sol cast	100	1st		494.5	58.7	41	41
		2nd		494	55.6	39	39
		post qnch		491.9	61.8	44	44

Main melting peaks for PBT/PC 0.0 mole % 25/75 blend can be seen at 496.3 K (Figure 4.15(a)). Further heat cycles, Figure 4.15(b-c), result in a slight lowering of the SPBT/PC melting point, however this reduction is only 6 K. Generally speaking, the depression of T_m a crystalline polymer in a blend results from morphological, kinetic and thermodynamic effects. A double melting peak was observed for PBT/PC 0.0 mole % 75/25 at 480 K with T_m at 496 K as shown in Figure 4.17(b) during the second scan. However, single main melting peak at 493 K in the post quench scan was observed along with a broad asymmetric low temperature endotherm at 325 K (Figure 4.17(c)). The appearance of this endotherm may be caused by a mobility of a small segment of polymeric chain.
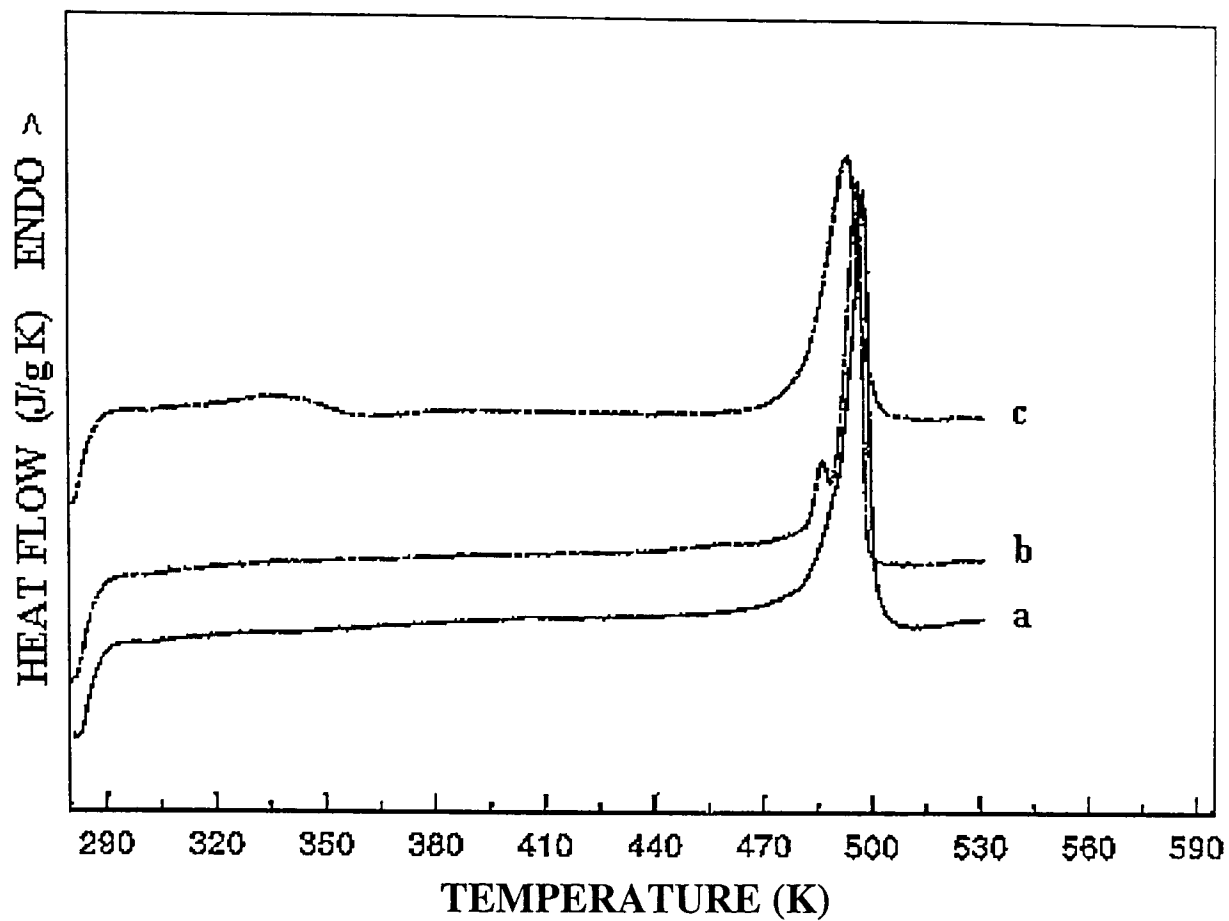
Figure 4.17 0.0 mole% PBT/PC 75/25 a) first scan,

b) second scan, c) post quench.
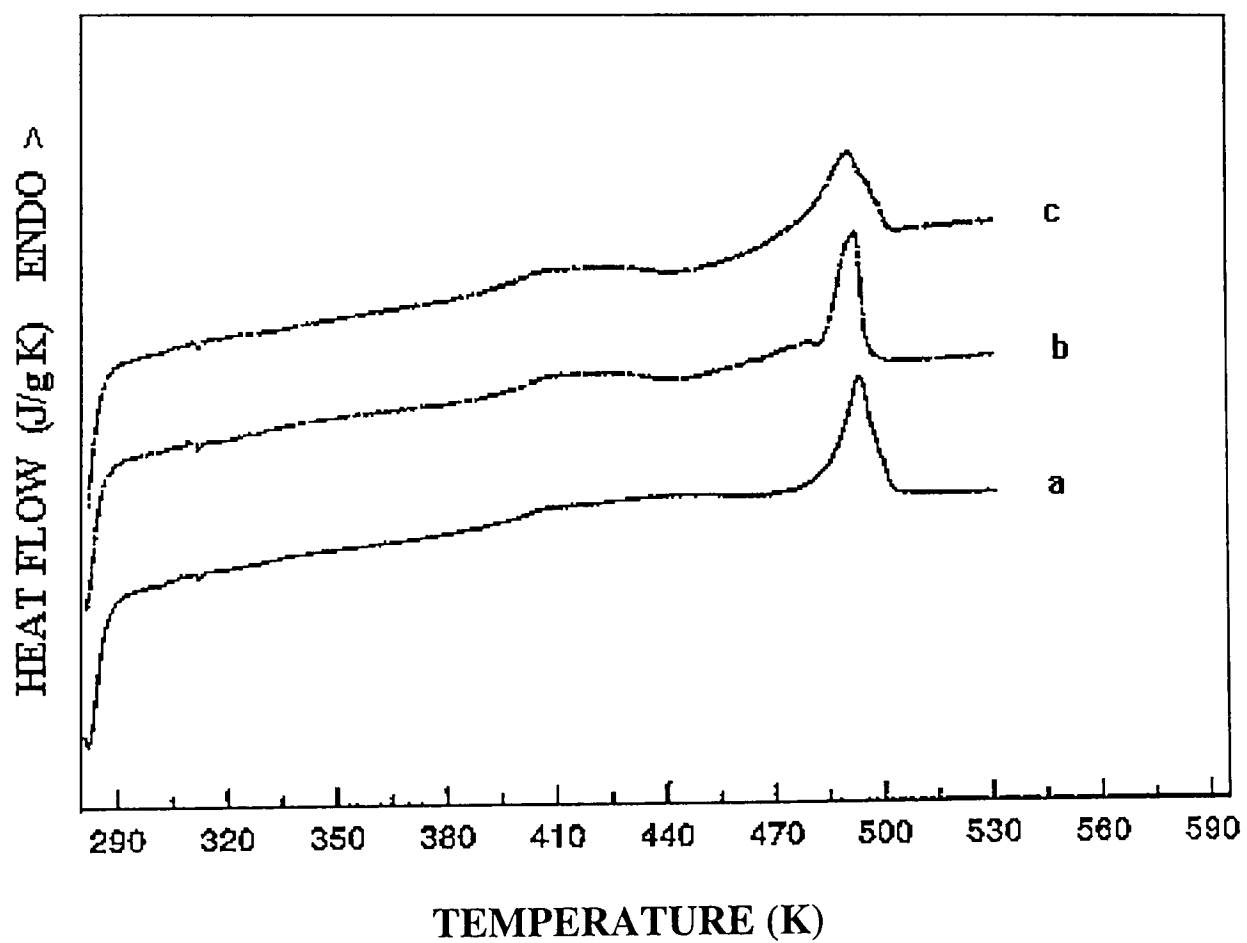
Figure 4.18 3.5 mole% SPBT/PC 25/75 a) first scan,

b) second scan, c) post quench.

Some authors[15-16] have reported differences between the melting behaviour of pure semicrystalline polymers and their blends with other polymers. For the 0.0 mole % sample, i.e. the PBT/PC blends, there was a dramatic reduction of melt temperature on thermal cycling, with the change in melting temperature ΔT_m peaking at 11.5 K at a blend composition of 50 % SPBT/PC. Results are gathered in Table 4.5. For the other blends ΔT_m was typically 2 K across the composition range. The observable T_m of the semicrystalline homopolymer is depressed in partially miscible blends due to the reduction in the crystallinity upon sulphonation and also blending with amorphous material such as PC[17-18].

Table (4.5)   DSC data 7.9% SPBT/PC blends & associated runs.

Sample	% SPBT	Thermal scan	T_g (K)	T_m (K)	H (J/g)	(100H)/ 142	% Crystallinity
PC sol cast	0	1st	415			0.00	
		2nd	417			0.00	
		post qnch	419			0.00	
7.9/25	25	1st	403	489.8	15.2	10.70	44
		2nd	418	489.1	7.33	5.16	21
		post qnch	419	487.8	8.84	6.23	25
7.9/50	50	1st	405	490.4	22	15.49	31
		2nd	415	490.1	18.2	12.82	26
		post qnch	415	489.6	18	12.68	26
7.9/75	75	1st	316/393	490.7	37.9	26.69	36
		2nd	317/399	489.3	25.2	17.75	24
		post qnch	316/407	488.9	25.3	17.82	24
7.9 sol cast	100	1st		491.8	45.7	32.18	32
		2nd		490.3	38.3	26.97	27
		post qnch		490.8	37.3	26.27	27

Table (4.6)　DSC data 11.1 % SPBT/PC blends & associated runs.

Sample	% SPBT	Thermal scan	T_g (K)	T_m (K)	H (J/g)	(100H)/ 142	% Crystallinity
PC sol cast	0	1st	415			0.00	
		2nd	417			0.00	
		post qnch	419			0.00	
11.1/25	25	1st	406	487.2	5.2	3.66	15
		2nd	419	485.5	6.8	4.79	19
		post qnch	422	485.7	6.9	4.86	20
11.1/50	50	1st	403	488.4	16	11.27	22
		2nd	318/418	486.3	12.7	8.94	
		post qnch	318/421	485.9	13.6	9.58	19
11.1/75	75	1st	406	488.1	27.4	19.30	26
		2nd	317/413	486.3	25.3	17.82	24
		post qnch	318/414	485.2	25.6	18.03	24
11.1 sol cast	100	1st		488	44.1	31.06	31
		2nd	318	488.1	34.7	24.44	24
		post qnch	318	488.3	34.7	24.44	24

Well-defined multiple melting peaks were not observed in any of the blends (cf. previous section on melting behaviour of SPBT samples), although there were asymmetries (Figures 4.15(b) and 4.16(b)) in the melting endotherms of some of the 0.0 and 3.5 mole % samples (Figures 4.18(b)). These are probably a combination of two unresolved endotherms. A similar feature is evident for SPBT/PC 3.5 mole % 25/75, as described before for the homopolymer SPBT 3.5 mole % powder sample: a small exotherm at 480 K followed by T_m at 492 K was observed in the second scan.

Figure 4.18(b) shows two high temperature melting endotherms at 410 K and 492 K for 25/75 blend. However 50/50 blend exhibited crystallisation at 435 K followed by main melting peak at 491 K during the post quench scan as shown in Figure 4.19(c).

The appearance of shoulder at 491 K near main melting peak in Figure 4.19 (b) may be due to the melting of unusual crystallites of SPBT in the blend. For all other blend compositions single symmetrical melting peaks (T_m) were obtained.

4.2.3 Glass transition temperatures

Measurement of the glass transition temperature of polymer blends provides a straight-forward method of assessing blend miscibility. A miscible amorphous blend of two polymers will exhibit a single glass transition at a temperature between the glass transition temperature of the homopolymers.

The blends produced from mixing the 0.0 and 3.5 mole % SPBT with PC showed no signs of miscibility originally, but showed partial miscibility following melting and quenching as can be seen in Figures 4.15(b-c) and 4.18(a-c) respectively. Glass transition in PBT/PC 0.0 mole % 25/75 blend composition appears at 401 K and 403 K during the second and post quench scans, respectively (see Figure 4.15 (b-c)). However, in the 50/50 and 75/25 (0.0 mole % blends), no evidence was found for T_g's even in the second and post quench cycles (see Figures 4.16-5.17(a-c)). Figures 4.18-4.20 (a-c) show DSC scans of blends of SPBT/PC 3.5 mole % for the compositions 25/75, 50/50 and 75/25 respectively. For 3.5 mole %, 25/75 blends (Figure 4.18(a-c)) the evidence of T_g can be seen at 394 K, 401 K, and 398 K during first, second, and post quench scans. A glass transition was visible for the 50/50 composition in the second scan (Figure 4.19(b)), and for 75/25 composition again single T_g s were recorded during the heating cycles at 396 K, 391 K, and at 388 K (Figure 4.20(a-c)). Blends for 75/25 3.5 mole % showed a decrease in the glass transition temperature during the cyclic scans (to an estimated accuracy of +/- 5 %). Furthermore an appearance of T_g's for PBT/PC 0.0 mole % with 25/75 blend composition in the second and post quench scans and for SPBT/PC 3.5 mole % blends indicate partially miscibility.
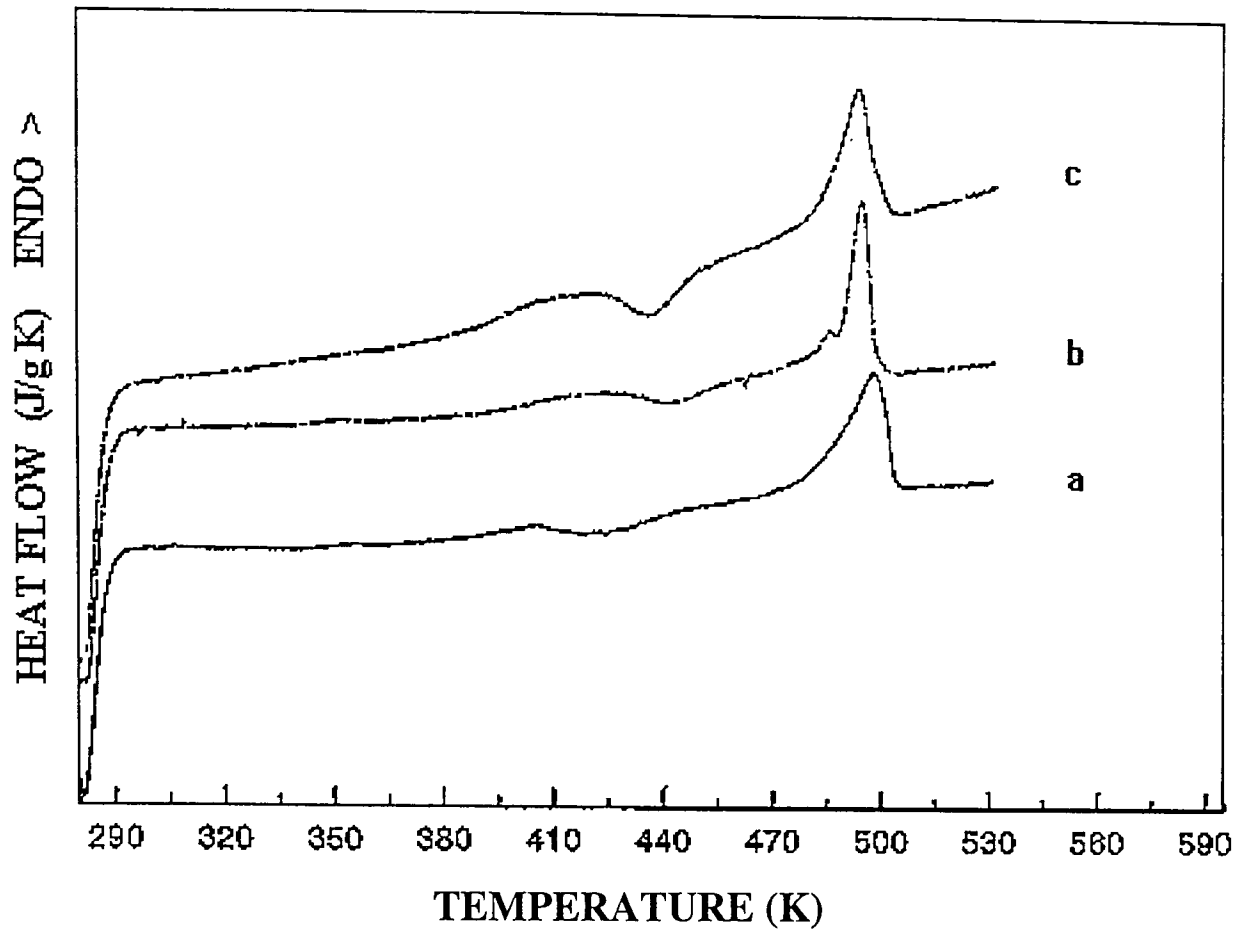
Figure 4.19 3.5 mole% SPBT/PC 50/50 a) first scan,

b) second scan, c) post quench.
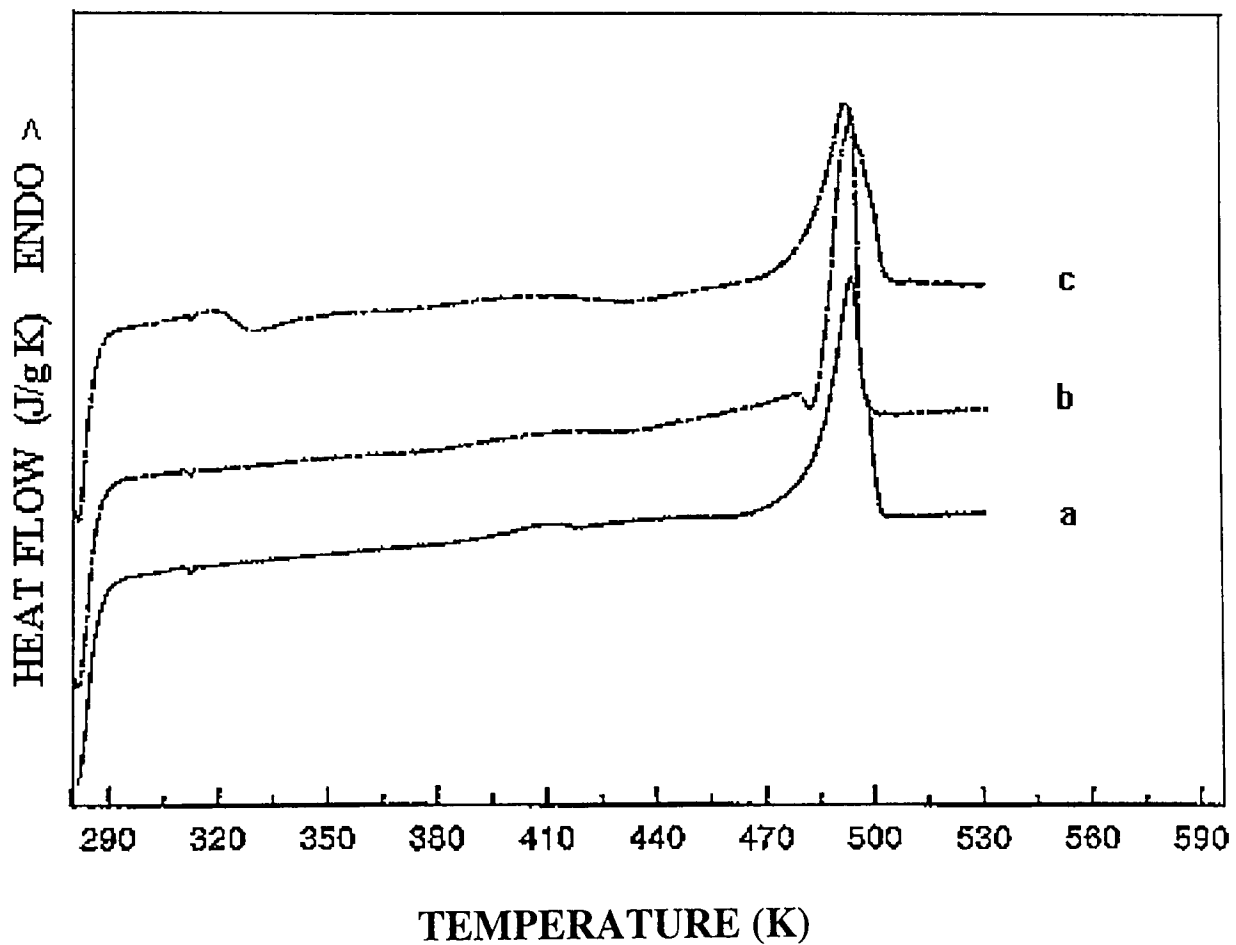
Figure 4.20 3.5 mole% SPBT/PC 75/25 a) first scan,

b) second scan, c) post quench.

Samples with higher sulphonation levels, namely the 7.9 and 11.1 mole % SPBT, showed partial miscibility as cast but, judging from the T_g data, appear to have phase separated following melting and quenching. Blends of SPBT/PC 7.9 mole % and 11.1 mole % showed some evidence for two distinct glass transitions. Figure 4.21(a-c) shows two T_g's, T_{g1} at 316 K and T_{g2} at 393 K during first scan for SPBT/PC 7.9 mole % 25/75. Figure 4.23(b) shows DSC endotherm with T_{g1} at 317 K and T_{g2} at 399 K in the second scan. After post quench T_{g1} at 316 K and T_{g2} at 407 K were just visible, as seen in Figure 4.23(c). Single T_g's were recorded for 25/75 and 50/50 blends at 403 K, 418 K and 419 K. Also at 405 K, 415 K, and 415 K during heating cycles, respectively, as illustrated in Figures 4.21-4.22(a-c). A sharp increase in glass temperature of 15 K is apparent for 25/75 and 50/50 blends during the cyclic heating. The shift in the glass temperature values may be due to the presence of strong interactions. e.g. of dipole-dipole type between SPBT-PC polymer pairs, which suggests that they may be partially compatible. The SPBT/PC 11.1 mole % blend showed a very distinct glass transition, similar to that of the 7.9 mole % blends of compositions described above. Figures 4.24-4.26(a-c) show DSC thermograms for SPBT/PC 11.1 mole % 25/75, 50/50, and 75/25 compositions, respectively.

A rise in the T_g glass transition temperatures during the first, second and post quench is quite clear from the Figures 4.24(a-c) and 4.25(a-c) showing data for 25/75 and 50/50 compositions respectively. T_g's are seen at 406 K, 419 K, and 422 K for 25/75 blend. For 50/50, and 75/25 blend single T_g's were obtained at 403 K and 406 K during the first scans respectively. Figures 4.25-4.26(b-c) show two T_g's at 318 K, 418 K and 418 K, 414 K for 50/50 composition. Other T_g values are 317 K, 413 K, and 318 K, 414 K for 75/25 blend during second and post quench scans, respectively. It seems that the, 50/50 and 75/25 (11.1 mole %) and 75/25 (7.9 mole %) blends contain at least two amorphous phases. However, since their T_g's do not correspond to that of pure PBT (293 K) or PC as reported in the literature[18], these "phases" may be interpreted as a mixture of two polymers[20].
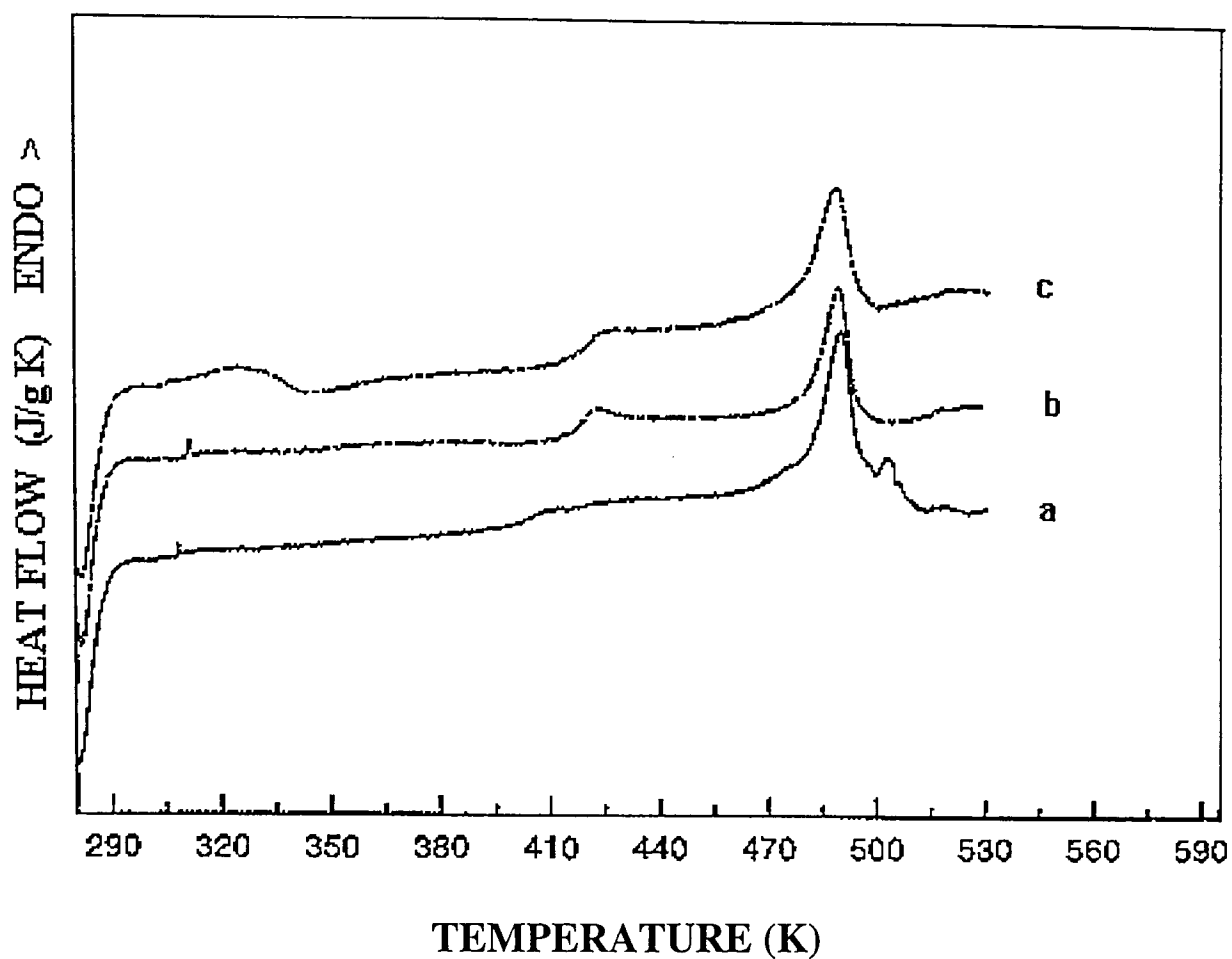
Figure 4.21 7.9 mole% SPBT/PC 25/75 a) first scan,

b) second scan, c) post quench.
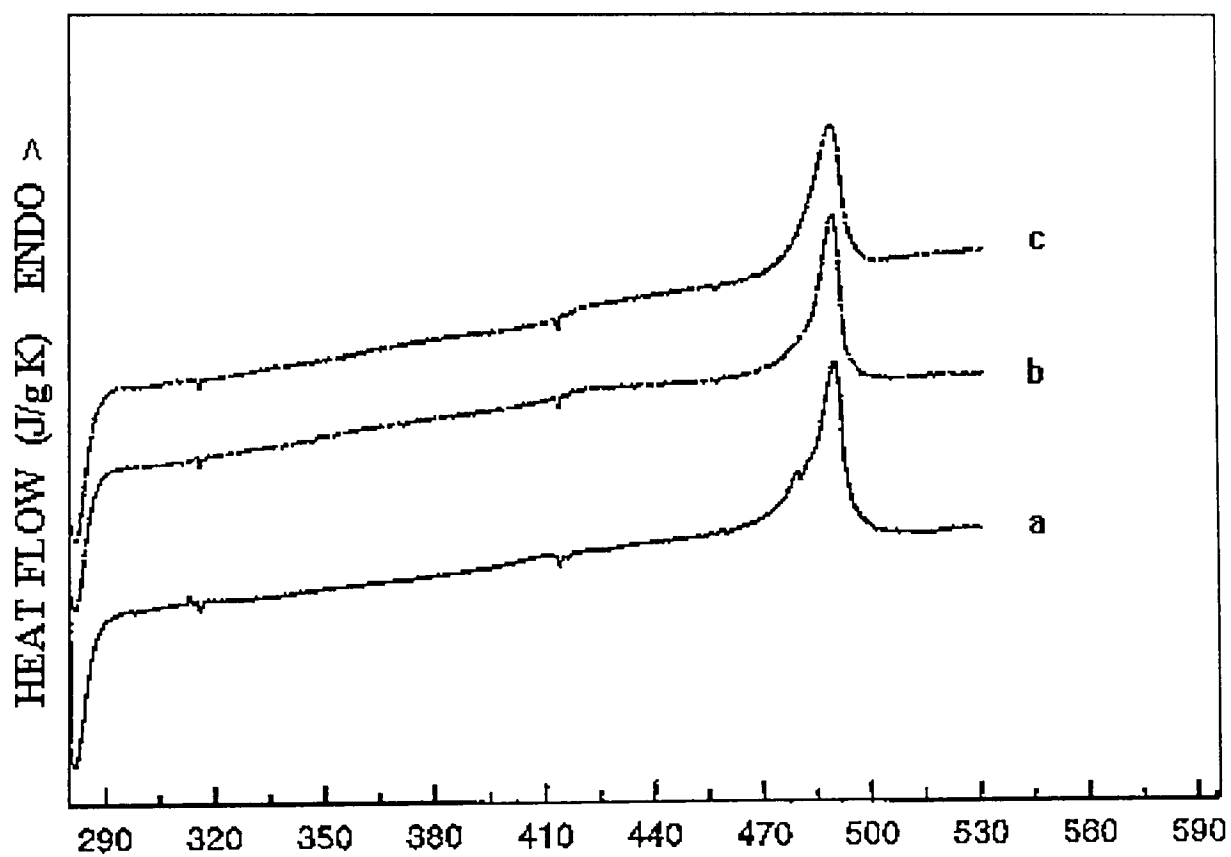
Figure 4.22 7.9 mole% SPBT/PC 50/50 a) first scan,

b) second scan, c) post quench.

Fox derived the following equation for the glass transition temperature of a two component amorphous polymer blend:

$$\frac{1}{T_g} = \frac{W_1}{T_{g_1}} + \frac{W_2}{T_{g_2}}$$ 4.4

where T_{g1} and T_{g2} are the glass transition temperatures of component 1 and 2, respectively. The quantities W_1 and W_2 are the weight fractions of component 1 and 2 in the miscible phase. In blends where one component is semi-crystalline the weight fractions (W_1 and W_2) refer to the amorphous phase. Using the data obtained from the DSC analysis on the degree of crystallinity of the SPBT/PC blends

TEMPERATURE (K)
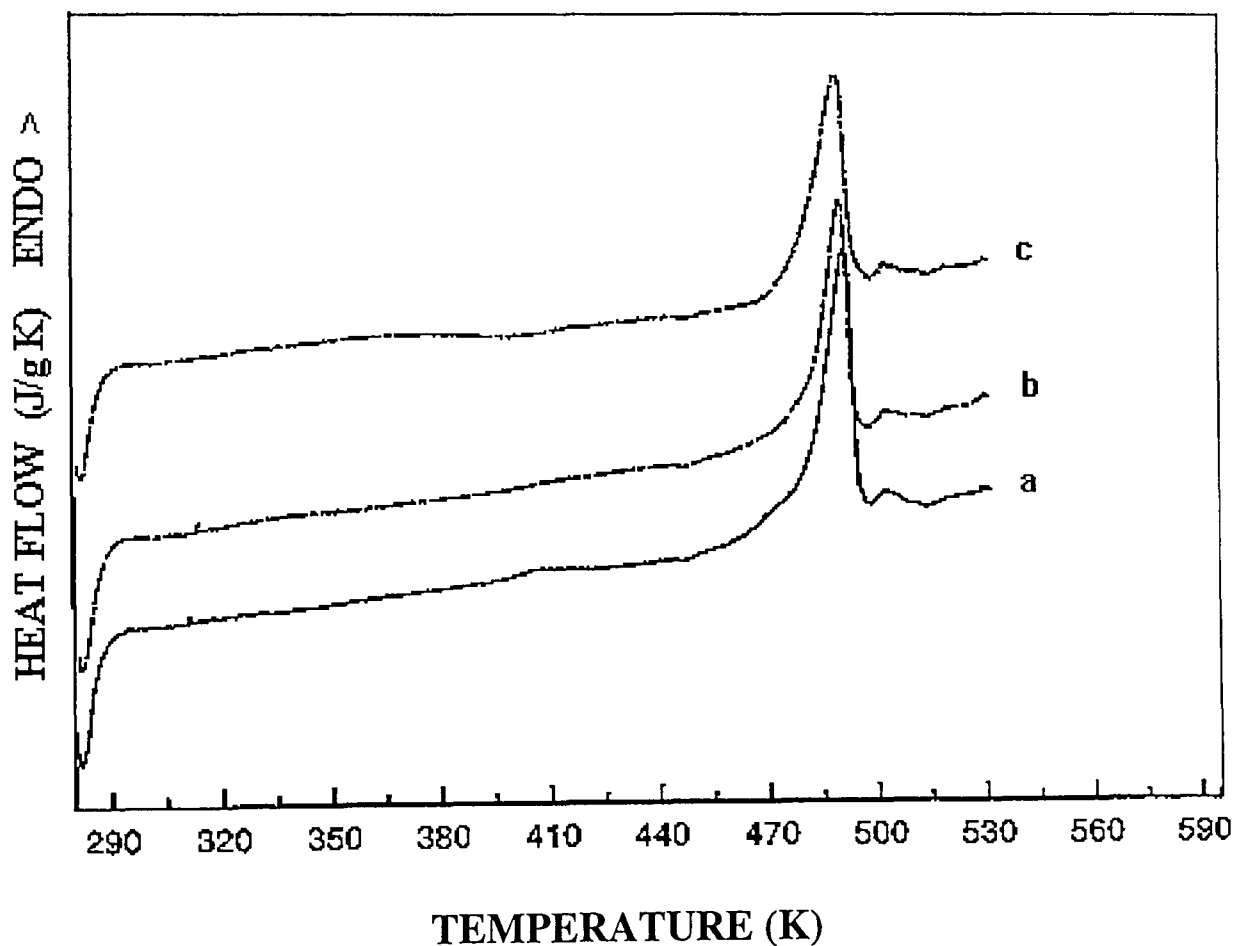
Figure 4.23 7.9 mole% SPBT/PC 75/25 a) first scan, b) second scan, c) post quench.
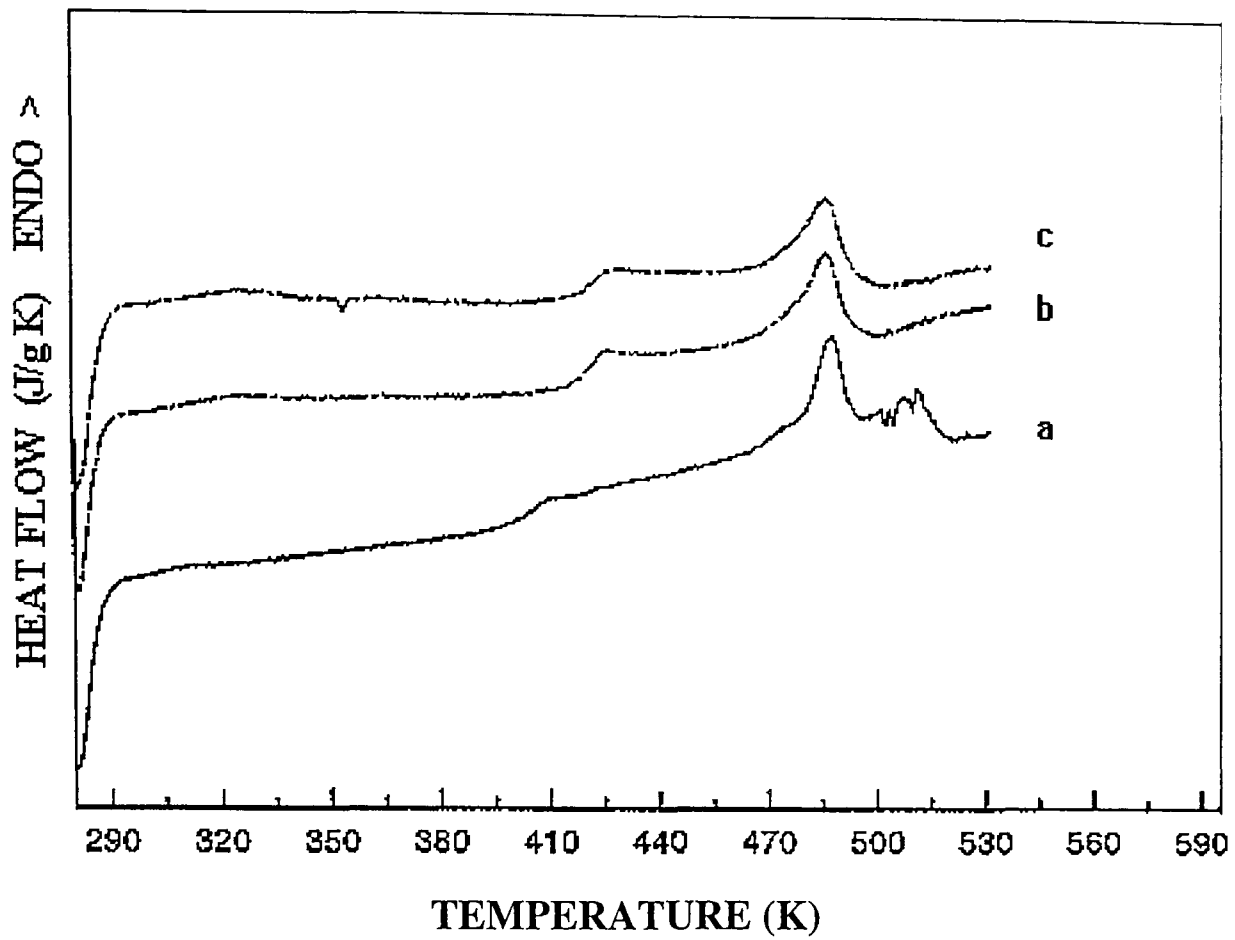
Figure 4.24 11.1 mole% SPBT/PC 25/75 a) first scan,

b) second scan, c) post quench.
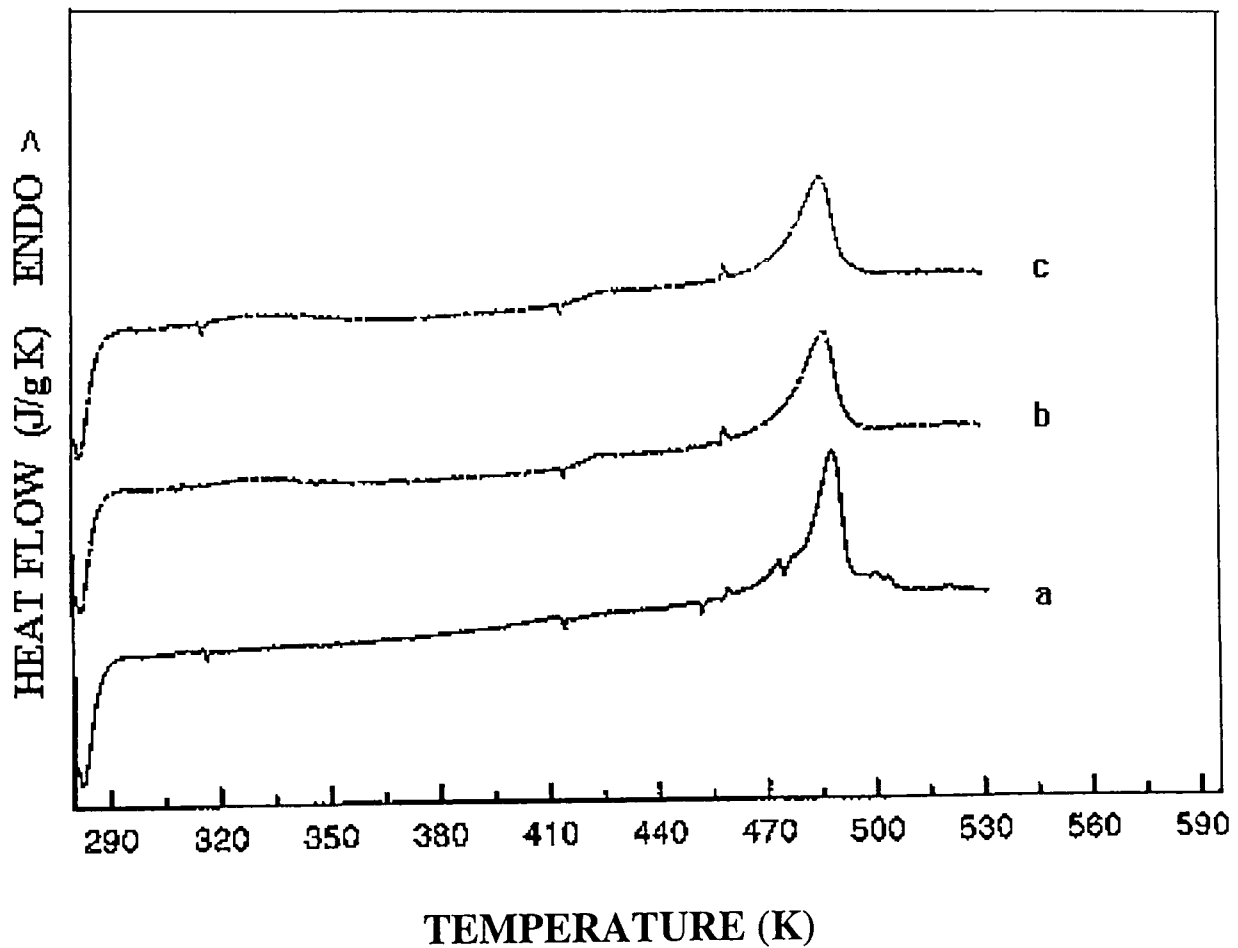

Figure 4.25. 11.1 mole% SPBT/PC 50/50 a) first scan,

b) second scan, c) post quench.
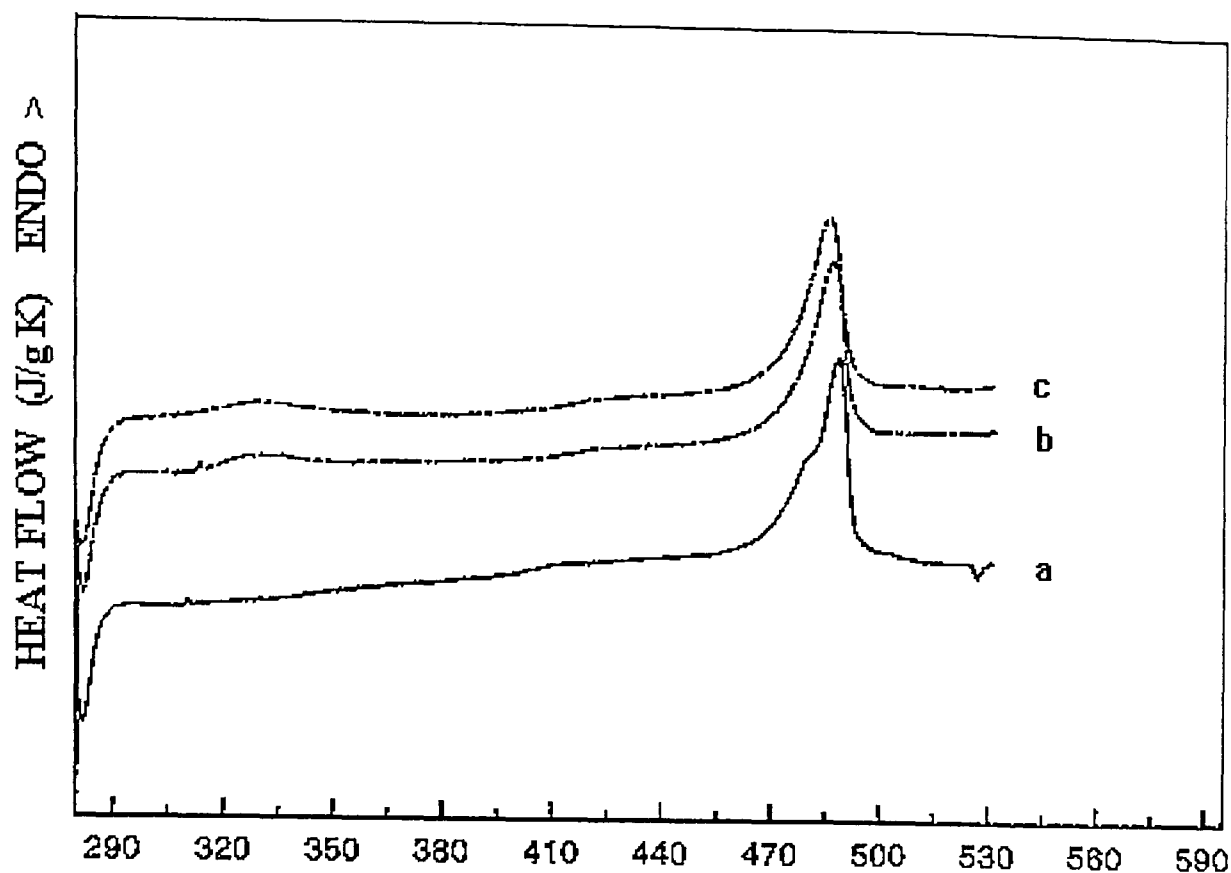
Figure 4.26. 11.1 mole% SPBT/PC 75/25 a) first scan,

b) second scan, c) post quench.

the mass fraction of amorphous SPBT has been calculated (to an estimated +/- 10% accuracy). The observed glass transitions, T_g, are shown in Figure 4.27 as a function of the mass fraction of amorphous SPBT for different levels of sulphonation. By comparison with the glass transition temperatures calculated from the Fox equation (also plotted in Figure 4.28), the data gives an indication of the degree of miscibility of the amorphous phases in the PBT/PC blends as determined by DSC.

Figure 4.29 illustrates the melting temperature depression with thermal cycling of the PBT/PC 0.0 mole % blends. A maximum depression in the melting point T_m of 13 K for 50/50 composition is evident following the cyclic heating. Depression in melting point was observed for 3.5, 7.9, and 11.1 mole % sulphonation level in the SPBT/PC blends of same compositions (Figures 4.29-4.32). It can be seen from Figure 4.29 and Figure 4.32 that the melting point T_m decreased from 496 K for 0.0 mole % 25/75 composition in the first scans to 485.5 K for 11.1 mole % 25/75 composition. This is yet another indication for an increased miscibility of 7.9 mole % and 11.1 mole % blends compared to those made with unsulphonated PBT.
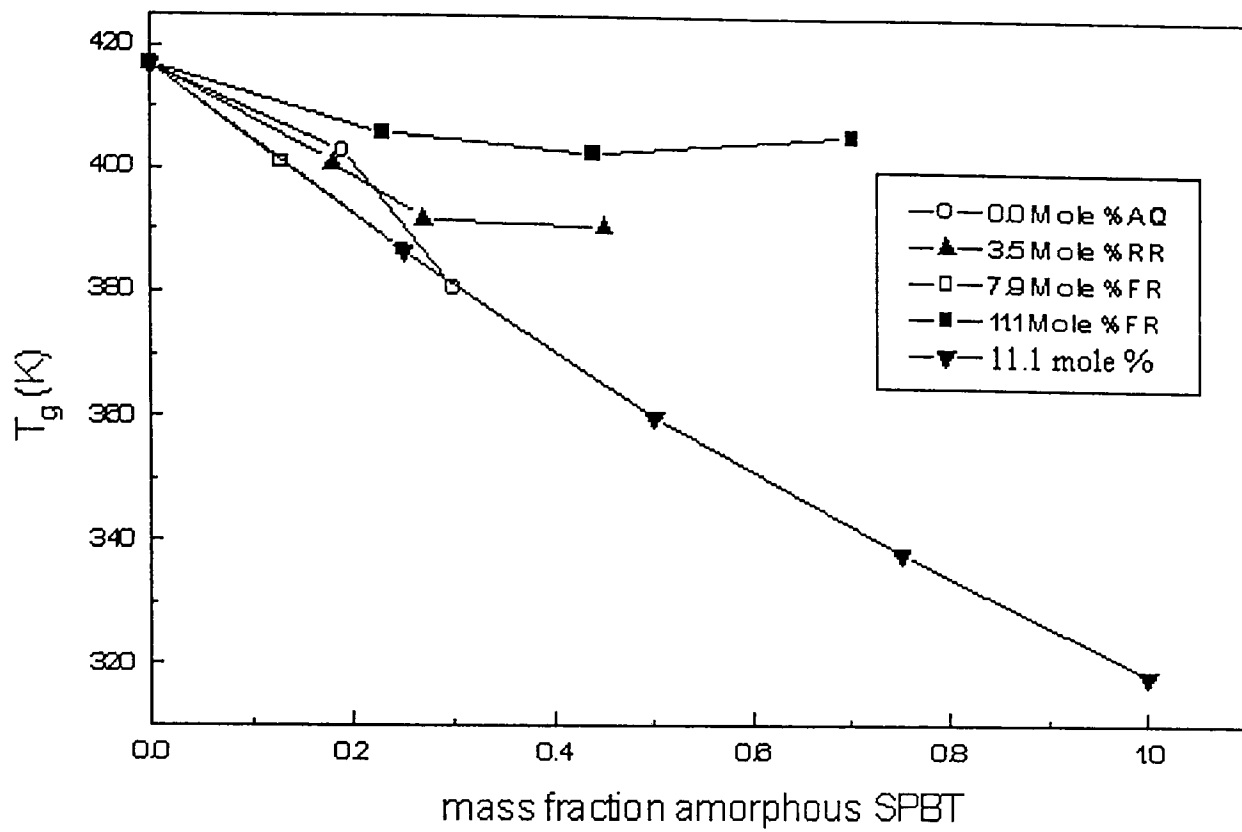
Figure 4.27 Glass transitions as a function of the mass fraction of amorphous SPBT for different levels of sulphonation.
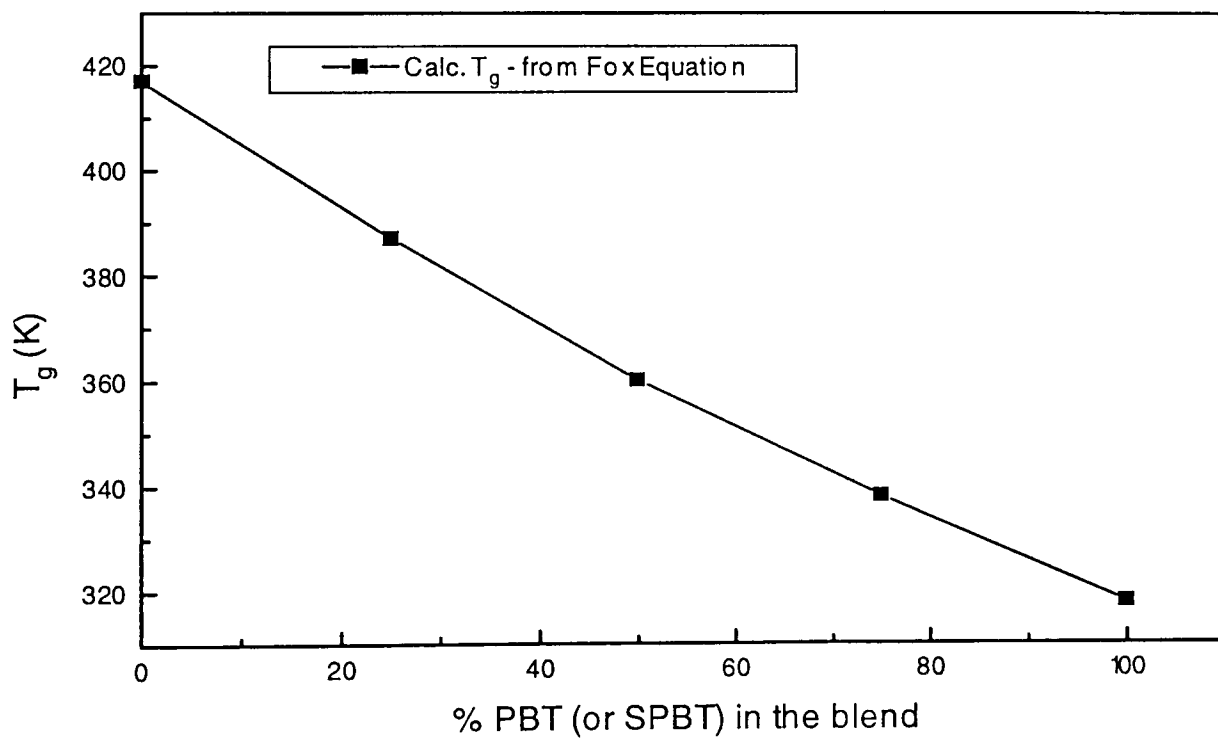
Figure 4.28 Glass transitions calculated from Fox equation versus % PBT in the blend.
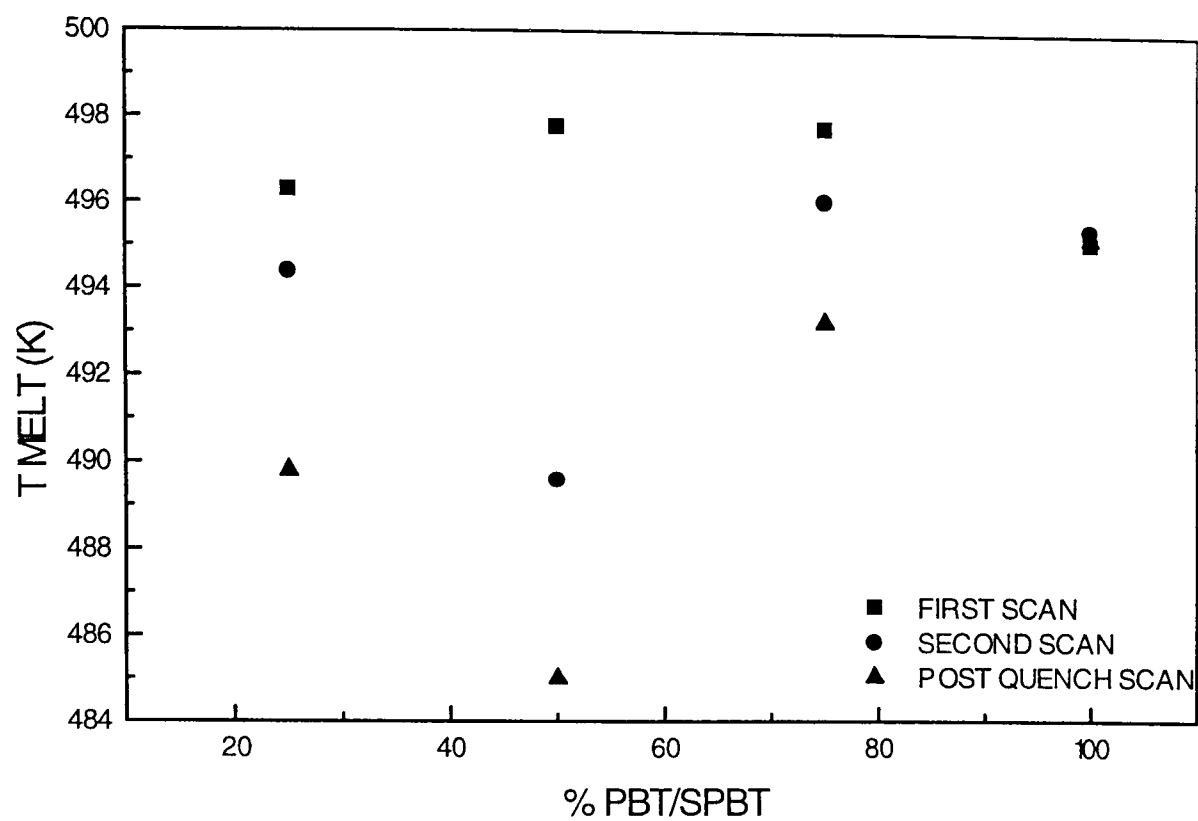
Figure 4.29 Melting point versus % PBT 0.0 mole %

during first, second and post quench.
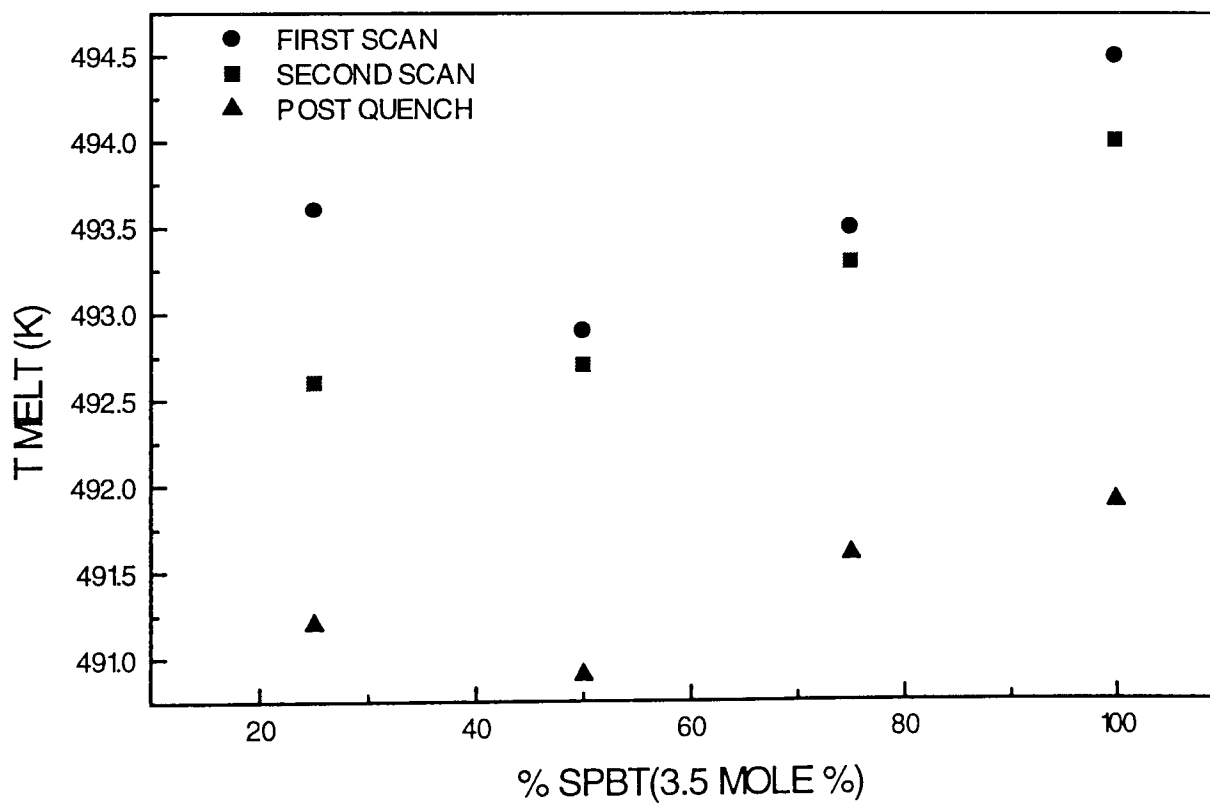
Figure 4.30 Melting point versus % SPBT 3.5 mole %

during first, second and post quench.
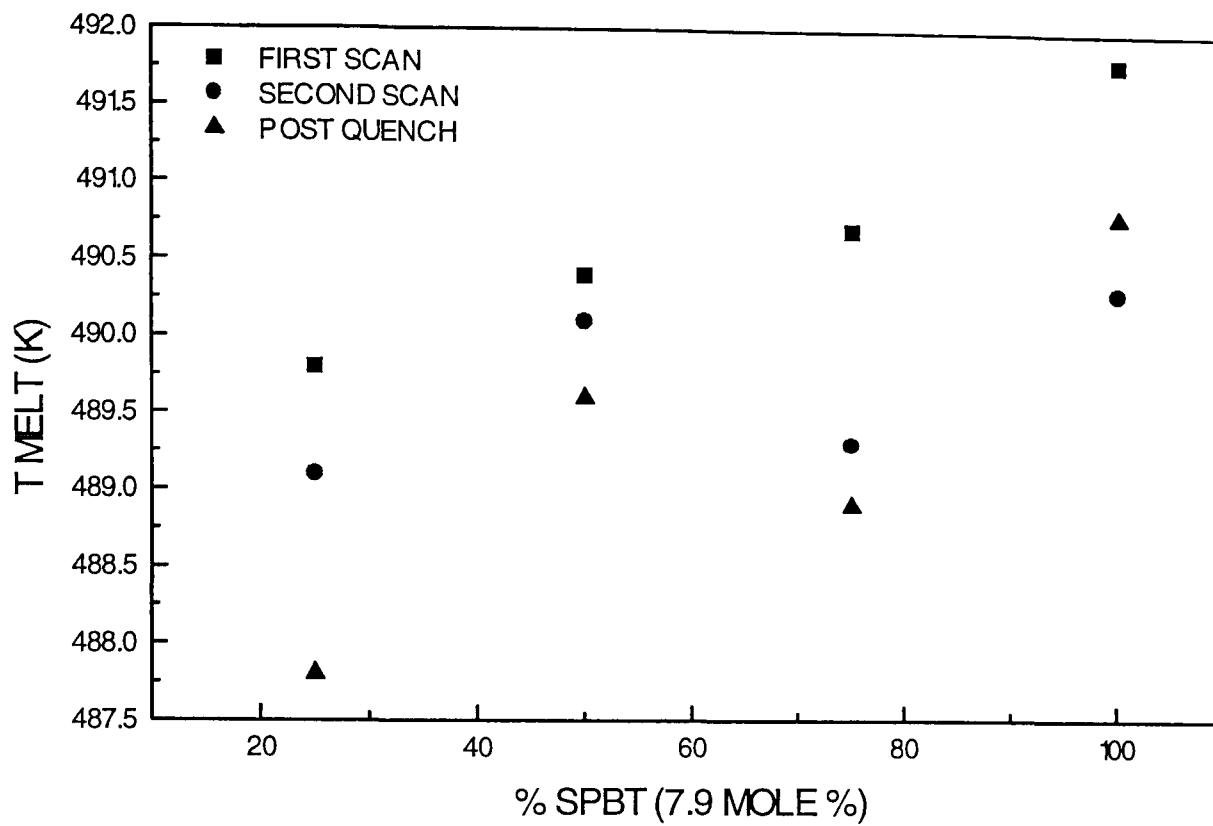
Figure 4.31 Melting point versus % SPBT 7.9 mole %

during first, second and post quench.
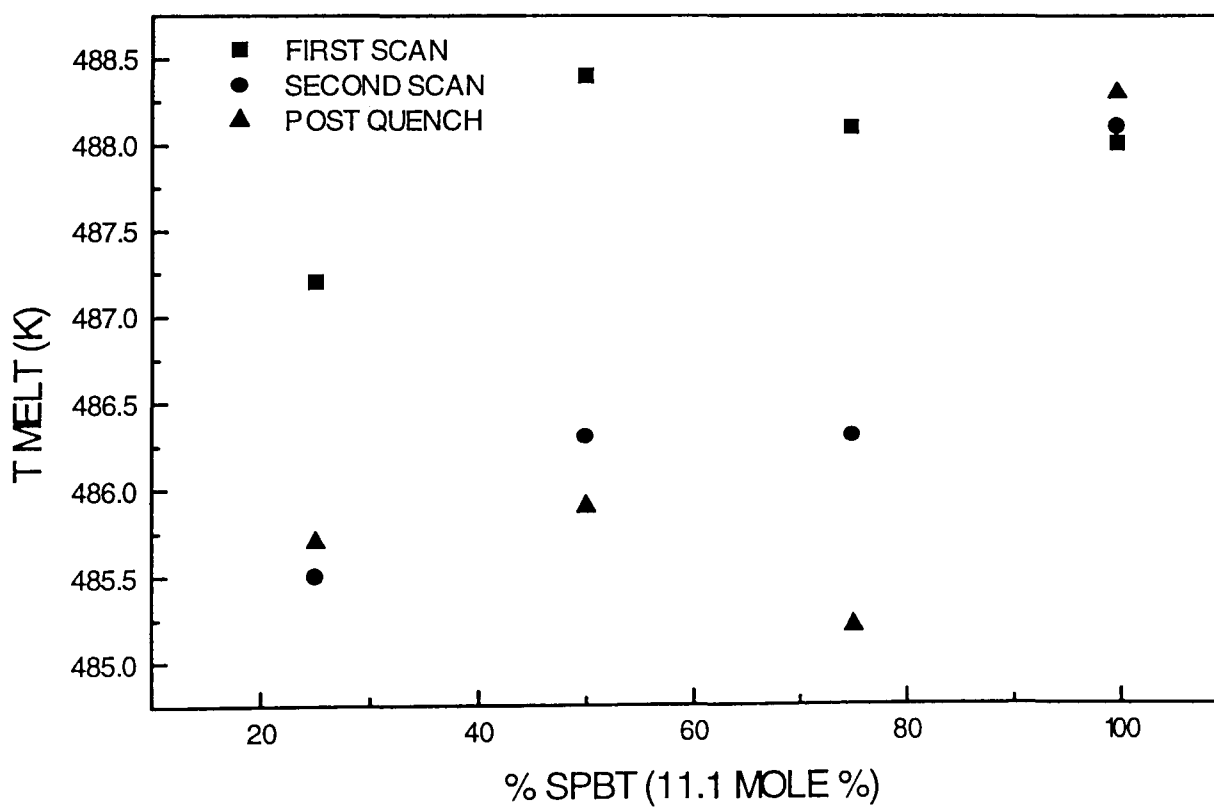
Figure 4.32 Melting point versus % SPBT 11.1 mole %

during first, second and post quench.

4.3 RESULTS AND DISCUSSION for PS AND PS-IONOMERS

4.3.1 Differential scanning calorimetry analysis (DSC)

For comparison DSC measurements were performed on model random ionomer, sulphonated polystyrene. DSC thermograms for PS, sulphonated PS, iso-PS and iso-sulphonated polystyrene (iso-SPS) samples (first scan and second scan) taken with baking were obtained. Results obtained for the samples the samples used in this study are presented in Table 4.7 and Table 4.8 during first and second scans, respectively. Figure 4.33 shows the DSC thermogram of iso-polystyrene (iso-PS) 0.0 mole % obtained during the first scan. Here multiple high temperature melting endothermic peaks can be seen.

TEMPERATURE (K)
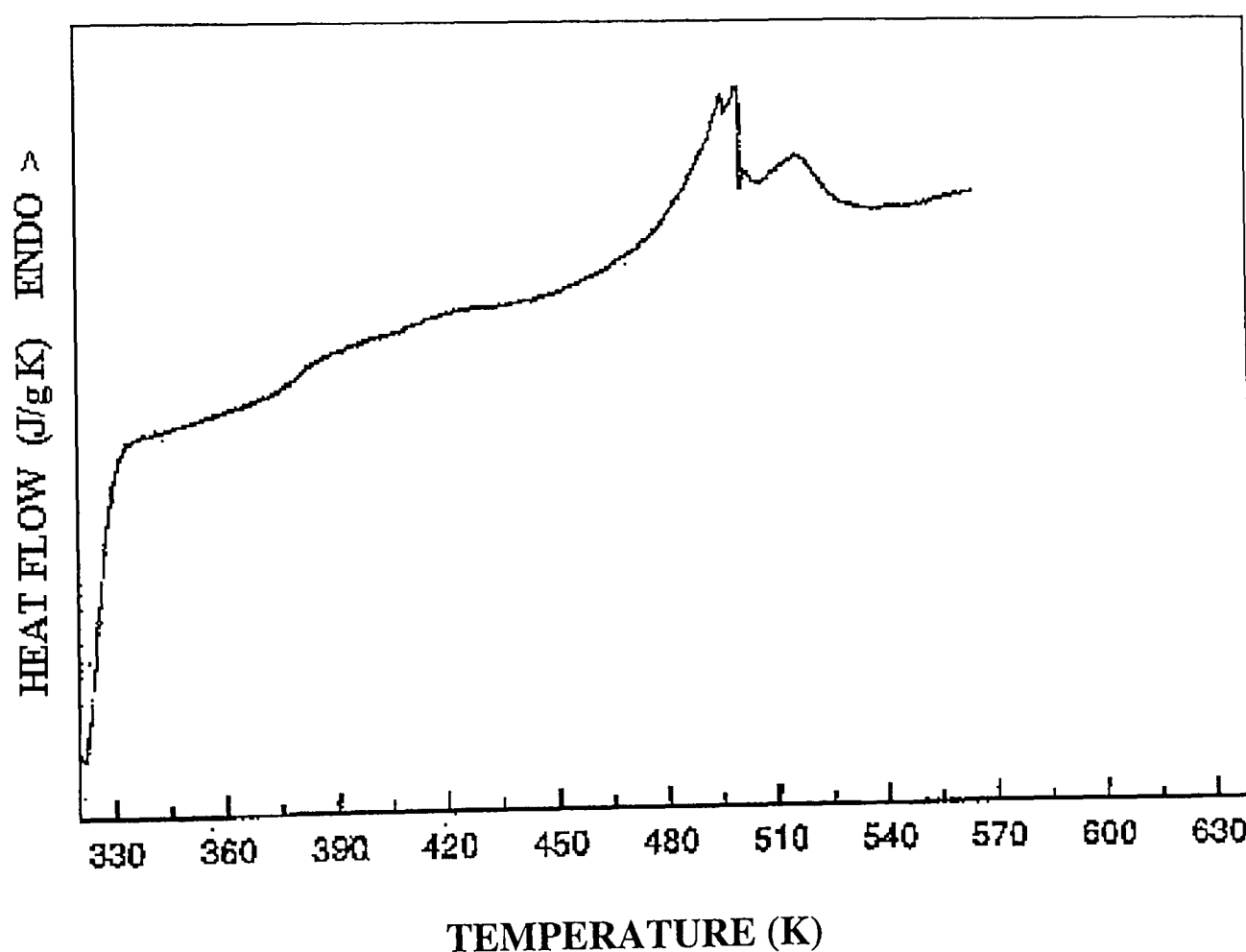
Figure 4.33   DSC thermogram of iso-PS 0.0 mole %
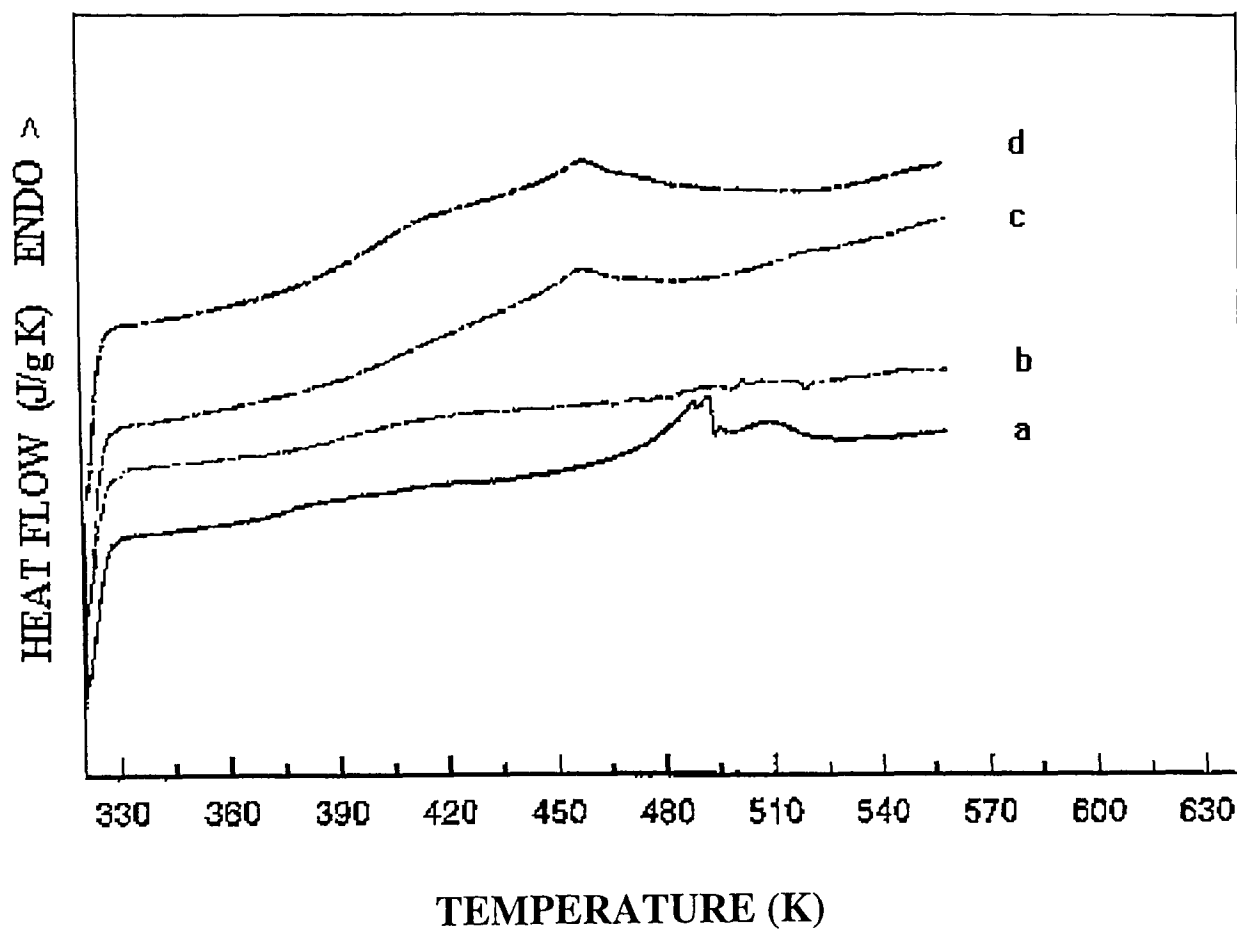
Figure 4.34 DSC thermogram of samples a) iso-PS 0.0 mole % b) iso-SPS
8.8 mole % c) iso-SPS 10.5 mole % d) iso-SPS 94.5 mole % (First scan).
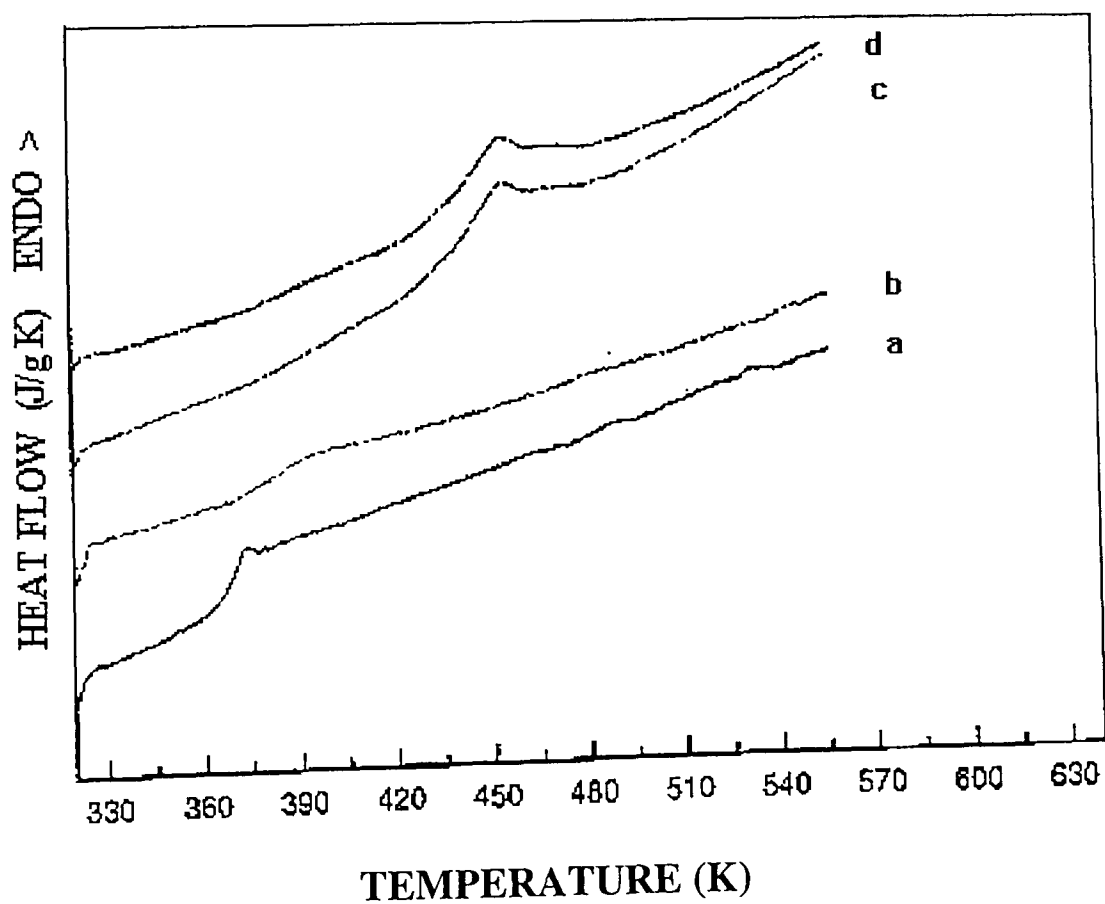
Figure 4.35 DSC thermogram of samples a) iso-PS 0.0 mole % b) iso-SPS
8.8 mole % c) iso-SPS 10.5 mole % d) iso-SPS 94.5 mole % (second scan).

Table (4.7)   DSC data for PS/SPS (first scan).

sample	mole %	glass transition T_g (K)	melting point T_m (K)	crystallinity %
iso-SPS	0.0	369	482	13
iso-SPS	8.8	406		-
iso-SPS	10.5	420		-
ios-SPS	94.5	453		-
SPS Chain deuterated		371		-
SPS Ring deuterated	6.3	385		-
SPS Ring deuterated		377		-
SPS	8.4	390		-

Table (4.8) DSC data for PS/SPS (second scan).

sample	mole %	glass transition T_g (K)
iso-SPS	0.0	365
iso-SPS	8.8	389
iso-SPS	10.5	438
iso-SPS	94.5	458
SPS (Chain deuterated)		378
SPS (Ring deuterated)	6.3	387
SPS Ring deuterated		379
SPS	8.4	392

Figure 4.33 shows a large melting peak at 493 K with a shoulder at 487 K followed by a small high temperature melting peak at 509 K. A T_g at 369 K was also observed. It is worth pointing out that these endothermic peaks appeared in the first scan but, vanished in the second scan (see Figure 4.35(a)). However, a T_g at 365 K, about 4 K lower than that observed in the first scan was noticed during the second scan. The appearance of endothermic melting peak in Figure 4.33 is related to the melting process of the partially crystalline material[21].

The DSC thermograms for sulphonated iso-polystyrene (iso-SPS) 8.8 mole % in first and second scans are given in Figures 4.34(b) and 4.35(b). A broad T_g at 406 K and no specific fusion peak could be traced in first scan.
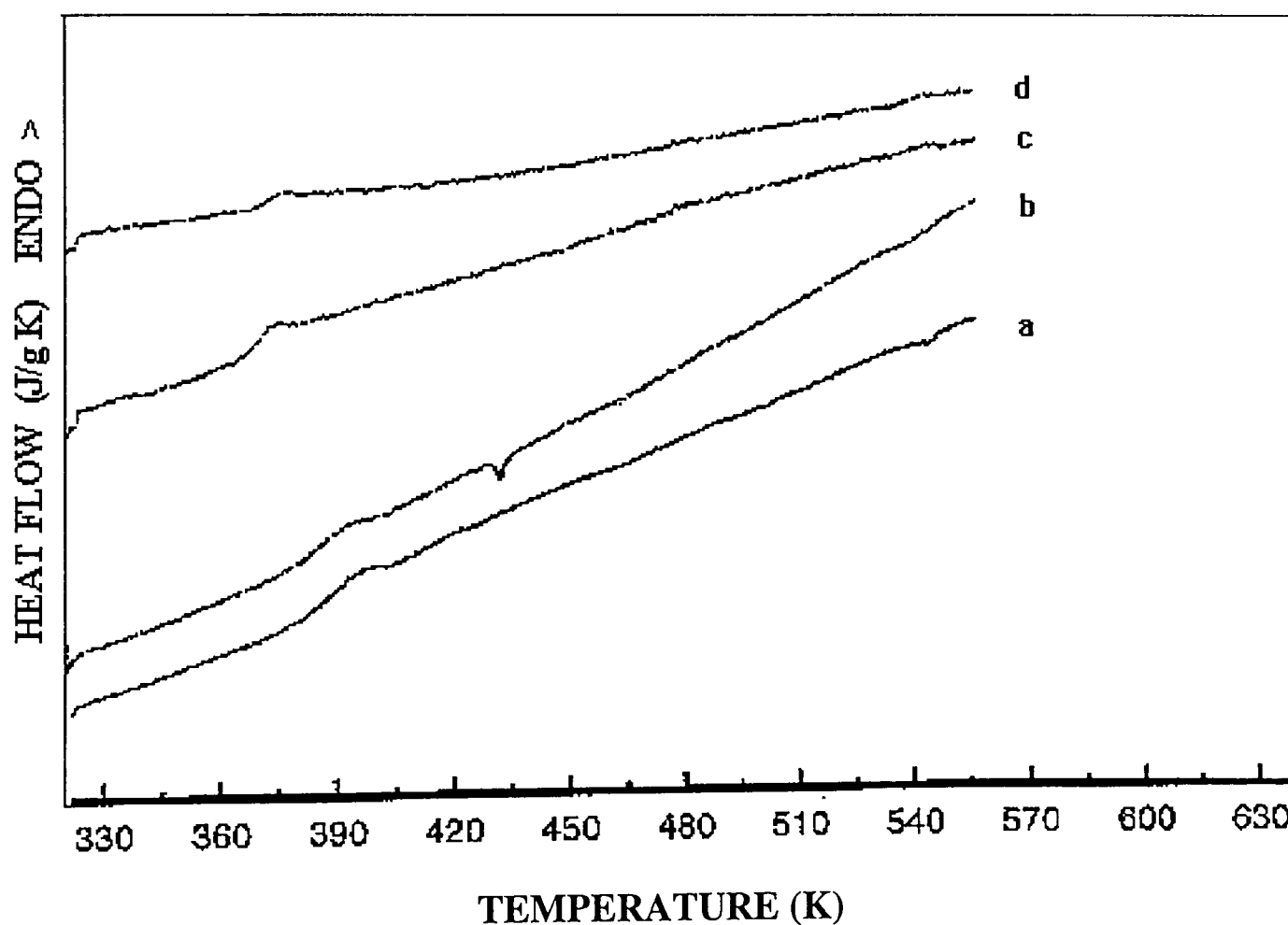
Figure 4.36 DSC thermogram of samples a) iso-SPS 8.4 mole % b) SPS R.DEU 6.3 mole % c) SPS R.DEU d) SPS C.DEU (First scan).
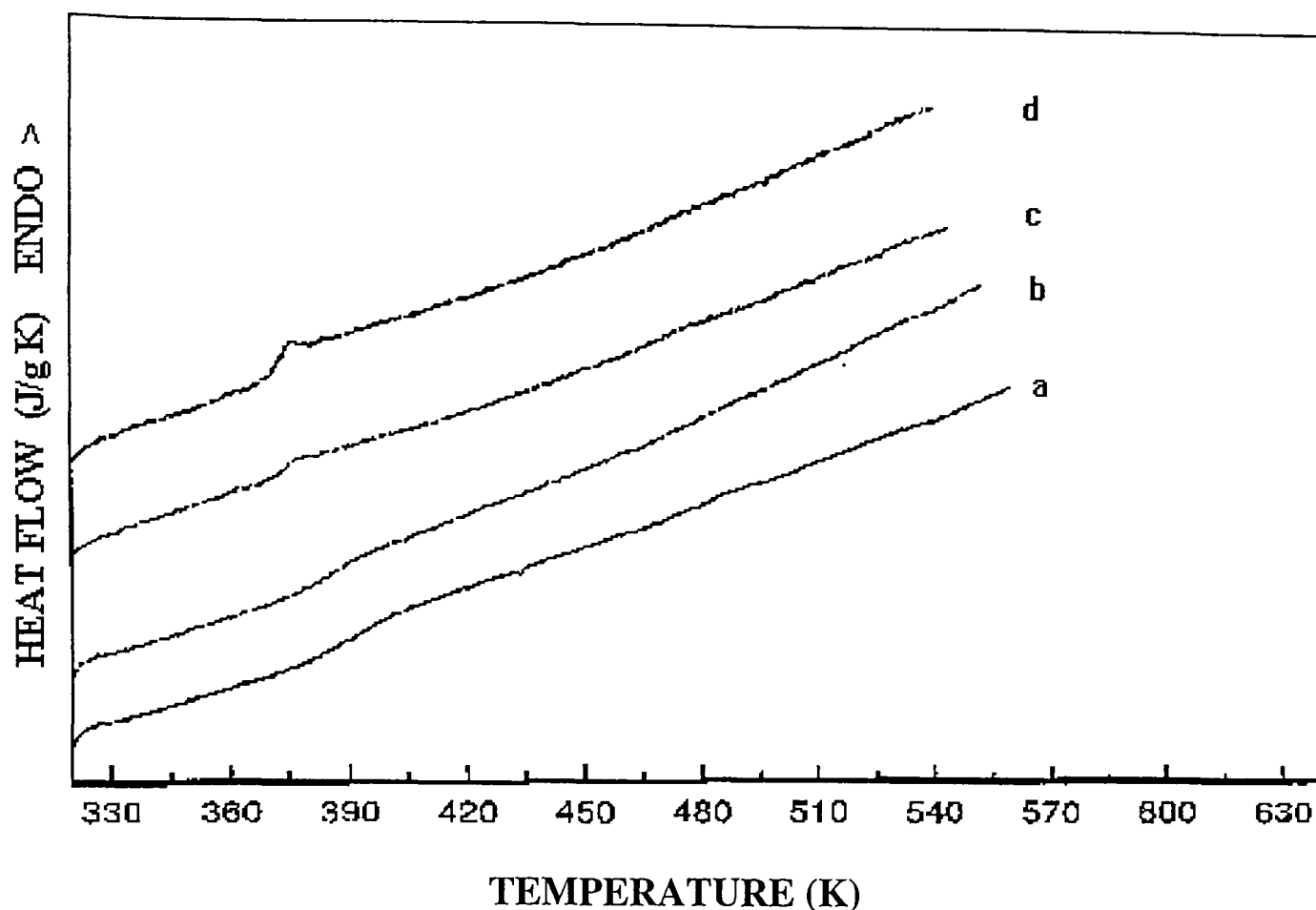
Figure 4.37 DSC thermogram of samples a) iso-SPS 8.4 mole % b) iso-SPS R.DEU 6.3 mole % c) SPS R.DEU d) SPS C.DEU (second scan).

DSC thermogram for iso-SPS 8.8 mole % is shown for the re-heating cycles in Figure 4.35(b). A T_g at 389 K is evident, a reduction in T_g of 7 K is noticed in the re-heating scan. Figure 4.34 (c) gives the T_g at 420 K for iso-SPS 10.5 mole % in first scan and a higher T_g at 438 K appeared in second scan as shown in Figure 4.35(c). There is a significant shift in the T_g position towards higher temperature by 18 K during the second scan (to an estimated +/- 5 % accuracy). From the DSC thermograms, it is evident that upon increase in the level of sulphonation a change in the state of material has been produced i.e., partial crystalline state to complete amorphous state[22].

Furthermore, a T_g at 458 K is shown in Figure 4.34(d) for sulphonated iso-polystyrene (iso-SPS) 94.5 mole % obtained during first scan. However, an increase of 5 K in T_g was evident in the second scan shown in Figure (4.35(d), compared with T_g obtained in First scan. No endothermic fusion peaks have been observed during these DSC scans for the iso-SPS samples.

The DSC thermogram for sulphonated polystyrene ring deuterated (SPS R.DEU) during the first scan is given in Figure 4.36(c). It shows a T_g occurs at 377 K. In second scan T_g was found at 379 K (Figure 4.37(c)). Sulphonated iso-polystyrene chain deuterated (SPS C.DEU) shows the same feature, a T_g at 371 K and 378 K in first and second scans, respectively. This is plotted in Figures 4.36(d) and 4.37(d). Another slight difference in T_g position at 390 K and 392 K is seen for SPS 8.4 mole % during first and second scans (Figures 4.36(a)), 4.37(a)). Figures 4.36(b) and 4.37(b) show the data of SPS R.DEU 6.3 mole %, with T_g points at 385 K and 387 K in the first and second scans, respectively. This data can be interpreted on the basis of the EHM model.

A significant rise in the T_g temperature upon increase of level of sulphonation is evident from the data Tables 4.7-8. This increase is attributed to ionic interactions occurring in the ionic domains which limit the mobility of the ionomer backbone. Therefore sulphonated polystyrene absorbed more thermal energy to execute the transition to glassy state compared to un-functionalised polystyrene.. In general, ionic associations would tend to be more effective at altering molecular motions as temperature is increased: system gains thermal energy to the point where the strength of associations begins to decrease and localised molecular motions become faster. Hence a change in the state of the polymer takes place i.e. from solid to a glassy one.

4.4 Thermo-gravimetry analysis (TGA)

4.4.1 PBT/SPBT (Powder samples)

Poly (butylene terephthalate) (PBT) and its ionomers have been studied by thermogravimetry (TG). This technique was used to investigate the thermal stabilities, and the influence of the amount of ionic content on the loss of weight in the PBT ionomers (powder samples) with 0.0, 3.5, 7.9, and 11.1 mole % level of sulphonation. Programmed heating conditions have been employed, using air and nitrogen atmospheres. Figures 4.38-4.41 show the residual wt. % of the sample with increasing temperature (runs were conducted at 20 K/min). The TG curves for PBT 0.0 mole %

in air and an inert atmosphere are shown in Figure 4.38(a-b). A three stage decomposition was observed for PBT 0.0 mole % in air, and a single stage decomposition is seen in nitrogen atmosphere. The decomposition zones are as follows: the first zone has between 350 K to 415 K which is characterised by a degradation of the large organic molecules formed in the preliminary stage (volatisation). In the second zone, in the range 430-490 K, reactions of dehydrogenation and thermal cracking take place.
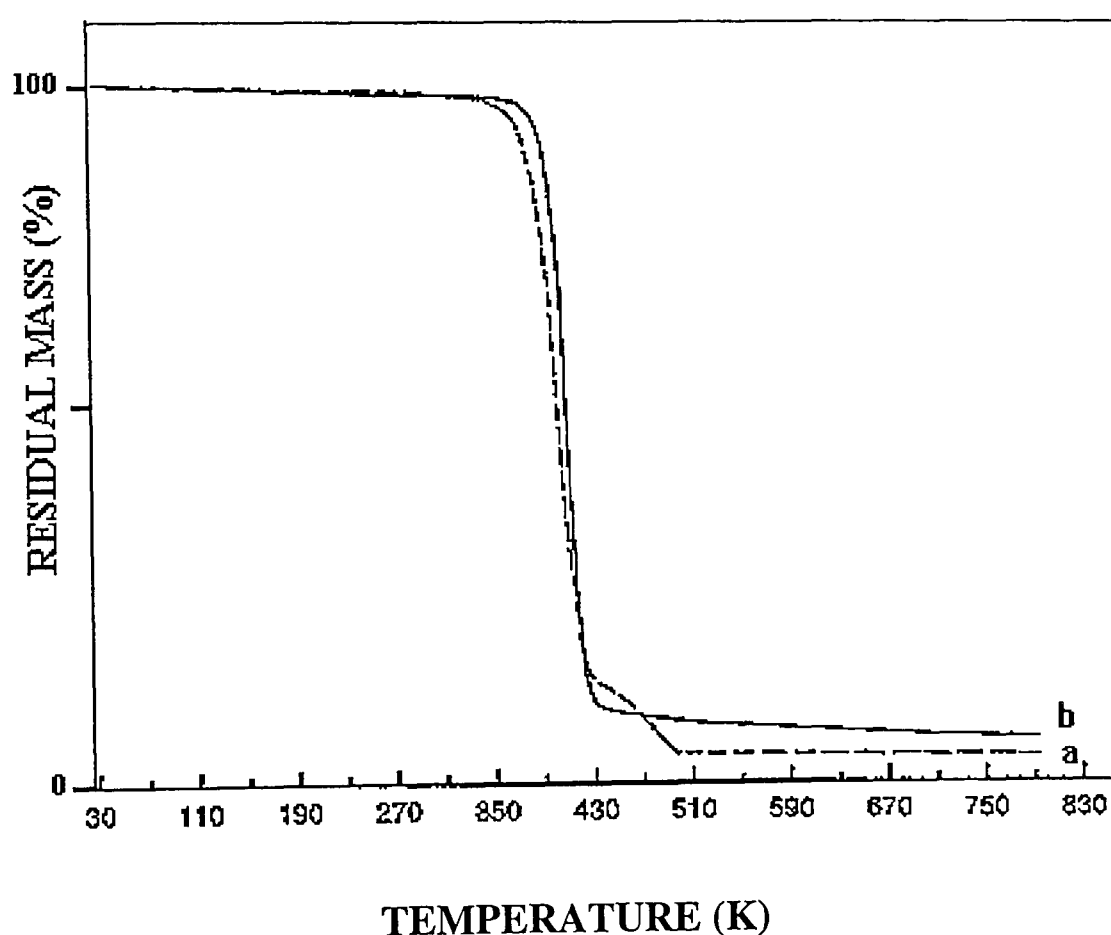
Figure 4.38 TGA curves of samples of PBT 0.0 mole %

a) in air b) in nitrogen atmosphere.
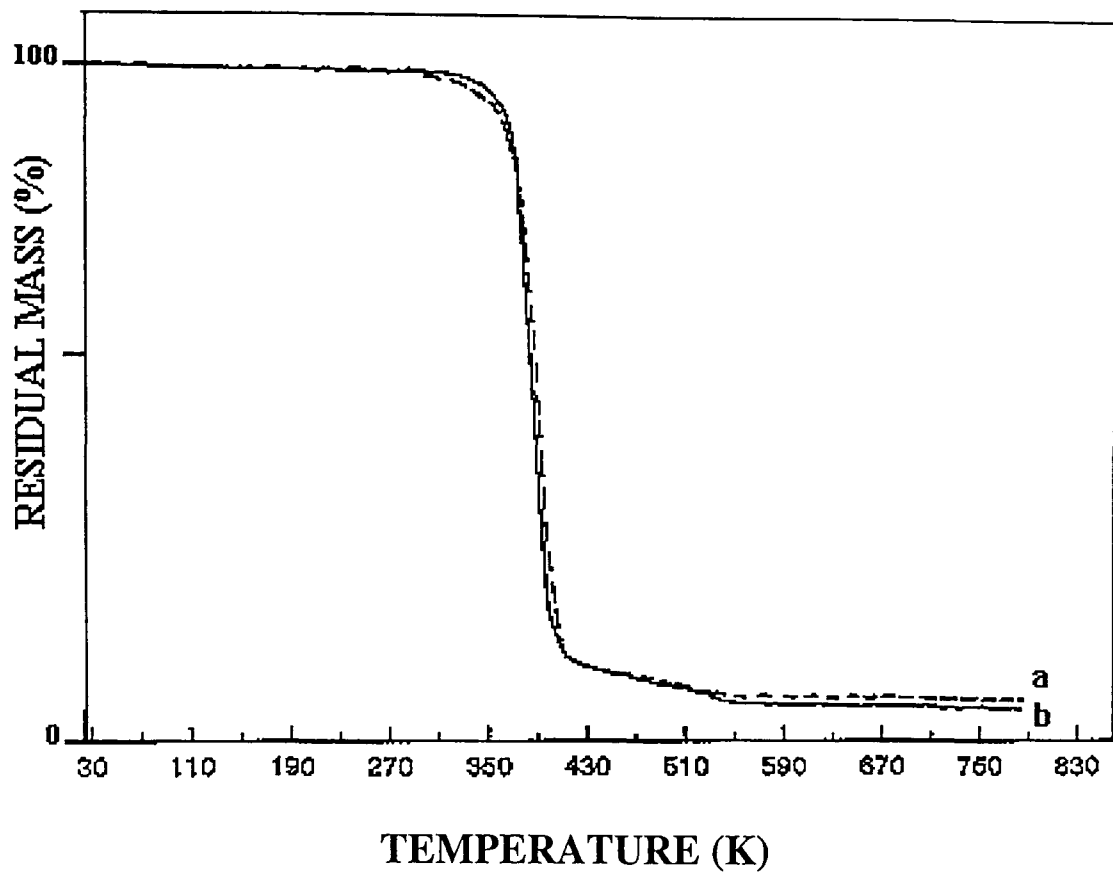
Figure 4.39 TGA curves of samples of SPBT 3.5 mole %

a) in air b) in nitrogen atmosphere.
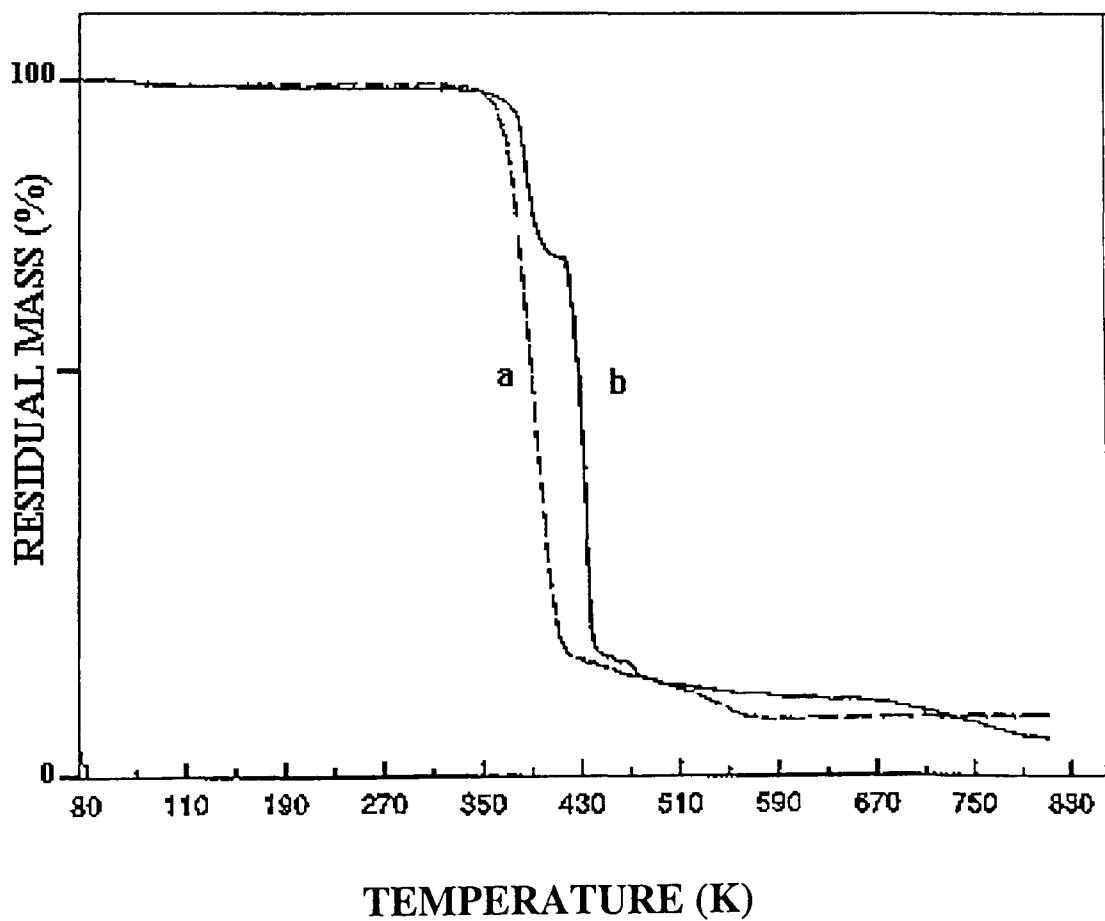
Figure 4.40 TGA curves of samples of SPBT 7.9 mole %

a) in air b) in nitrogen atmosphere.
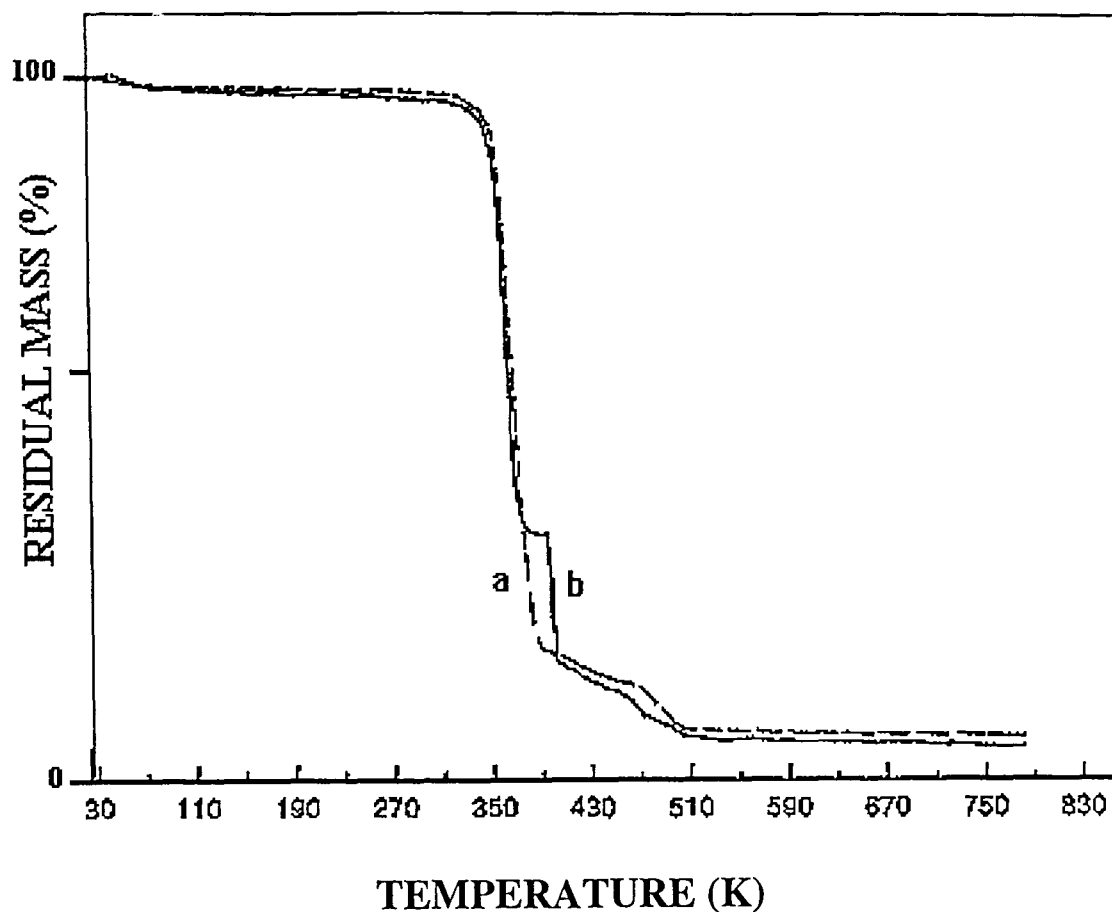
Figure 4.41 TGA curves of samples of SPBT 11.1 mole %

a) in air b) in nitrogen atmosphere.

In the third stage, at temperature higher than 500 K, fusion, disproportionation and gassification occur.[23]. In first stage, 88 % weight loss of PBT occurs which may be due to chain end cleavage[24]. The second stage, corresponding to 10 % weight loss, implies almost total decomposition. The amounts of residue at 773 K is less than 1 % weight loss (particularly for PBT in air atmosphere compared to 4.65 % weight loss in inert atmosphere).

Figure 4.39 (a-b) shows the rate of weight loss with increasing temperature for SPBT 3.5 mole %. Three stage decomposition is evident in the air and nitrogen atmospheres. The maximum rate of weight loss is in the range 360 - 400 K. No significant difference in the weight loss was observed for this sample in different atmospheres.

SPBT 7.9 mole % showed a four and three stage weight loss on heating in the nitrogen and air atmospheres respectively as shown in Figure 4.40 (a-b). In the first stage the

maximum weight loss of 86 % in the range of 350-410 K was noticed. However, a weight loss of 25 % in the range of 360 - 420 K was observed in the first stage, and the maximum weight loss of 61 % in the temperature range 425-440 K can be seen in Figure 4.40(b) for nitrogen atmosphere. About 3% weight loss occurred in the third stage (440 - 470 K) and the amount of residue at 800 K of 1.73 % is apparent in the final stage in nitrogen atmosphere.

SPBT 11.1 mole % sample showed a thermal degradation in four and three steps in nitrogen and air atmospheres, respectively, as shown in Figure 3.41. It is similar to SPBT 7.9 mole % as described above, however the maximum weight loss of 65 % took place in the range of 340 - 380 K for nitrogen atmosphere and 83 % in same temperature range for air atmosphere. In the second stage further loss of weight in the range of 360 - 390 K is apparent in Figure 4.41 (b). A further weight loss of 11 % occurred in the final stage. The residue weight at 780 K was found to be 3.15 %.

Taking the curves in Figures 4.38-41(a-b) into consideration, it can be seen that the apparent thermal stability of the polymers with regards to level of ionic content and atmospheric conditions increases with the increase of the level of sulphonation. At elevated temperatures (780 K) sulphonated PBT samples were found to be more thermally stable compared to unfunctionalised counter parts. Thermal stability of SPBT (four step degradation) with mole % > 5 is described to the specific interactions involved in the ionomers due to the presence of ionic interactions which originate either from a proton transfer or coulombic interactions between the sulphonic group and carbonyl group[25].

4.4   SUMMARY

i)   PBT/SPBT Powder Samples

Crystallinity

Powder samples having sulphonation levels of 0.0 to 5.0 mole % were found to have typically 40 % crystallinity which reduces to 30 % after melting and rapid cooling (40 degree per minute). The level of crystallinity was not significantly reduced on subsequently melting and quenching in liquid nitrogen. Samples with higher levels of sulphonation (from 5.0 to 11.1 mole %) were found to have 24 - 30 % crystallinity which was unchanged on melting and rapidly cooling. Crystallinity data obtained for the melt processed films (melt processed at least two years prior to these measurements) confirmed the above findings, having approximately 30 % crystallinity throughout the sulphonation range. There was no significant change following rapid cooling or quenching in liquid nitrogen from the melt. The reduction in the overall crystallinity is mainly due to the ionic effects in the bulk.

Melting behaviour

The appearance of multiple melting endotherms is well recorded[5] although their precise origin remains a subject of debate. Similar multiple endotherms have been observed in this work for SPBT samples with up to 5.0 mole % sulphonation whilst only a single melting melting peak is found for material with higher ion content. Previous work on SPBT identified the presence of two distinct crystallite forms in SPBT with less than 5.0 mole % sulphonation but only one form was observed in samples with higher levels of sulphonation. It is therefore believed that the appearance of the double melting peaks is due to the presence of these two distinct crystalline forms.

The melting temperature of SPBT, taken as the maximum of the main melting peak, is found to decrease with increasing sulphonation level. Data obtained has been analysed

in accordance with Flory's model for the melting of random copolymers. Strictly the theory is only valid under equilibrium conditions, however the our data fits the theory remarkably well indicating the random distribution of the sulphonate groups within the copolymer and that these groups are indeed excluded from the crystalline regions. Slight deviation from Flory's theoretical curve was taken to be indicative of polymer polymer interaction.

Glass transition temperature (T_g)

Due to the high degree of crystallinity in the samples and the close proximity of the glass transition temperature to room temperature, it has proved difficult to obtain accurate and unambiguous values of T_g. Glass transitions were not observed for the melt pressed samples where ageing effects resulted in sharp peaks at the transition, the peaks however making an unambiguous determination of T_g impossible. Overall data obtained indicated a glass transition at approximately 318 K with no defined trend in T_g with increasing sulphonation level.

ii)   PBT/PC blends

Crystallinity

The degree of crystallinity of the SPBT portion of the PBT/PC blends made from 0.0 and 3.5 mole % SPBT remains at the same level as found in the homopolymers (40% as prepared reducing to 30 % following melting). However, for blends produced from the highest level of sulphonation (11.1 mole %) the degree of crystallinity of the SPBT is reduced to 20 % in the SPBT/PC 50/50 blend, representing therefore only 10 % overall crystallinity in the sample. This may be due to the existence of well-separated microdomains, the so-called "cluster phase". This is a characteristic of many random ionomers, and therefore one could propose that the sulphonate groups are found in the amorohous phases of SPBT.

Glass transition temperature (T_g)

DSC investigations of the solution cast blends indicate that there may be a partial miscibility occurring in the amorphous phases, as indicated by a slight reduction in the glass transition temperature, T_g, of the polycarbonate portion. No such shift in T_g for the solution cast PC control sample was observed, thereby excluding the possibility of this due to an influence of a solvent. Glass transition temperatures calculated from the Fox equation also gives indication of the blends miscibility.

Melting behaviour

The melting temperature for the PBT/PC 0.0 mole % blends, shown a remarkable reduction of melt temperature on thermal cycling. The change in melting temperature ΔT_m peaked at 11.5 K at a blend composition of 50 %. It is ascribed to the low specific interactions and high molecular mobility compared to the funtionalised blends.

Defined multiple melting peaks were not observed for blends with level of sulphonation > 5 mole % due to the formation of crystallies of the same type. However there were asymmetries in the melting endotherms for 0.0 and 3.5 mole % SPBT/PC blends which are not easily interpreted an the basis of SAC data alone.

Miscibility

PBT/PC blends with sulphonation level less than 5.0 mole % were found not miscible due to high level of crystallinity of PBT. However, blends with sulphonation level greater than 5.0 mole % were found partially miscible. Furthermore, it was found by the DSC investigations that SPBT/PC 7.9 mole % 25/75 and 11.1 mole % 50/50 blends are the candidates for the best composition due to a greater degree of miscibility compared with other blend compositions and level of sulphonation.

References

1   J Kim, M E Nichols and R E R, *J. Polym. Sci, Polym. Phys*, **32** 887 (1994).

2   M Aubin and R E Prud'home, *Polym. Eng. and Sci*, **24** 5 (1984).

3   A Eisenberg, B Hird and R B Moore, *Macromoleculecules*, **23** 4098 (1990).

4   H K Yip and H L Willams, *J. Appl. Polym. Sci*, **20** 1209 (1976).

5   J T Yeh and J Runt, *J. Polym. Sci, Polym. Phys. Ed*, **27** 1543 (1989).

6   M E Nichols and R E Robertson, *J. Polym. Sci. Polym. Phys*, **30** 755 (1992).

7   S Y Hobbs and C F Pratt, *Polymer*, **16** 462 (1975).

8   R S Stein and A Misra, *J. Polym. Sci, Polymer Phys*, **18** 327 (1980).

9   H J Ludwing and P Eyer, *Polym. Eng. Sci*, **28** 143 (1988).

10   KR Gorda and DG Peiffer, *J. Polym. Sci. Polym. Phys*, **30** 281 (1992).

11   G Pompe, L Häubler and W. Winter, *J. Polym. Phys. Ed*, **34** 211 (1996).

12   R L Scott, *J. Chem. Phys*, **17** 279 (1949).

13   P J Flory, "Principles of Polymer Chemistry", Cornell Uuiversity Press, Ithaca, N Y (1953).

14   T Nishi and T T Wang, *Macromolecules*, **8** 909 (1975).

15   K T Kwei and H L Frisch, *Macromolecules*, **11** 1267 (1978).

16   D J Blundell, *Polymer*, **28** 2248 (1987).

17   J Devaux, P Gogard and J P Mercier, *Polym. Eng. Sci*, **22** 229 (1982).

18   P Sanchez, P M Remiro and J Nazabal, *J. Appl. Polym. Sci*, **50** 995 (1993).

19   K H Illers, *Coll. Polym. Sci*, **258** 117 (1980).

20   D C Wahrmund, D R Paul and J W Barlow, *J. Appl. Polym. Sci*, **22** 2155 (1978).

21   Gixue, Y Lu, G Shi and Q Dai, *Polymer*, **35** 892 (1994).

22   O Scharpf, B Gabrys and D G Peffier, "ILL report 90 SC26T, Part A and Part B" Institute Laue-Langevin, Grenobel France (1990).

23   C. N. Cascaval, D. Rosu, and I. Agherghinei, *Polym. Degradation and Stability*, **52** 253 (1996).

24   I Luderwald and N Grassise, *Appl. Sci*, **2** 77 (1977).

25   D E Bergbreiter and C R Martin, in "Functional Polymers", Plenum Press, London and New York (1991).

CHAPTER 5

<div align="right">

MATERIAL CHARACTERISATION

</div>

5.1   Introduction

This chapter describes with the characterisation of poly (butylene terephthalate) (PBT) and polystyrene (PS) ionomers and their unsulphonated counterparts. The results from the wide angle X-ray diffraction (WAXD) and optical microscopy studies on PBT/PC blends are presented. The results are discussed at each stage to put them in the context with the results of rest of the work and provide clarity in the following chapters.

The aim of these experiments was to investigate the effect of increasing ion content on the structure of PBT and PS ionomers on the disorder in the bulk material caused by the ions. The results of these studies were then used to interpret data obtained on SPBT/PC blends: an increasing disorder and loss of crystallinity due to sulphonation of SPBT resulted in a more transparent blend.

5.2   Wide angle X-ray diffraction

Poly (butylene terephthalate) (PBT) belongs to the triclinic system with space group $P\ 1\text{-}C_1^1$ or group $P\ \bar{1}\text{-}C_i^1$. Each unit cell contains one molecular chain; the cell dimensions are $a = 4.95$ Å, $b = 5.94$ Å, c (fibre axis) $= 11.59$ Å, $\alpha = 99.7°$, $\beta = 115.2°$, and $\gamma = 110.8°$[1].

Wide angle X-ray diffraction (WAXD) was used to study the morphology of PBT and sulphonated poly (butylene terephthalate) (SPBT). Hot pressed thin films of ~ 0.5 mm thickness and powder samples (with ion content level (0.0 to 13.5 mole %)) have been investigated. The peak positions were indexed and compared using peak programme for generation of unique reflection set written by M. J. Cooper. Samples used for these

measurements are given in Table 5.1.

Table 5.1 PBT, SPBT (hot pressed film (F) & powder (P)), and PS samples.

SAMPLE	% ionic content	SAMPLE	% ionic content
PBT (P)	0.0	atactic PS	0.0
PBT(F)	0.0	isotactic PS	0.0
PBT (P)	3.5	syndiotactic PS	0.0
PBT(F)	4.9	sulphonated PS chain-deuterated	
PBT (P)	7.9	sulphonated isotactic PS ring deuterated	6.3
PBT(F)	8.4	sulphonated isotactic PS	8.4
PBT (P)	11.1	isotactic PS	8.8
PBT(F)	13.5	sulphonated isotactic PS	10.5
		fully sulphonated isotactic PS	95.0

5.2.1 i) Diffraction patterns from PBT/SPBT film samples

The wide angle X-ray diffraction profiles taken at atmospheric pressure for the PBT and SPBT film samples are shown in Figures 5.1-5.4(a) for angles 2θ between $7°-50°$. Figures

5.4 and 5.8 present the X-ray diffractograms of all the PBT/SPBT film and powder samples respectively, with origins of the scattering curves shifted vertically for clarity. Bragg's equation $2dsine\theta = n\lambda$, was used to analyse WAXD data .
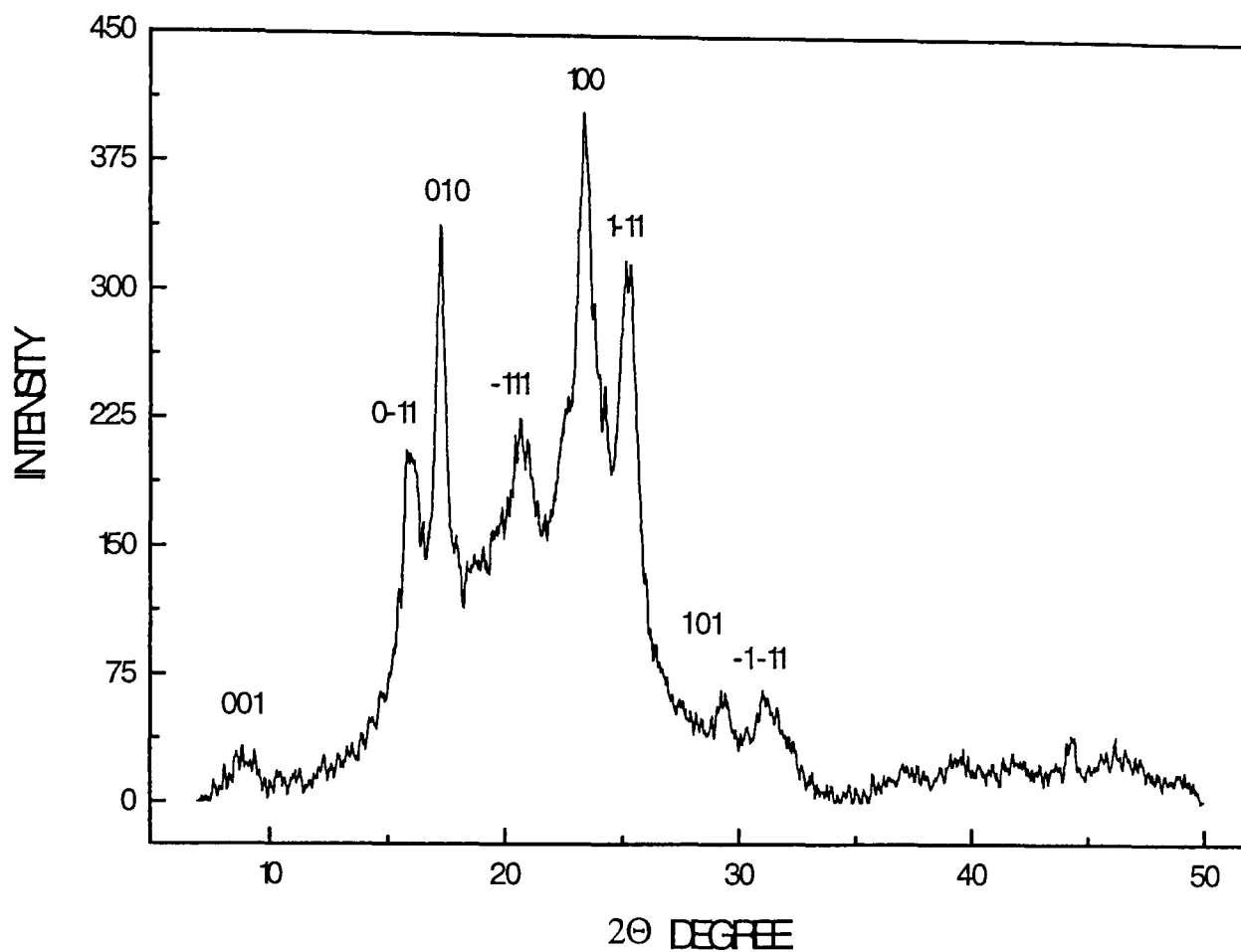
Figure 5.1 Wide angle X-ray scattering profile of PBT 0.0 mole %.

Figure 5.1 shows the reflection WAXD pattern of un-sulphonated PBT. Three main peaks, (010), (100), and (1-11) are visible. In addition, there are two broad, medium intensity, peaks (0-11) at 15.88° (5.58 Å) and (-111) at 20.69° (4.29 Å). The weak intensity, low order halo (001) is at 2θ of 8.78° corresponding to 10.06 Å), however, higher order halos (101) at 29.30° (3.04 Å) and (-1-11) appear at 31.02° (2.88 Å). In Table 5.2 2θ angle, d-spacing, relative intensity and hkl values describing the spectrum of PBT are listed. The sharp diffraction peak (010) at 17.25° (2θ) has a d-spacing of 5.14 Å which corresponding to the projected length of the crystal unit ordered along the chain axis. However, this

value is smaller than the X-ray diffraction value for crystalline PBT of b = 5.94 Å determined by Yokouchi et al [1]. This can be attributed to the difference in crystallinity of PBT used in this study was not grown as crystal.

Table 5.2 Peak positions (as Equivalent Bragg Spacings d) for PBT 0.0 mole %.

peak number	2-theta angle 2Θ	d-spacing Å	Relative Intensity	hkl
1	8.78	10.06	5	(001)
2	15.88	5.58	50	(0-11)
3	17.25	5.14	83	(010)
4	20.69	4.29	54	(-111)
5	23.34	3.81	100	(100)
6	25.25	3.52	75	(1-11)
7	29.30	3.04	14	(101)
8	31.02	2.88	15	(-1-11)

For the SPBT 4.9 mole % film, the WAXD profile is shown in Figure 5.2. A number of relatively sharp reflections can be observed indicating partial ordering in the material. The reflections are tabulated in Table 5.3. The (100), (010), and (1-11) peaks are apparently the same, within experimental error, as those of the parent polymer. The broadening of the spectrum of SPBT 4.9 mole % compared to unfunctionalized PBT is not observed. The maximum crystallinity for this material is observed for a 3.5 mole % of sulphonation, as seen from DSC results (Chapter 4).

Figure 5.3 shows the spectrum of a SPBT 8.4 mole % film and results are presented in Table 5.4. Two major effects are observed in this pattern: broadening of the peaks at

(0-11), (010), (-111), (100), and disappearance of the (001), (1-11), (101) and (-1-11) peaks. Instead, a broad feature appears at (-103) position. Such a broadening is indicative of a general destruction of crystalline order[2-3]. This destruction can be caused by a loss of either intra or inter-molecular ordering. Intra-molecular ordering takes place when monomers of a polymer molecule are oriented, and in the case of inter-molecule ordering orientation between the chains takes place. Because the scattering patterns contains tens of both intra and inter-molecular origin, it is impossible to distinguish between them a position without detailed investigation on oriented samples. Furthermore, the peak at (001) disappeared, which could be due to loss of crystallinity and ordering in the polymer caused by increasing number of ionic groups. It can be seen from Table 5.2, 5.3, 5.4, and 5.5 that the maximum relative intensity from the (100) plane remains unchanged upon sulphonation for all the SPBT films compared with unfunctionalised PBT. It is due to the assembly of the phenyl groups (see Figure 5.9) which are aligned in parallel at the corners of the unit cell[1].
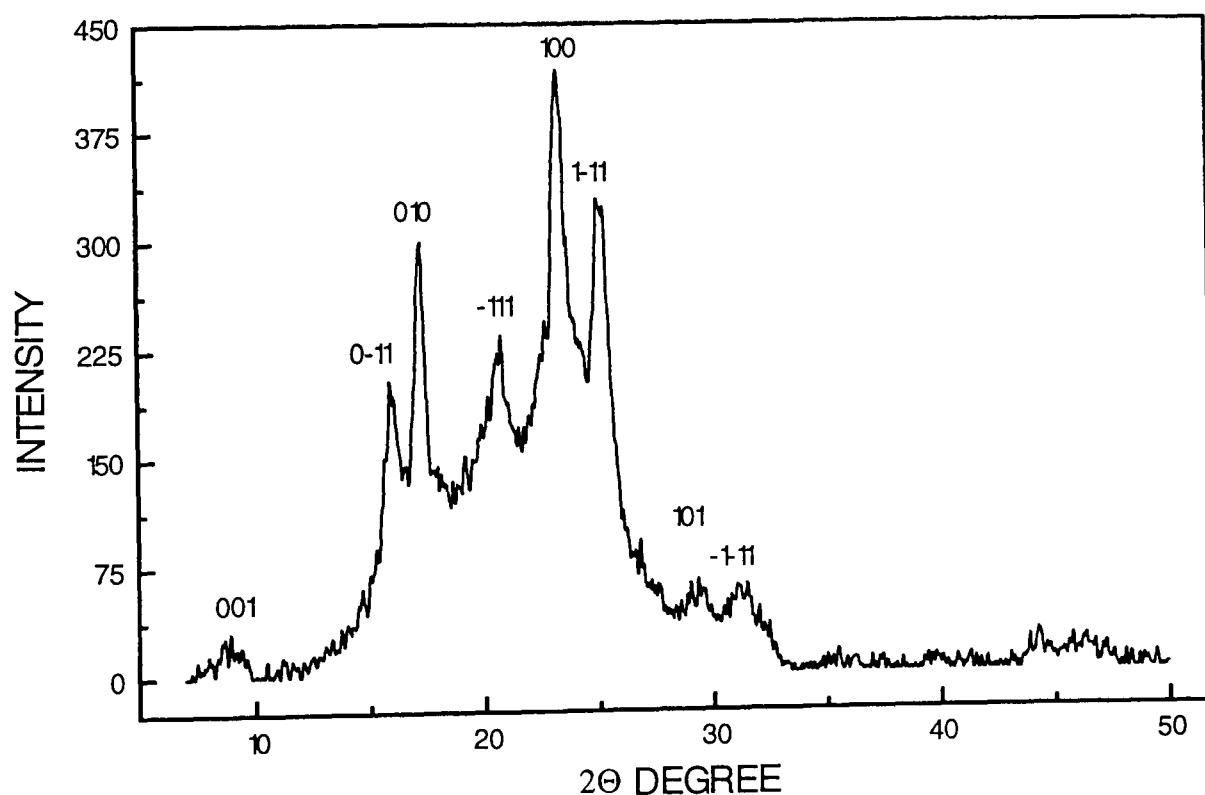

Figure 5.2 Wide angle X-ray scattering profile of SPBT 4.9 mole %.

That the scattering pattern becomes more diffuse as the sulphonate content increases (Figure 5.4(a)) may be due to a decrease of short range order caused by sulphonation, as shown for PS by Gabrys et al[4]. The broadening of diffraction pattern indicates decreasing crystallinity when ionic content becomes more than 5 mole %. This phenomenon is attributed to a decreasing rate of crystallisation which results less perfect crystals formed in the material due to specific ionic interactions and contribution of hydrogen bonding[5-6].

The diffraction pattern changes significantly with increasing degree of sulphonation and only one broad peak is observed at the highest sulphonate content (13.5 mole %). The diffraction patterns for these samples are collected in Figure 5.4. The absence of WAXD crystalline reflections confirms that high levels of functionality prevent the formation of crystallites in the initially easily crystallisable PBT. However there are still traces of crystallinity present in the ionomer samples as found by DSC (Capter 4). The reduction in the crystallinity can be explained due to the introduction of comonomer into a crystallisable polymer chain. Since same phenyl rings now contain bulky $Na^+SO_3^-$ group.

As a result, the presence of ionic groups on an otherwise molecularly symmetric backbone that favours crystallisation will generally lead to a reduction in the rate of crystallisation. Furthermore, the retardation of crystalline kinetics, the introduction of imperfections in the polymer chain, and the greater energy required to align the polymer chains, will tend to reduce the overall level of crystallinity in a functionalised PBT when compared to unsulphonated PBT[7].

These X-ray study results that are in general agreement with those quoted in the literature for other ionomer systems [4,8-10]. In order to describe data more quantitatively interlamellar distance t was estimated (to an estimated +/-5% accuracy) from WAXD patterns using the Scherrer relationship [11].

$$t = \frac{K\lambda}{FWHM\cos\theta}$$ 5.1

Where λ is the wavelength of the x-ray radiation source, K is a constant, assumed to be equal to units, and $FWHM$ is the full width at half maximum of the X-ray reflection peak. Where possible, peak widths were estimated from the diffraction pattern, lamellar sizes "seen" in different directions of the lattice estimated, and results summarised in Table 5.6. Inspection of Table 5.6 demonstrates that the inter-lamellar distance increases upon sulphonation compared with PBT 0.0 mole % which is surprising. Figure 5.10, illustrates the variation of the inter-lamellar size t with change in mole % of ion content for (hkl) values of (100). It also follows from Table 5.6. that t increases slightly for reflections (100), and becomes very large for 13.5 mole %. However this last value has to be treated with cation. No systematic trend is observed for other reflections.

Table 5.3 Peak positions (as Equivalent Bragg Spacings d) for SPBT 4.9 mole %

peak number	2-theta angle 2Θ	d-spacing $\mathring{A}$	relative intensity	hkl
1	8.93	9.900	7	001
2	15.93	5.56	49	0-11
3	17.31	5.12	72	010
4	20.80	4.27	56	-111
5	23.38	3.80	100	100
6	25.10	3.54	79	1-11
7	26.84	3.32	21	101
8	29.09	3.06	13	-1-11
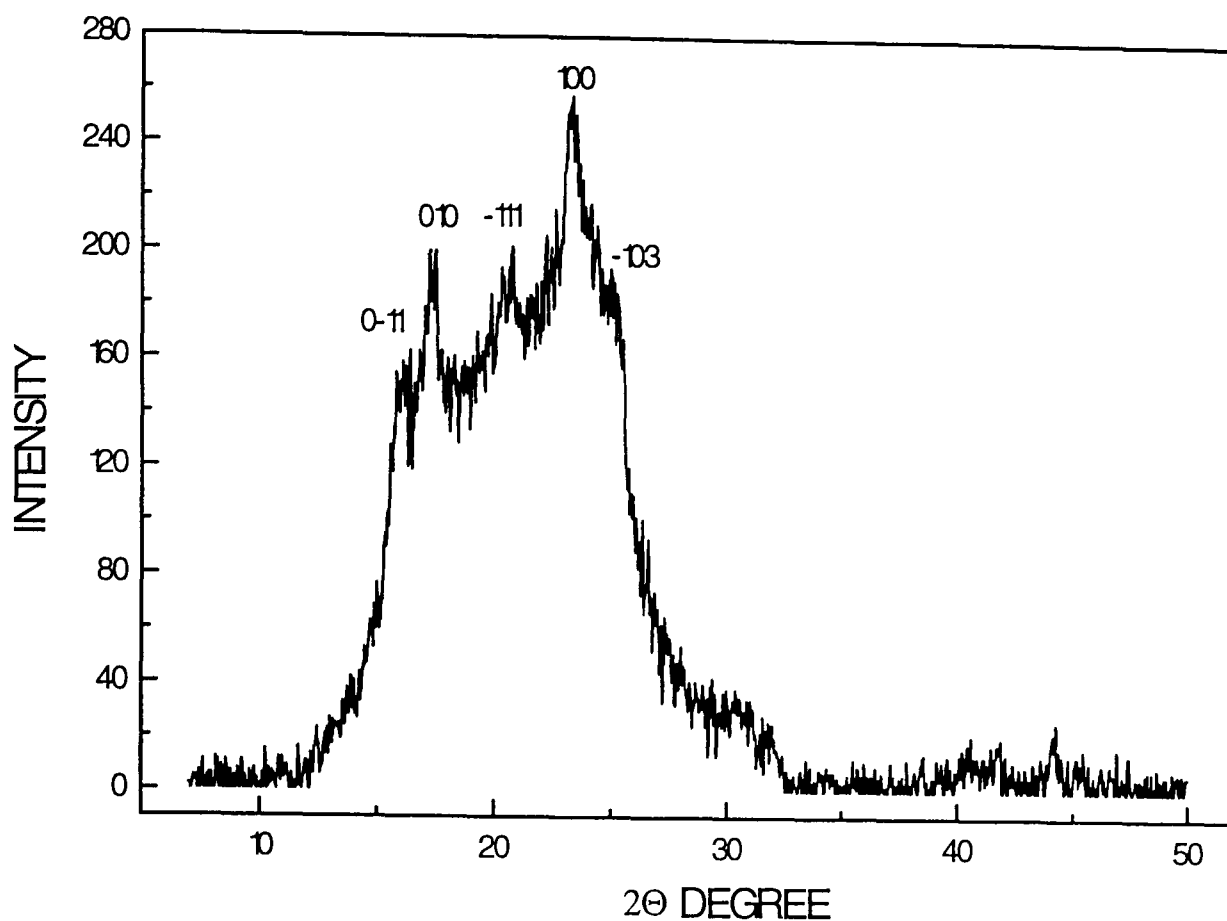
Figure 5.3 Wide angle X-ray scattering profile of SPBT 8.4 mole %.

Table 5.4 Peak positions (as Equivalent Bragg Spacings d) for SPBT 8.4 mole %

| peak number	2-theta angle 2Θ	d-spacing Å	relative intensity	hkl
1	15.93	5.56	59	0-11
2	17.21	5.15	79	010
3	20.71	4.28	80	-111
4	23.32	3.81	100	100
5	25.00	3.56	75	-103
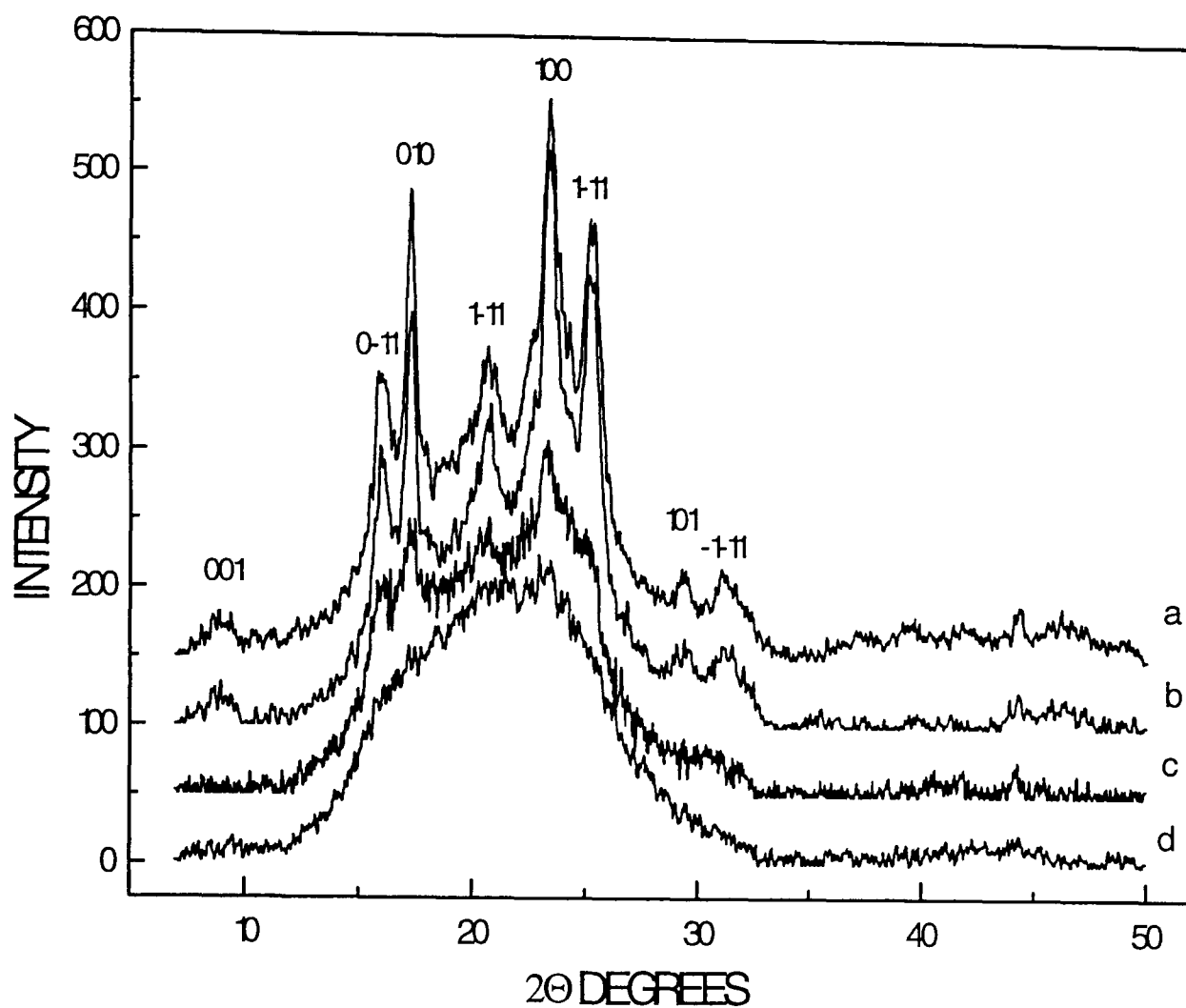
Figure 5.4 Wide angle X-ray scattering profile of

a PBT b SPBT 4.9 c SPBT 8.4 d SPBT 13.5 mole %.

Table 5.5 Peak positions (as Equivalent Bragg Spacings d)

for SPBT 13.5 mole %

peak number	2-theta angle 2Θ	d-spacing Å	relative intensity	hkl
1	23.09	3.85	100	100

Table 5.6 Variation in the interlamellar distance with sulphonation for PBT film samples.

mole %	crystal size Å hkl (0-11)	crystal size Å hkl (010)	crystal size Å hkl (-111)	crystal size Å hkl (100)	crystal size Å hkl (1-11)
0.0	154.8	178.4	124.6	119.3	149.4
4.9	268.8	211.8	136.3	116.9	126.2
8.4	-	161.5	192.0	127.5	-
13.5	-	-	-	323.6	-

Moreover for reflections (010) and (0-11) t increased for PBT 4.9 mole % compared to PBT. For the sample with 13.5 mole % sulphonation level, however all but (100) peak disappeared due to the significant decrease in the crystallinity of the material upon sulphonation with 13.5 mole % sulphonation level, however all peaks disappeared due to the significant decrease in the crystallinity of the material upon sulphonation. It was therefore not possible to determine t values for other reflections except from (100) plane of sample with highest level of functionality.

This analysis indicates that the interlamellar distance t is not a very good measure for ionomer samples, since it leads to an apparent contribution. This issue is further discussed in this chapter, after description of results collected on powder samples.

5.2.2 ii) PBT/SPBT powder samples

The X-ray powder pattern of the polymer PBT 0.0 mole % is shown in Figure 5.5 The X-ray powder patterns of the hot pressed film samples differ significantly from those of the powder samples. The first point to be noted is that the crystallinity of the unfunctionalised PBT 0.0 mole % hot pressed film sample is found to be higher compared

to PBT 0.0 mole % powder sample where sharp X-ray diffraction peaks were obtained (cf Figure 5.1). Moreover the absence of high 2θ reflections of (101), (-1-11) planes and low 2θ reflection from (0-11) plane and the broadening of the sharp main reflections support our findings. This effect may be attributed to the crystallisation process taking place during the cooling of the PBT film samples from melt, see Figure 5.1.
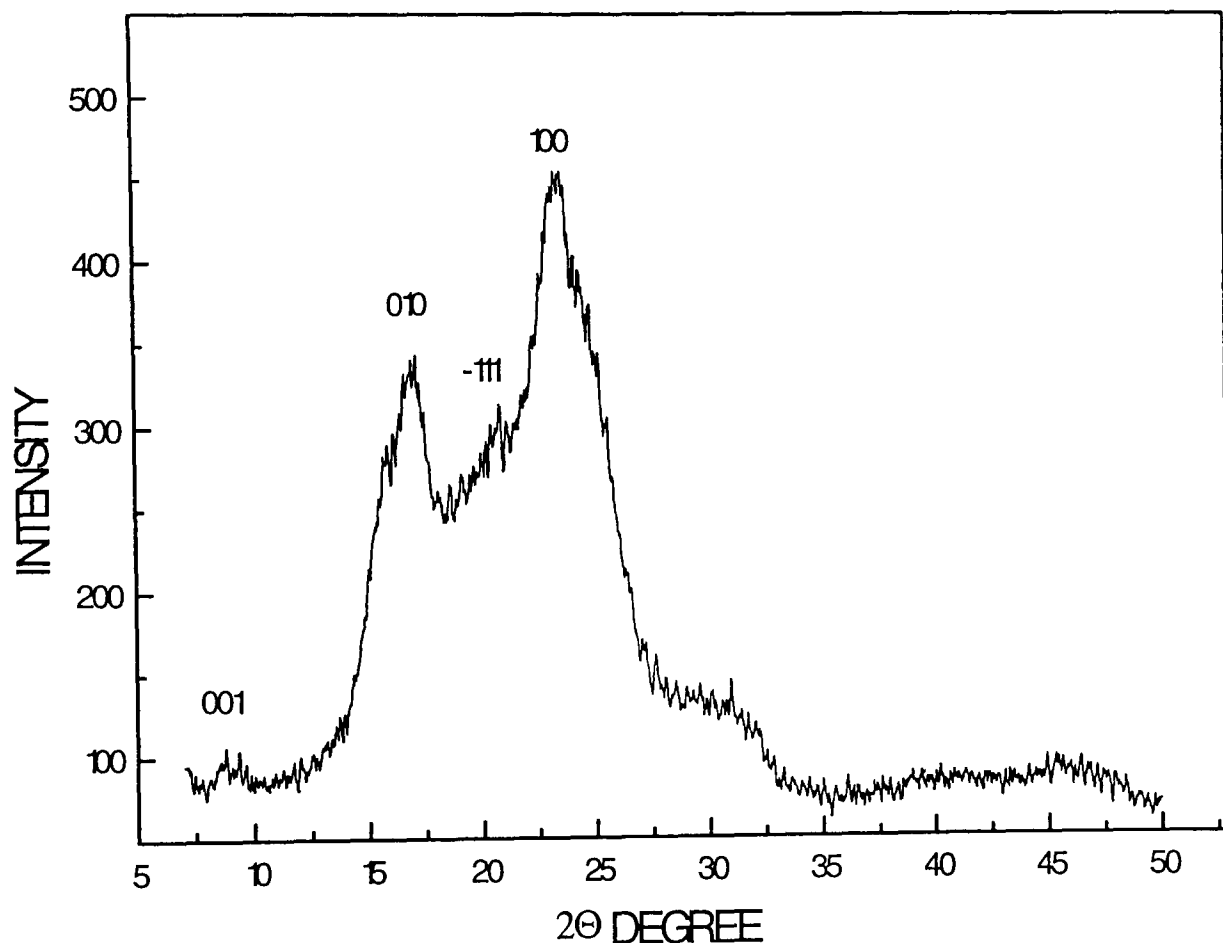

Figure 5.5 Wide angle X-ray scattering profile of

PBT 0.0 mole % powder sample.

In Figure 5.5 the main features of WAXD pattern for unsulphonated PBT are identifies as the (010) and (100) broad reflections occurring at 2θ values of $17.14°$ and $23.5°$, with corresponding d spacing 5.1 Å and 3.8 Å. A weak peak at $8.76°$ (d-spacing of 10 Å) is identified as the (001) reflection.

Table 5.7 Peak positions (as Equivalent Bragg Spacings d) for PBT(P) 0.0 mole %.

peak number	2-theta angle 2Θ	d-spacing Å	relative intensity	hkl
1	8.76	10	22	001
2	17.14	5.1	74	010
3	20.9	4.2	70	-111
4	23.5	3.8	100	100

Figure 5.6 shows the spectrum of a SPBT 3.5 mole % sample. A number of somewhat sharper reflections than those appearing in the PBT 0.0 mole % sample can be observed at an angle 2Θ of 17.1° (5.2 Å), 20.5° (4.3 Å) and 23.5° (3.8 Å), with corresponding reflections from the planes with the hkl indices (010), (-111), and (100) respectively. Appearance of two small peaks at (0-11) and (1-11) does not coincide with those found in PBT 0.0 mole % (Figure 5.5), but can possibly be due to the structural change caused by the sulphonated groups introduced to the PBT sample. In unsulphonated PBT, the flat phenyl rings belonging to the neighbouring chains are aligned. When the bulky sulphonate group is substituted, there would be conformational changes due to geometrical constraints. However, without modelling, it is difficult to pinpoint them.

In this study it has been observed that for all the samples (powder and films) the maximum intensity peak comes from (100) plane. The (100) reflections arise from the layer spacing between two main chains. The side chains, which are fully interdigitated and tilted with respect to the rigid main chain come to occupy this domain between the main chains. A lateral packing of main chains giving the (010) reflections forms each layer. As a result, the lateral spacing of the main chain is 3.8 Å, which is close to the Van der Waals radius of the phenyl ring (3.45 Å). This suggests that the two phenyl rings of PBT/SPBT have
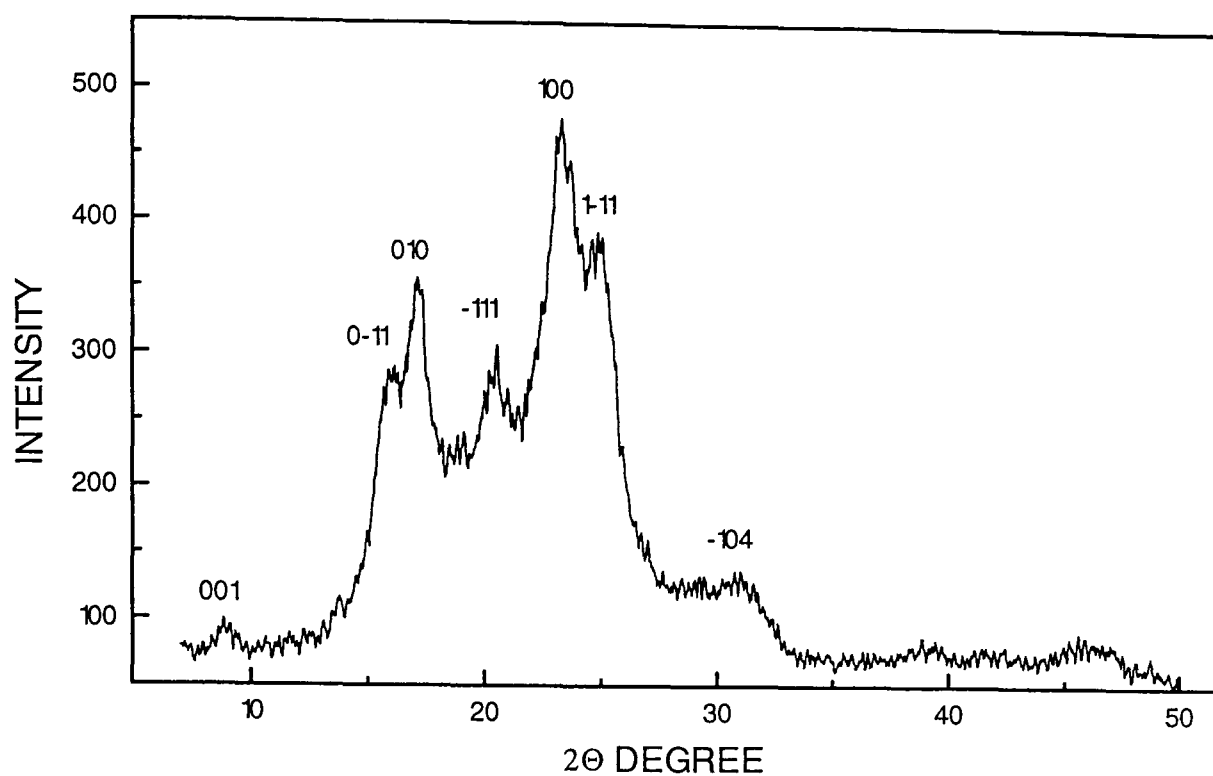
Fig. 5.6 Wide angle X-ray scattering profile of

SPBT 3.5 mole % powder sample.

Table 5.8 Peak positions (as Equivalent Bragg Spacings d) for SPBT(P) 3.5 mole %.

| peak number	2-theta angle 2Θ	d-spacing $\mathring{A}$	relative intensity	hkl
1	8.87	9.9	20	001
2	16.05	5.5	60	0-11
3	17.10	5.2	76	010
4	20.55	4.3	65	-111
5	23.34	3.8	100	100
6	24.9	3.6	80	1-11
7	30.8	2.9	27	-104
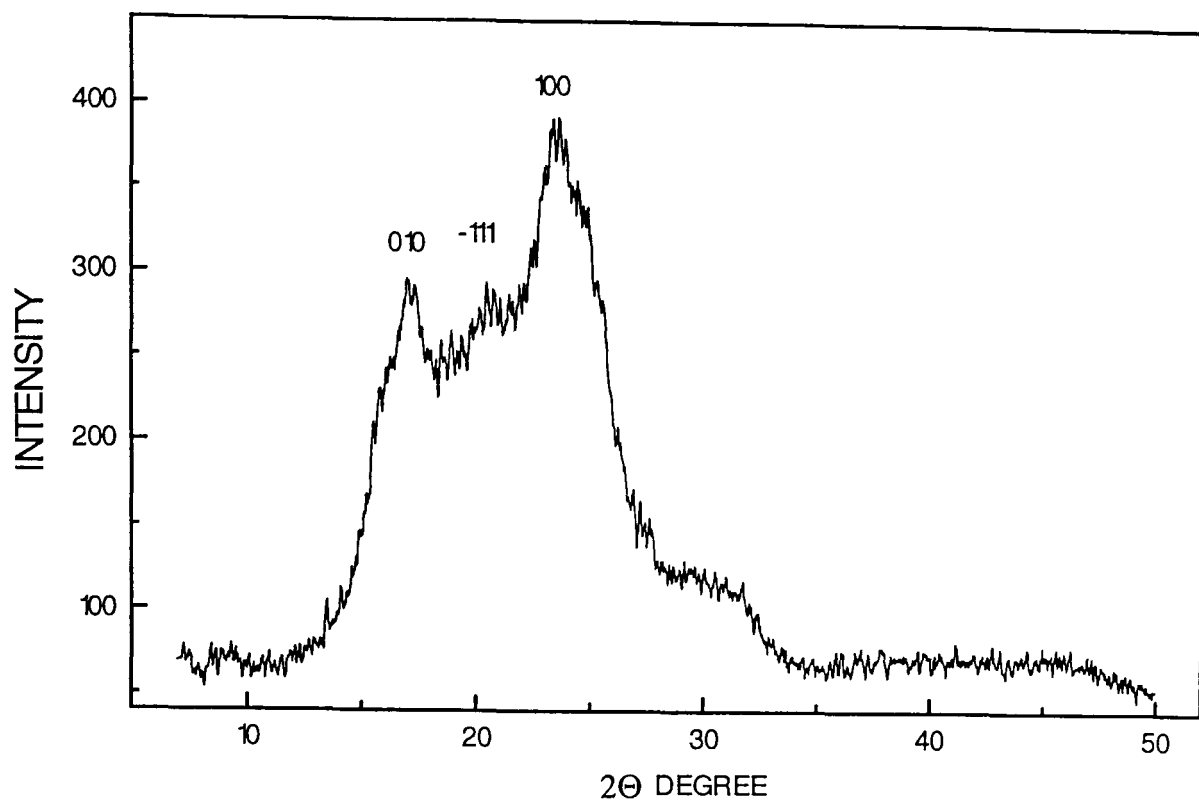
Figure 5.7 Wide angle X-ray scattering profile of

SPBT 7.9 mole % powder sample.

Table 5.9 Peak positions (as Equivalent Bragg Spacings d) for SPBT(P) 7.9 mole %.

| peak number	2-theta angle 2Θ	d-spacing Å	relative intensity	hkl
1	17.0	5.2	75	010
2	20.4	4.4	74	-111
3	23.36	3.8	100	100
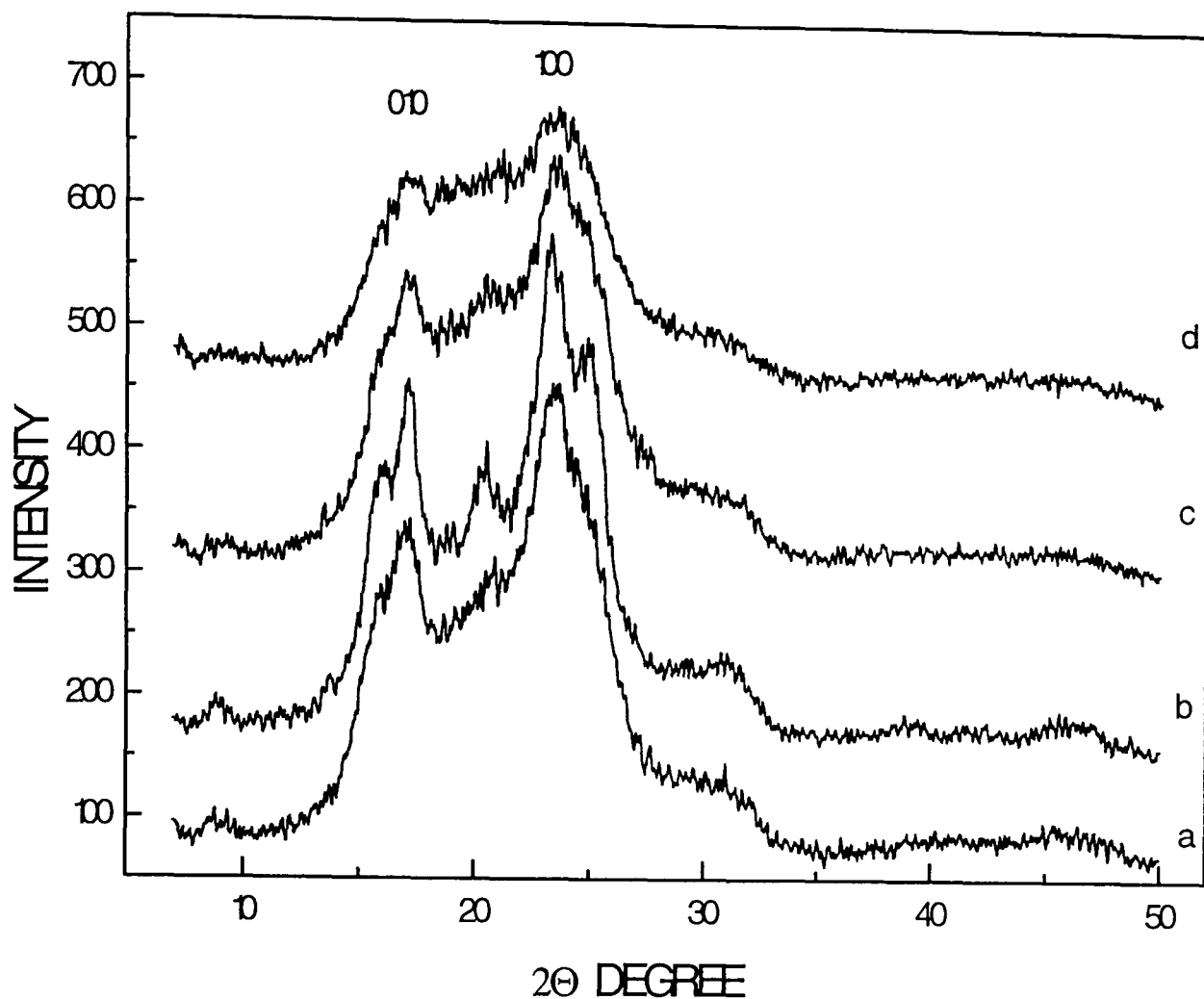
Figure 5.8 Wide angle X-ray scattering profiles of

a PBT 0.0 b SPBT 3.5 c SPBT 7.9 d SPBT 11.1 mole %.

Table 5.10 Peak positions (as Equivalent Bragg Spacings d)

for SPBT(P) 11.1 mole%.

| peak number	2-theta angle 2Θ	d-spacing Å	relative intensity	hkl
1	16.98	5.2	81	010
5	23.63	3.7	100	100
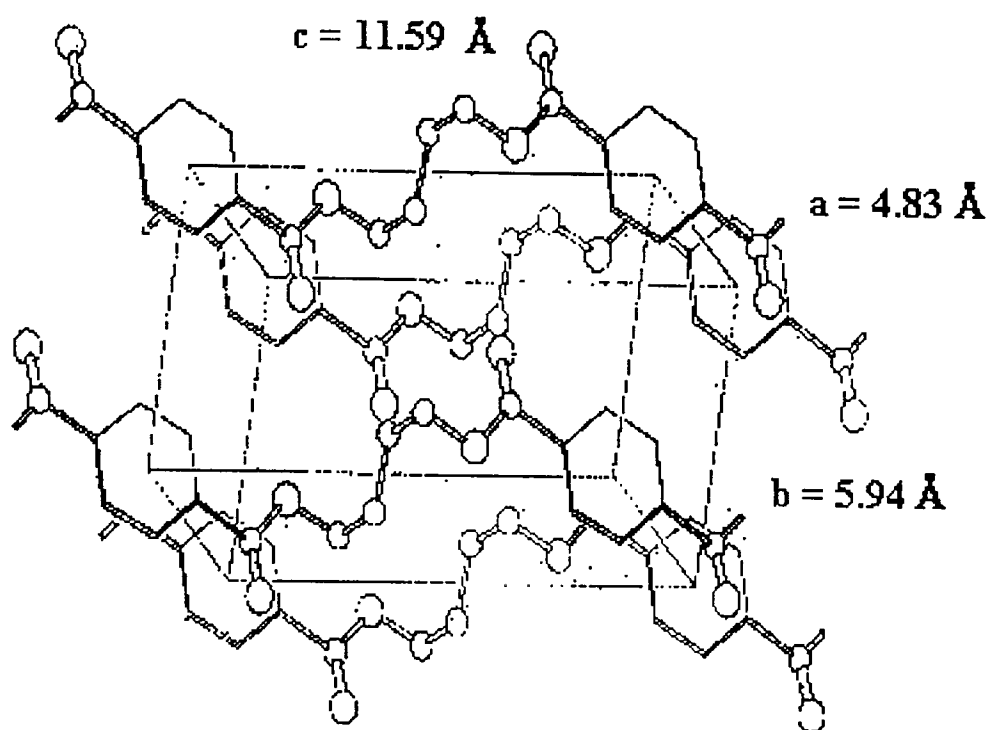
Figure 5.9 Arrangement of molecules in the crystal of PBT[1].

nearly coplanar arrangements. Figure 5.7 illustrates the X-ray diffractogram for the SPBT 7.9 mole %. The sulphonation effect on the structure of the polymer is quite evident here: a more diffused pattern is obtained with the increase of the of ionic content. Hence one can conclude that a significant change in the morphology and structure occurs in samples apparent for those with sulphonation level higher than 5 mole %.

The diffraction pattern shows only two main broad, small and low intensity diffraction peaks at the Bragg angle of $2\theta = 17°$ and $23.36°$ corresponding to the (010) and (100) planes, respectively. The the diffraction peaks for planes (-111), (001), (101) and (-1-11) were not detected, which means that the PBT copolymer showed reduced crystallinity compared to unfunctionalised PBT 0.0 mole % sample. Figure 5.7 demonstrate that the relative intensities of diffraction peaks at $2\theta = 17°$ and $20.4°$ and reduced remarkably for SPBT with a sulphonation level of 7.9 mole %.

In the case of SPBT 11.1 mole % a very broad X-ray diffraction pattern was obtained with

only small elevations at $2\theta = 16.98°$ and $23.63°$. That indicates further reduction in crystallinity, and the data recorded are shown in Figure 5.8 (d). From all above discussed results obtained for both films and powder samples it is concluded that the increasing ion content prevents the formation of crystallites in the highly crystallisable PBT and thus changes a semi-crystalline material into an amorphous one.
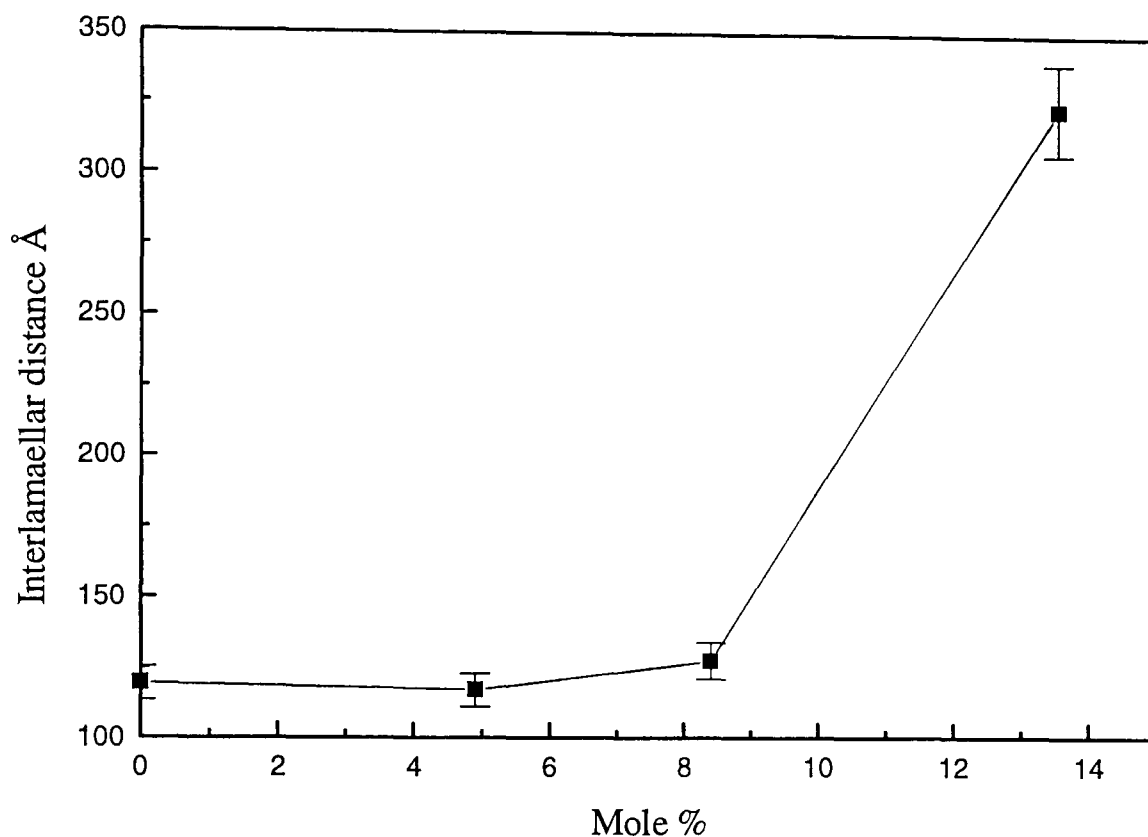

Figure 5.10 Plot of interlamellar distance versus mole % for (100) plane as a function of sulphonation level for SPBT samples.

In what follows only a tentative explanation is offered, since the patterns of polycryatalline samples are notoriously difficult to interpret. The changing material orientation of crystallites in an amorphous matrix may cause diffraction peaks to broaden or even completely disappear. Hence the discussion will concentrate on the most prominent peak only, that the hkl index (100). If the crystal size is interpreted as the size of the lamellae, than its increase for (100) reflection could be thought of as an increase in the distance between lamellae (Figure 5.10).

From our the X-ray results on sulphonated PBT samples described above, it is apparent that with an increase of ionic content, the crystallinity decreases in the material. A possible explanation for the expansion in interlamellar distances in the crystalline domains upon increase of ionic content may be the need to accommodate the sulphonate groups in the bulk. In terms of the EHM model reduction in the overall % of crystallinity is attributed to the segmental mobility of a chain which is lowest near the location where an attached ion pair is incorporated within a multiplet and anchored to the multiplet. Moreover, reduction in the crystalline domains in the crystalline phase is attributed to a formation of a region of restricted chain mobility, or 'skin' around multiplets[10]. It produces disorder in crystalline phase in the bulk and results in the increase of the interlamellar distances of remaining lamellae, as schematically shown in shown in Figure 5.11(b).
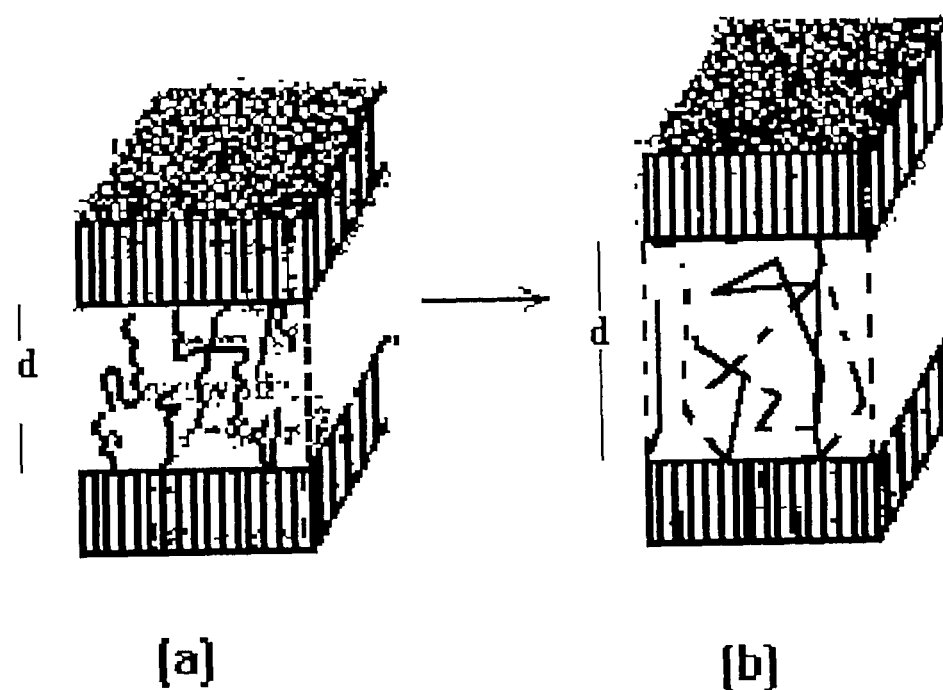

Figure 5.11 (a) Schematic representation of crystalline regions in PBT

(b) Amorphous region: dashed curve located in the

interlamellar region of SPBT.

Figure 5.11 (a) shows crystalline domains in the unsulphonated semicrystalline PBT. A possible explanation is as follows. Upon sulphonation bulky sulphonate groups perform

two functions: firstly, they destroy the ordering within the lamella layers, hence bluring the peaks of the X-ray pattern. Secondly, they congregate in the amorphous phase contained between subsequent lamellae, hence causing an apparent increase in the crystal size.

5.3   PS/SPS samples results and discussion

For comparison, powder samples of polystyrene were investigated. Polystyrene is a model random ionomer, and the influence of the degree of sulphonation on the local order has been investigated extensively[12].

The wide angle X-ray diffraction patterns of polystyrene (PS) samples of different tacticities and sulphonated isotactic polystyrene with the sulphonation level of (0.0 to 10.5 mole %) are given in Figures 5.11 to 5.16. Samples are characterised in Table 5.1. Results obtained have been compared with those obtained for un-sulphonated PS in order to study the effect of ion content on the structure of the material. Moreover WAXD parameters such as 2θ, d-spacings and relative intensities are tabulated in Tables 5.11-5.14 for each sample. Peaks were indexed for syndiotactic polystyrene (see Figure 5.16) as it was done in the case of PBT/SPBT. However peaks were not indexed for atactic and isotactic PS samples.

The X-ray diffraction profile of iso-PS 0.0 mole % is shown in Figure 5.11. A few relatively sharp reflections can be observed indicating partial ordering in the material. The main diffraction peak observed was at $2\theta = 18.02°$ (Bragg spacing d = 4.9 Å).
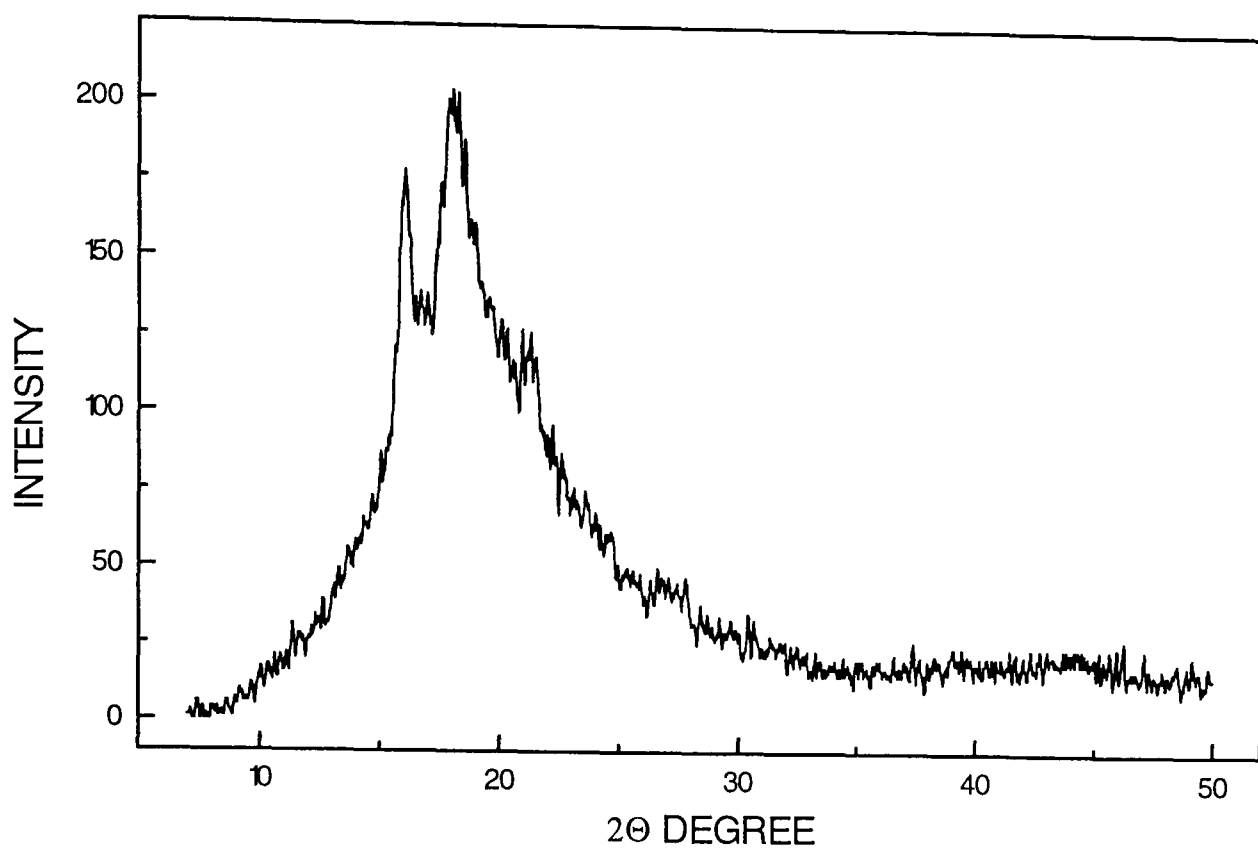
Fig. 5.11 Wide angle X-ray scattering profile of

iso-PS 0.0 mole %.

Table 5.11 Peak positions (as Equivalent Bragg Spacings d)

for iso-PS 0.0 mole %.

| Peak number	2-theta angle 2Θ	d-spacing Å	relative intensity
1	16.03	5.52	85
2	18.02	4.9	100
3	20.94	4.2	61
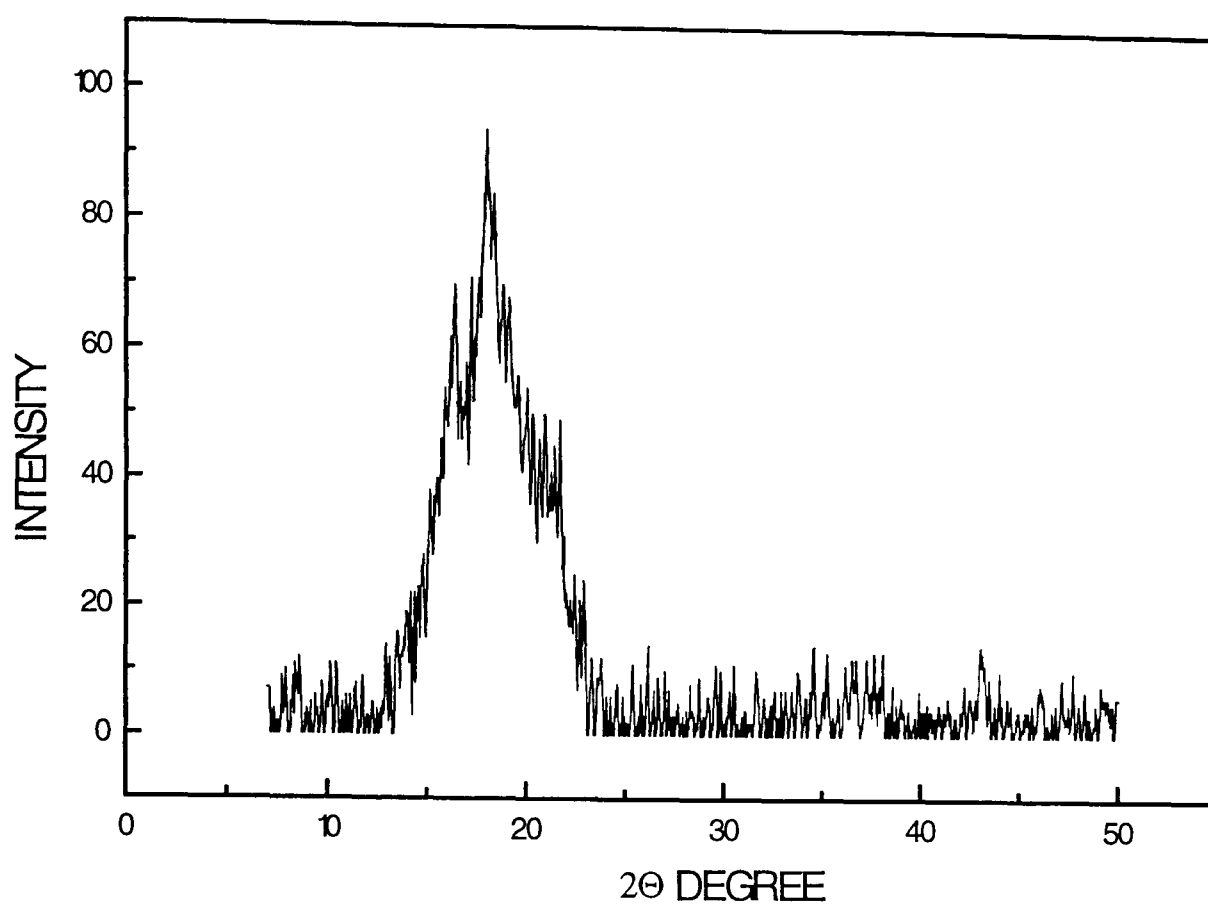
Fig. 5.12 Wide angle X-ray scattering profile of

iso-SPS 8.8 mole %.

Table 5.12 Peak positions (as Equivalent Bragg Spacings d)

for iso-SPS 8.8 mole %.

| Peak number	2-theta angle 2Θ	d-spacing Å	relative intensity
1	16.41	4.93	58
2	18.00	4.43	100
3	20.92	4.24	54
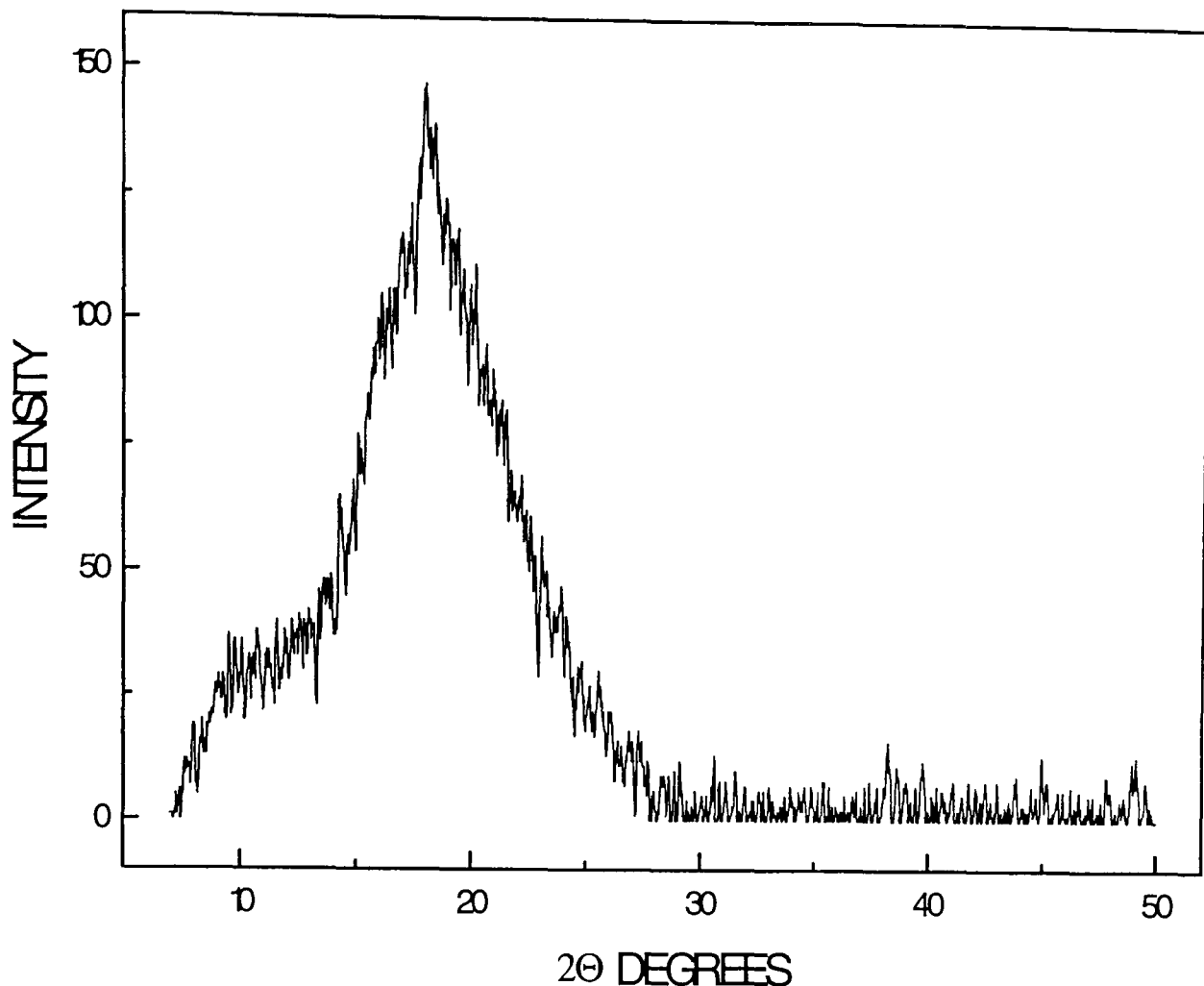
Fig. 5.13 Wide angle X-ray scattering profile of

iso-SPS 10.5 mole %.

Another sharp, high intensity reflection is visible at $2\theta = 16.03°$ and d-spacing of 5.52 Å. The subsidiary peak at $2\theta = 20.94°$ (d-spacing 4.2 Å) showed a relatively low intensity. one conclude that the 4.2 Å reflection observed here corresponds to the extended conformation of chains of the material in bulk[13-14]. Results for PS 0.0 mole % are summarised in Table 5.11. Figure 5.12 shows the X ray powder pattern of the sulphonated iso-PS 8.8 mole %. A significant change in the reflection at $2\theta = 16.41°$ is due to the influence of ion content on the structure of the material. Compared to iso-PS 0.0 mole %, there is a decrease of d-spacing from 5.52 Å to 4.93 Å. Relative intensities and d-spacings are listed in Table 5.12.

Table 5.13 Peak positions (as Equivalent Bragg Spacings d) for iso-SPS 94.5 mole %.

peak number	2-theta angle 2Θ	d-spacing Å	relative intensity
1	18.21	4.8	87
2	19.22	4.6	100
3	23.57	3.8	89
4	25.65	3.5	86
5	32.10	2.8	90
6	34.09	2.6	72

In case of sulphonated iso-PS 10.5 mole % sharp diffraction peaks were not detected only one broad halo which means the polymer is amorphous. However, X-ray diffractogram of this system differs significantly from the pattern of pure iso-PS. Inspection of Figure 5.13 further reveals the presence of broad peak over the range of $12° < 2\theta < 30$ and may correspond to the diffraction from a poor intermolecular packing. These results suggest that a remarkable reduction in the % crystallinity is already found for samples with increasing level of sulphonation. Furthermore these WAXD measurements are in good agreement with DSC results, which have been described in Chapter 4, and will be briefly commented upon below. In addition, a fully sulphonated iso-PS sample was studied.
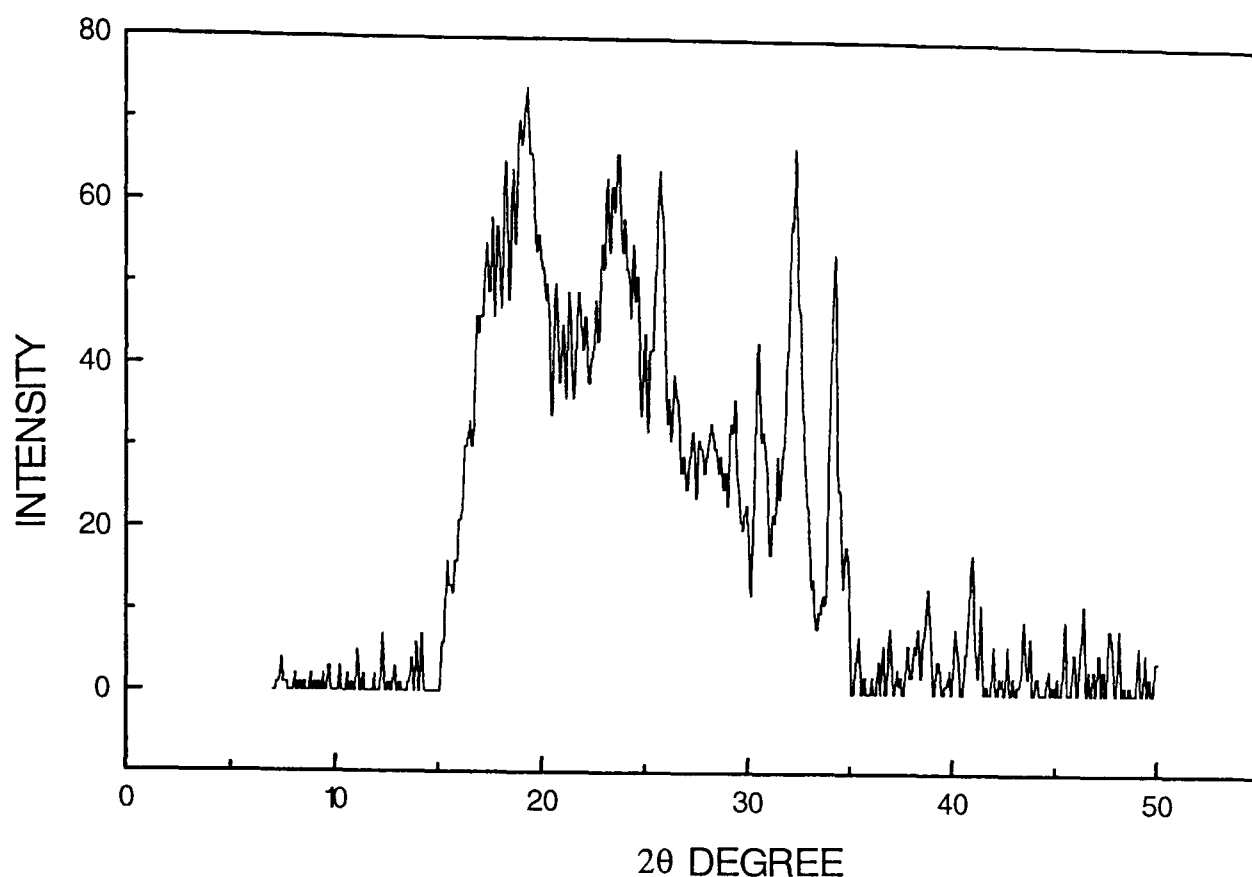
Figure 5.14 Wide angle X-ray scattering profile

of sulphonated iso PS 94.5 mole %.

The wide angle X-ray profile for the fully sulphonated iso-PS 94.5 mole % is illustrated in Figure 5.14. This spectrum is very different from that of the other ionomers: the sample showed two broad peaks at 2θ = 18.21° and 19.22° accompanied by three sharp high intensity new reflections at 2θ = 23.57°, 32.10° and 34.9°. This indicates a formation of new, crystalline-like structure. It is noteworthy that high intensity peaks were not detected for samples with 0.0 to 10.5 mole % of level of sulphonation. This new crystalline structure is attributed to the very high sulphonate group content[15]. Since now nearly all phenyl rings have a sulphonate group attached to them, the chain becomes very rigid. There is a little space to accommodate other chains, hence the structure will tend to have the minimum of conformational energy. The measured d-spacings are given in Table 5.13. From Figure 5.11, it can be seen that there were two main reflections which appeared at 2θ = 16.03° and 18.02° for iso-PS 0.0 mole %. In the case of iso-SPS 94.5 mole % no

reflections were observed at $2\theta = 16.03°$ which supports the hypothesis presented above of a new structure being formed. No further attempt was made to identify this structure.

For atactic polystyrene WAXD pattern is shown in Figure 5.15. As is well known[16-19], polystyrene displays two amorphous halos in the region of interest of this work. It is seen in Figure 5.15 that the low angle halo appear at $2\theta = 10°$ and another broad peak at $2\theta = 18.84°$. No other interesting diffraction pattern was observed.
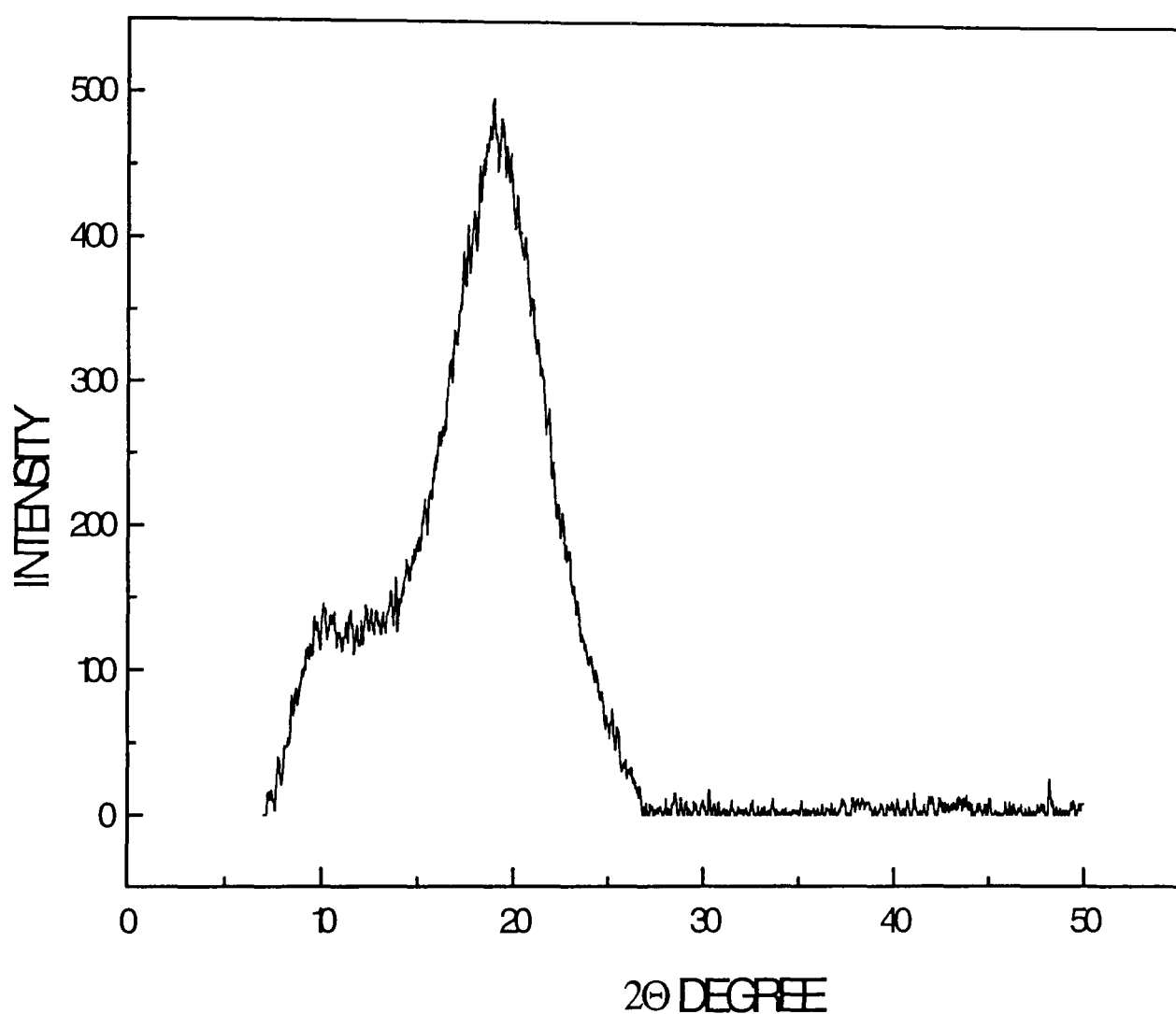

Figure 5.15 Wide angle X-ray scattering profile of atactic PS

Based on earlier studies syndiotactic polystyrene shows stable chemical and morphological properties due to its ordered chain configuration[15-16]. The structure of this polymer is

however quite complex and belongs to the hexagonal system with the space group 158.
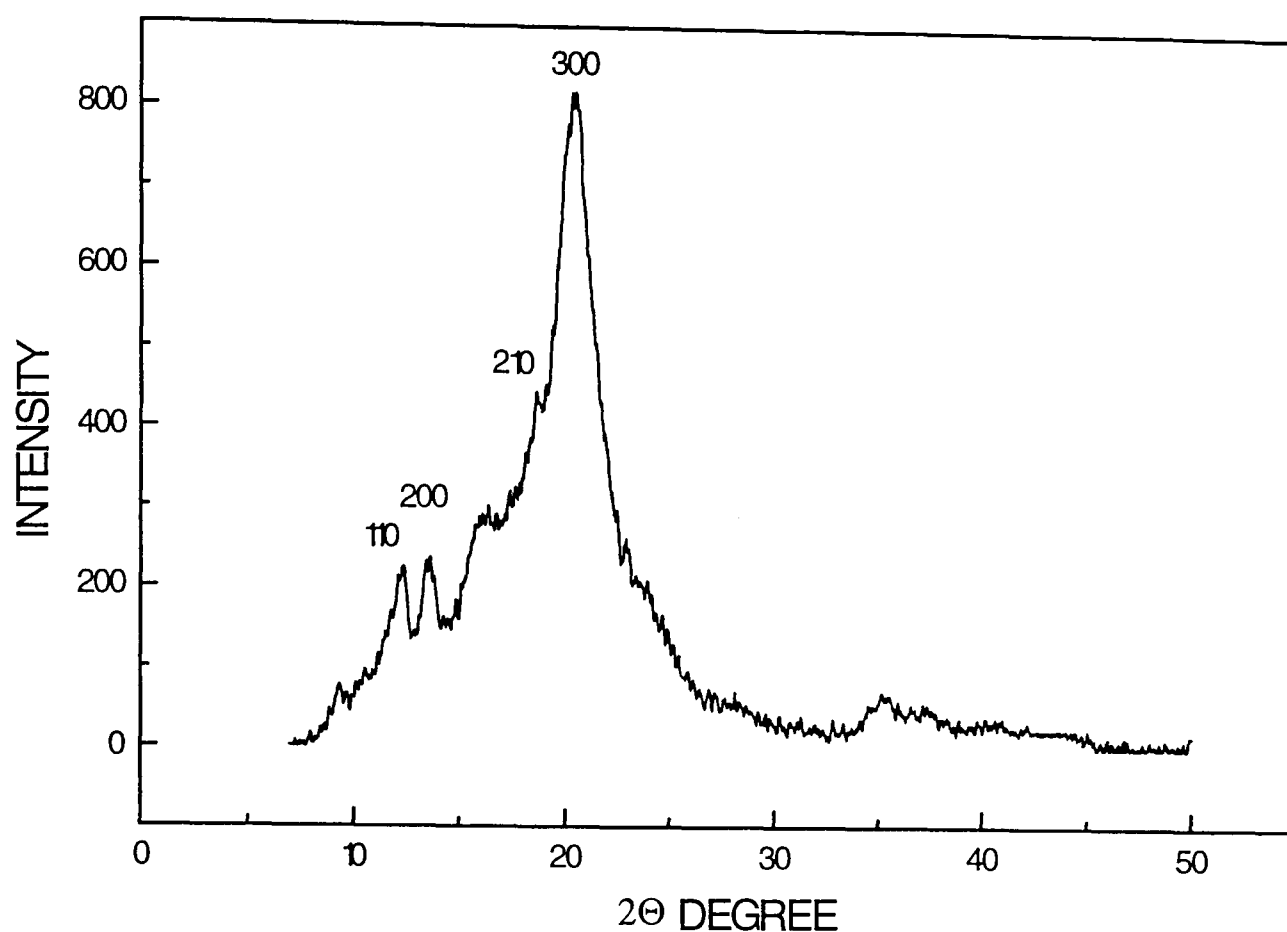
Figure 5.16 Wide angle X-ray scattering profile of syndiotactic PS.

Table 5.14 Peak positions (as Equivalent Bragg Spacings d) for syndiotactic PS 0.0 mole %.

peak number	2-theta angle 2Θ	d-spacing Å	hkl	relative intensity
1	12.35	7.1	110	27
2	13.59	6.5	200	28
4	18.63	4.8	210	54
5	20.50	4.3	300	100

The cell dimensions are a = 15.16 Å, b = 15.16 Å, c = 5.04 Å, α = 90°, β = 90°, and γ = 120°[20-22]. Figure 5.16 shows the X-ray profile of syndiotactic polystyrene 0.0 mole %. Three peaks are clearly seen at 2θ = 12.35°, 13.59°, 16.41° and 20.50°. The main peak has a d-spacing of 4.3 Å. The material was found to be partially crystalline.
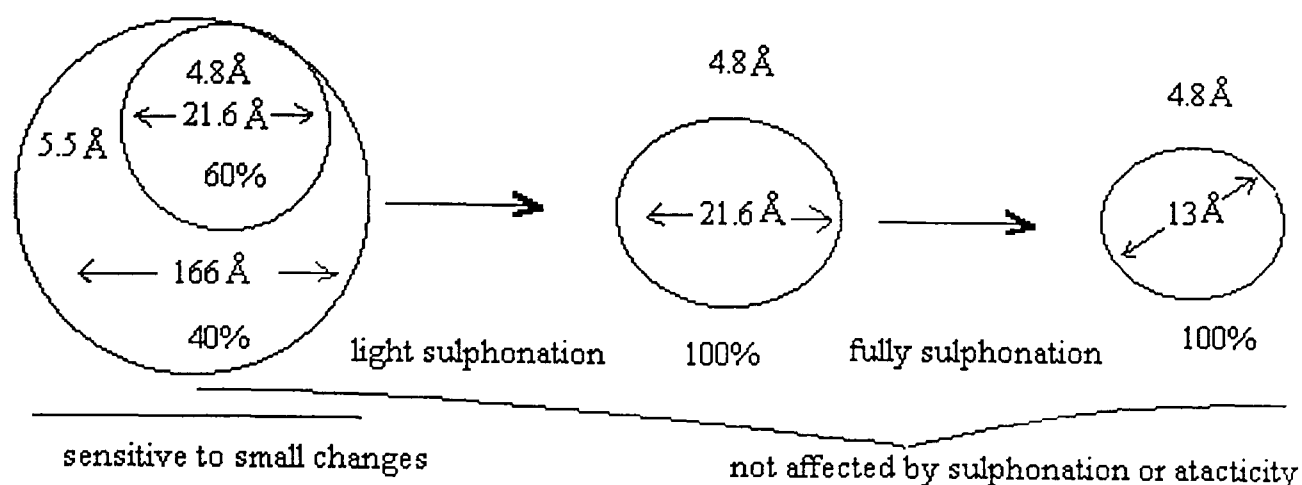

**Figure 5.17 A graph representation of disorder setting in
iso-PS upon sulphonation**

The diffraction pattern for syndiotactic-PS shows three main peaks, small and low intensity diffraction peaks at the Bragg angle of 2θ =12.3° and 13.59 ° corresponding to the (110) and (200) planes with d-spacings 7.1 Å and 6.5 Å, respectively. The main peak from (300) plane was detected at 2θ = 20.5°. Experimental results, relative intensities and d-spacings are shown in Table 5.14. WAXD diffraction pattern for atactic-PS showed only one high intensity broad peak at 2θ = 18.84°, isotactic-PS 0.0 mole % displayed two high intensity peaks, and syndiotactic-PS showed three sharp peaks, indicating partial ordering in the material compared to atactic-PS.

Several conclusions can be drawn from the above measurements. Firstly, that the X-ray data corresponds well to that obtained by Gabrys et al[4,23]. Despite lacking the advantage of absolute intensity offered by the scattering of spin-polarised neutrons with spin

polarisation option the X-ray powder patterns give a good idea of the short range order in present in PS samples. Secondly, the destruction of short range order upon sulphonation resembles the effect of acticity (cf patterns of sulphonated iso-PS with that of atactic-PS. Thirdly, that the disappearance of multiple melting endotherms upon sulphonation as observed for iso-PS (chapter 4) can be linked to the destruction of the larger "crystalline" region (~ 166 Å diameter) upon light sulphonation, crystalline region reduced to 13 Å upon further sulphonation (see Figure 5.17 (b))[23]. Then the iso-PS becomes more amorphous. The average distance between the neighbouring chain is 5.5 Å and crystallite size 4.8 Å. Finally, the conclusions drawn for polystyrene ionomers on the basis of WAXD and DSC data help to elucidate the results obtained for PBT.

5.4   Optical microscopy

5.4.1   Introduction

Wide angle X-ray diffraction studies on SPBT ionomers have established that increasing ionic content reduces crystallinity and increase disorder. This phenomena cab be explained as due to the formation of ionic aggregates in the amorphous phase of the material. Mixing ionomers with an amorphous material such as PC increases disorder further, and leads to optically clear blends. In order to obtain information about the microstructure of SPBT/PC blend, a series of SPBT/PC blends with different PC ratio was investigated by optical microscopy. Thin sections of samples were viewed in a microscope with the specimen being rotated between crossed polars to allow changes in birefringence to be observed. In this section the results of that investigation are recorded and discussed, and explanation of the observed structures is suggested.

Table 5.15   Compositions and % ionic content for the samples for optical microscopy measurements.

| SPBT/PC blends wt. %	% ionic content
25/75	0.0, 3.5, 7.9 and 11.1
50/50	0.0, 3.5, 7.9 and 11.1
75/25	0.0, 3.5, 7.9 and 11.1
100/0.0	0.0, 3.5, 7.9 and 11.1
0.0/100	-

Samples were prepared by solvent casting, detailed description is given in section 3.3.4 chapter 3.

5.4.2   Results and discussion.

Analysis by optical microscopy was undertaken on SPBT/PC blends, listed in Table 5.15. All samples were solution cast and some were subsequently baked. Magnification used was 200 times. Figure 5.18 shows a structure of PBT (0.0 mole %) film in the PBT/PC blend composition. The effect of blending crystalline PBT with amorphous PC is similar. The initiating sites for the growth of two-dimensional spherulites can be seen. As the name implies, spherulites are sphere-shaped crystalline structures that form in the bulk (cf section 2.3.2). The fine structure of the spherulites is not visible in this figure. In the PC-rich phase dispersed PC particles ranging 2-5 µm in diameter are seen as black balls. Figure 5.19 reveals the effect of increasing wt. % of PBT in the PBT/PC 75/25 composition and gives the evidence of a spherulitic superstructure[24].

Fine structure of the spherulites is visible with classical Maltese cross patterns. The diameters of the spherulites reach 90-100 µm. Figure 5.20 illustrates morphology of SPBT(3.5 mole %) solution cast film. Two types of spherulites usual (compare Figure 5.19) and unusual can be seen with narrow inter-spacing.

The ribbons of lamellae radiate out from the core of each large spherulite giving the wheat sheaf pattern. Although large spherulites do not exhibit Maltese crosses when viewed with crossed polarises (as in this micrograph), they do have the circular and fibrous characteristics of spherulites. Hence increase in the number of spherulite is due to the lamellae structures of PBT chains. The change of size and distribution of spherulites upon mixing SPBT (3.5 mole %) with decreasing amount of PC is shown in Figures 5.20-5.24. Figure 5.21 shows the effect of blending with PC on the morphology of SPBT(3.5)/PC 25/75 blend. Tiny crystallites are seen in the PC rich area, further reduction in the size of the small spherulites is evident. Possible explanation for the reduction in the size of crystallites is the influence of ionic groups which are randomly distributed in the amorphous phase and restrict the growth of spherulites. The same phase structure is also observed in Figure 5.22 which is a micrograph of SPBT(3.5)/PC 25/75 blend.
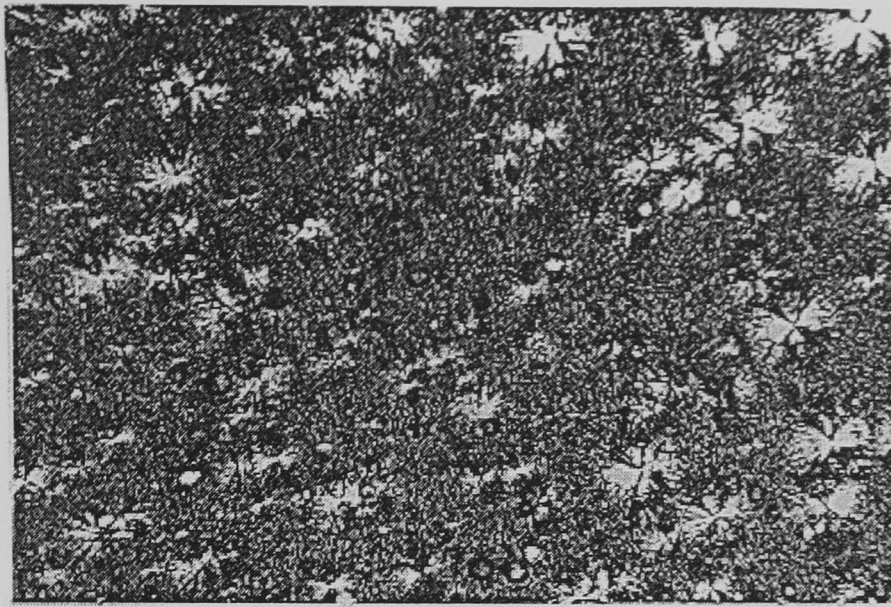
50 μm

**Figure 5.18 Polarised light micrograph (X 200) for PBT
in the PBT/PC 25/75 composition.**
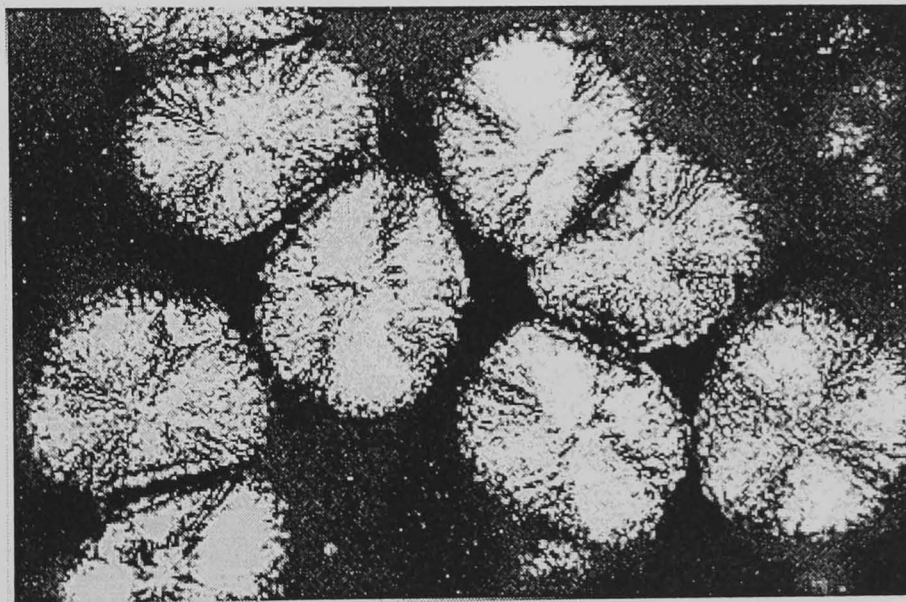
50 μm

**Figure 5.19 Polarised light micrograph (X 200) for PBT
in the PBT/PC 75/25 composition.**
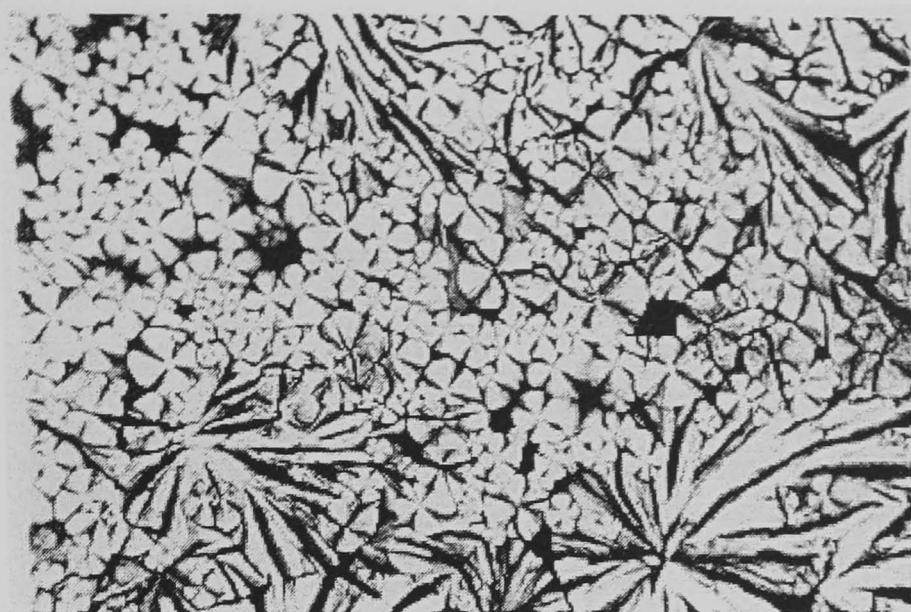
50 µm

**Figure 5.20 Polarised light micrograph (X 200) for
SPBT (3.5) Solution Cast.**
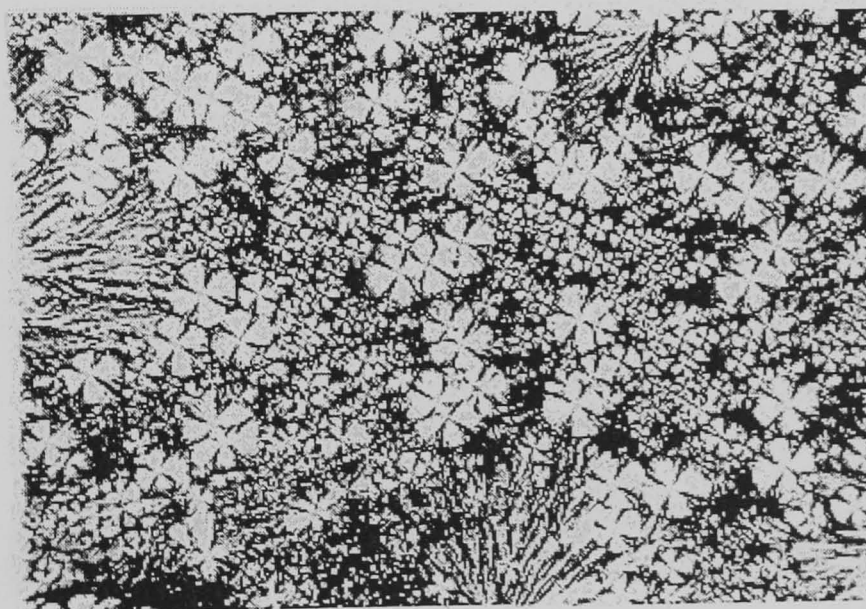
50 µm

**Figure 5.21 Polarised light micrograph (X 200) for
SPBT (3.5) in the SPBT/PC 25/75 composition.**
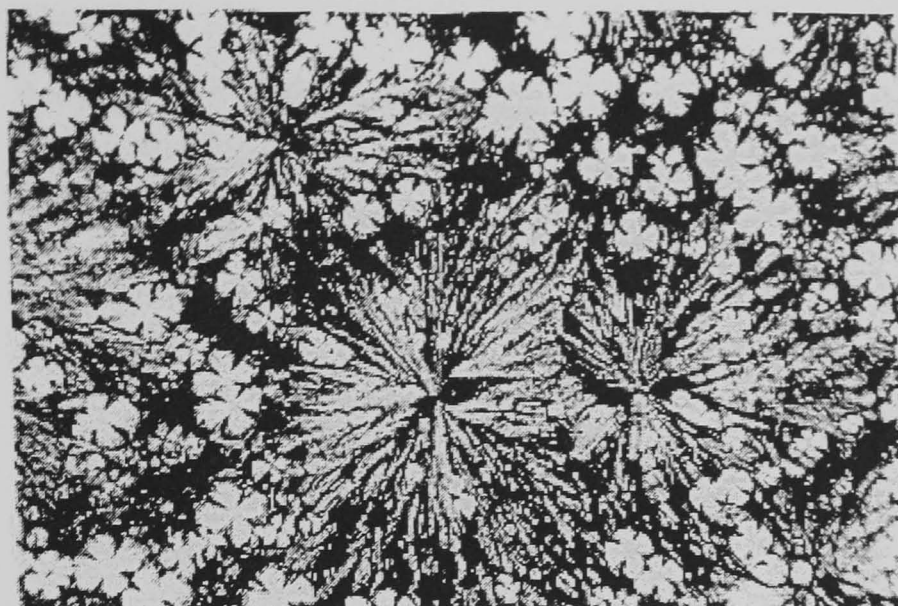
50 μm

Figure 5.22 Polarised light micrograph (X 200) for SPBT (3.5)
in the SPBT/PC 25/75 composition (baked).
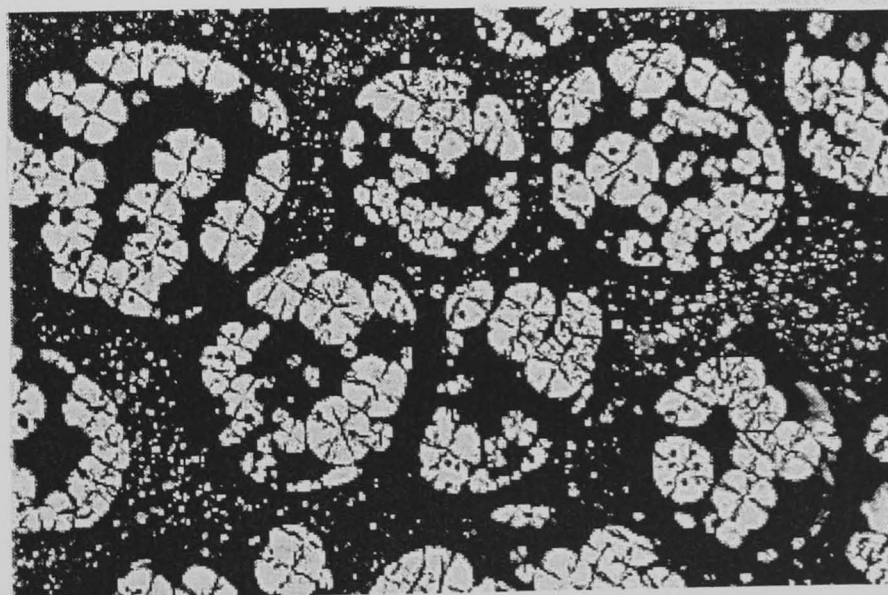
50 μm

Figure 5.23 Polarised light micrograph (X 200) for SPBT (3.5)
in the SPBT/PC 50/50 composition (baked).
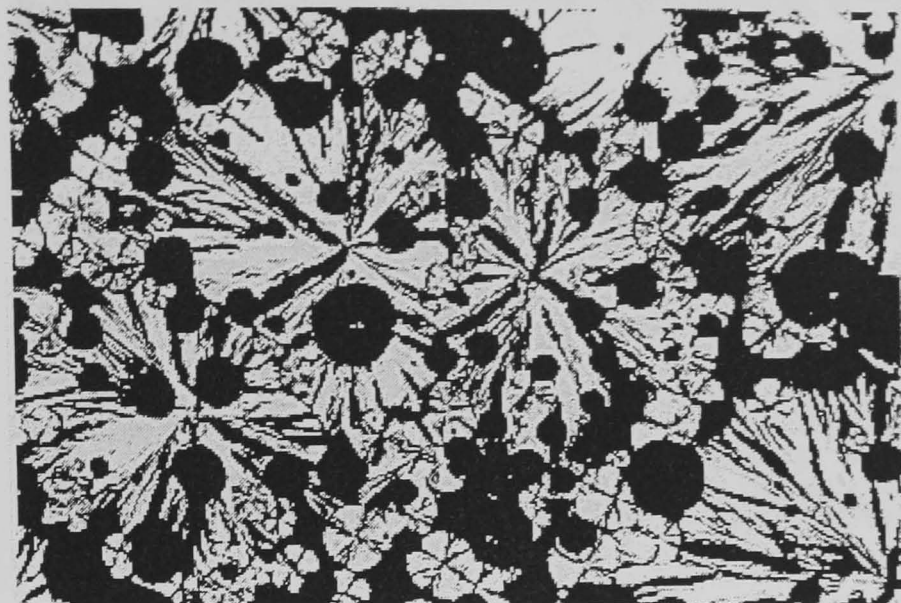
50 μm

Figure 5.24 Polarised light micrograph (X 200) for SPBT (3.5) in the SPBT/PC 75/25 composition (baked).
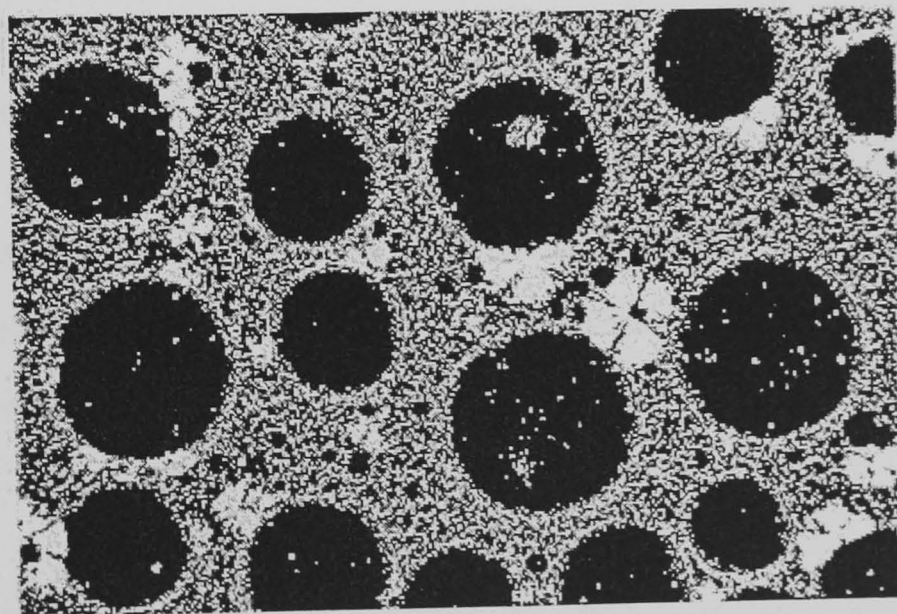
50 μm

Figure 5.25 Polarised light micrograph (X 200) for SPBT (7.9) Solution Cast (baked).
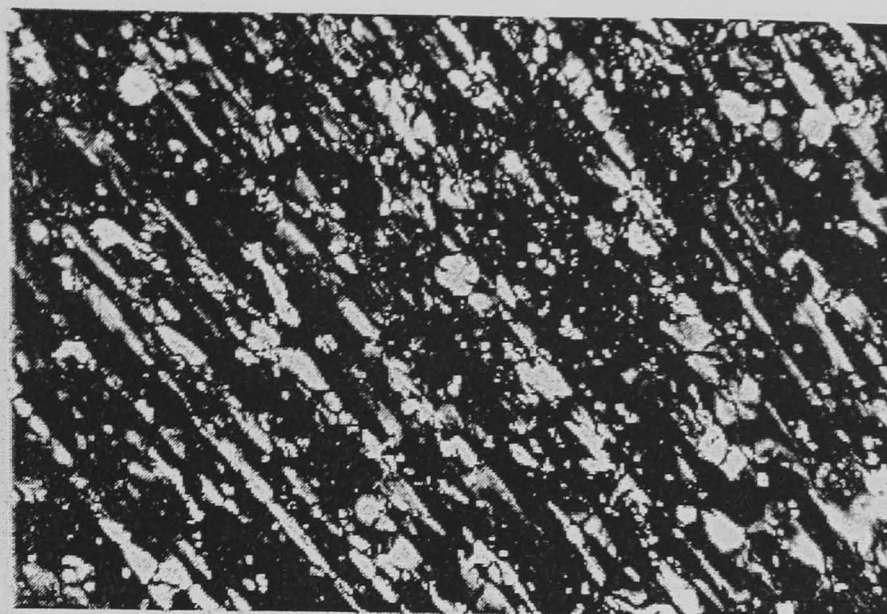
50 µm

**Figure 5.26 Polarised light micrograph (X 200) for SPBT (7.9)
in the SPBT/PC 25/75 composition.**

Phase separated domains of SPBT particle and extinction of spherulites in the amorphous phase (PC-rich area) between the channels is also clearly seen in Figure 5.23 for SPBT(3.5)/PC 50/50 (baked) blend. Size of the spherulites is reduced markedly compared to PBT /PC 75/25 to the order of 30 µm, usual crystallites dominate the field of view in the optical micrograph of SPBT-rich (crystalline) phase. SPBT domains are regularly distributed throughout the sample. Small PC particles are seen settled on the ribbons of some SPBT spherulites. Hence one can conclude that no evidence of miscibility for this particular composition in this sample is found. Reduction in the % of crystallinity is a result of coarsening of spherulites in the PC rich phase.

Random distribution of amorphous PC particles (with a diameter in the range of 20-50 µm) on the top of SPBT lamellae network is visible in Figure 5.24 which shows SPBT(3.5)/PC 75/25 (baked) blend. Comparison of Figure 5.21 and Figure 5.23 shows a change in the blend microstructure upon increase of wt.% of SPBT. Further increase in the size of large spherulites (Figure 5.24) upon increasing amount of SPBT has taken place and appearance of black spots (PC particles) is visible. It amounts to an immiscible composition. The location of PC particle on the top of SPBT spherulites

may be due to the low density (as compared to SPBT) of PC particles. Subsequently the level of sulphonation was increased to 7.9 mole % and blends with PC were made with identical weight ratio to those of SPBT 3.5 mole %.

Figure 5.25 shows SPBT(7.9) solution cast (baked) film. The structure is very different now: sulphonated SPBT particles that are somewhat aggregated in circles can be seen. Amorphous domains (large circular) are spaced far apart and filled with tiny, undeveloped, non-spherulitic semi-crystalline SPBT particles. A few grown spherulites in the gaps between adjacent circles are seen. Moreover, this picture suggests that the increase of ionic content has resulted in the formations of ionic aggregates in the amorphous phase. It is evident from this micrograph that crystallinity has been reduced markedly upon the increase of sulphonation.

Further changes occur upon blending with PC. The microstructure of SPBT(7.9)/PC 25/75 blend is seen in the Figure 5.26. Miscibility for this composition with lateral striations is clearly seen. No evidence of spherulitic microstructure was found and DSC results (chapter 4) also support the ionomers theory regarding formation of ionic aggregation in the amorphous region[25]. No evidence of Maltese cross spherulite structure was observed under optical microscope. This blend shows miscibility to a greater extent than SPBT(3.5)/PC blended was found optically clear to greater extent as well.

Despite rather high level of sulphonation, the spherulite structure is still present, but not lamellae with amorphous phase in the background as shown in Figure 5.27 for the SPBT(7.9)/PC 50/50 blend. Same spherulites of different sizes are visible. Therefore this blend has two phases PC is still the continuous phase, and SPBT domain has a wide size range, from a couple to several tens of micrometers[26]. This blend, however is partially miscible. Figures 5.27 and 5.28 afford a comparison between blends of the same composition (50/50), but prepared by melt-and solution casting techniques, respectively. There is a sudden change in the morphology of the SPBT(7.9)/PC 50/50 blend after melting on the hot plate, as shown in the Figure 5.29. The spherulite structure has vanished to a great extent with most of the crystalline material being
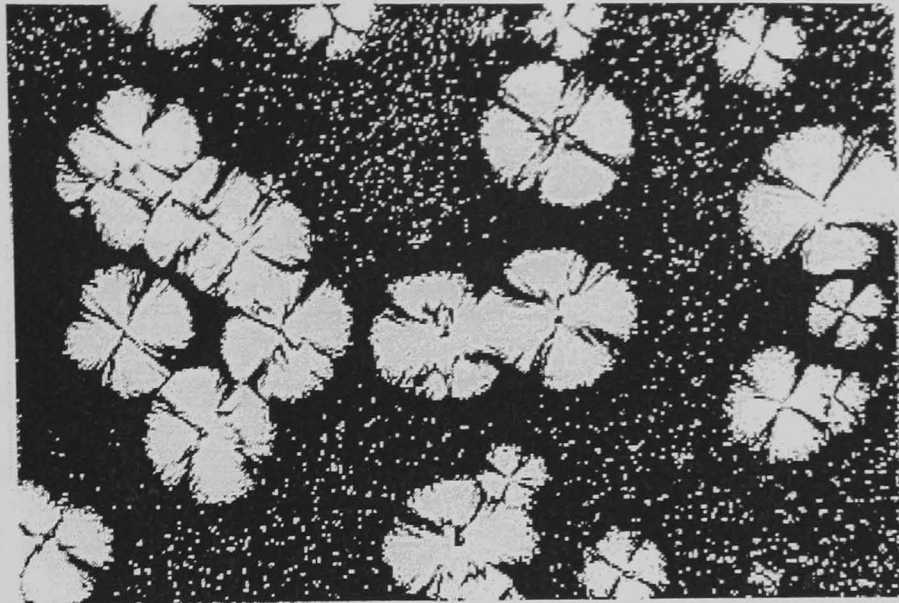
50 μm

Figure 5.27 Polarised light micrograph (X 200) for SPBT (7.9)
in the SPBT/PC 50/50 composition.
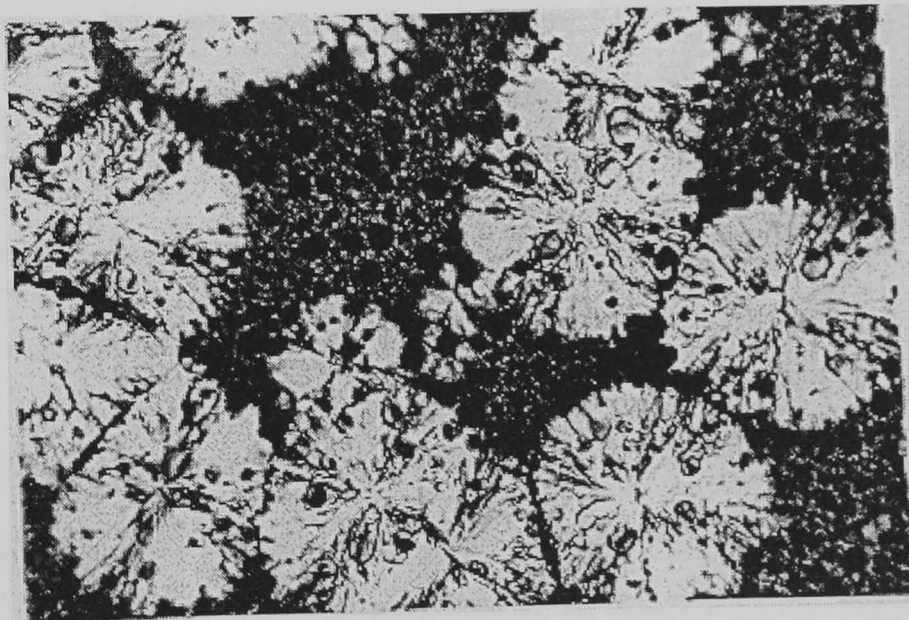
50 μm

Figure 5.28 Polarised light micrograph (X 200) for SPBT (7.9)
in the SPBT/PC 75/25 composition.

molten. This can be interpreted as coarsening of the crystallites leading to enhanced miscibility of two polymers. Figure 5.28 shows the micrograph for SPBT(7.9)/PC 75/25 composition. Typical spherulite appearance in this blend shows a round and elongated texture under cross polars. In this micrograph only one type of optically irregular large spherulites without Maltese-cross patterns is visible. Inclusions and PC encapsulate (black circles) are seen in the amorphous miscible phase, moreover discrete spheres of PC particles embedded outside of the spherulite are visible. Segregation of PC particles in the gaps between the spherulites is also evident. The site and amount of spherulites correspond to the increasing amount of SPBT, as also observed for a SPBT(3.5)/PC blend.

Figure 5.30 shows for SPBT(11.1) solution cast film. where spherulite structure, homogeneously distributed to the amorphous background, is visible. All the spherulites are of the same kind and almost of the same diameter of about 20 µm. Compared with Figure 5.20 (SPBT(3.5) solution cast) a clear change in the crystalline morphology of the material is seen. The size and the density of the spherulites have decreased with the increasing ion content, and a reduction in crystallinity of the material is observed. Furthermore two types of spherulites (Figure 5.20) changed to one kind only (Figure 5.30) with increasing degree of sulphonation (3.5 to 11.1 mole %, respectively). This findings are in agreement with the results obtained from thermal analysis on the same blends, as discussed in Chapter 4 and further elaborated in conclusions.

The extent of blending of SPBT 11.1 mole % and PC was studied on three weight composition, as described below. The extent of intermixing between SPBT(11.1) and (PC 25/75 wt %) in the solution cast blend is displayed in Figure 5.31. Optical micrograph shows apparently non-crystalline, non-spherulite structure and lateral striations, which implies partial miscibility for this composition. No evidence of Maltese cross spherulite structure was observed. This blend was also partially optically clear. Its morphology showed a remarkable resemblance to that of SPBT(7.9)/PC 25/75 (Figure 5.26). Only an increase in the thickness of lateral striations has taken place, which is attributed to the formation of ionic aggregates, and reduction of
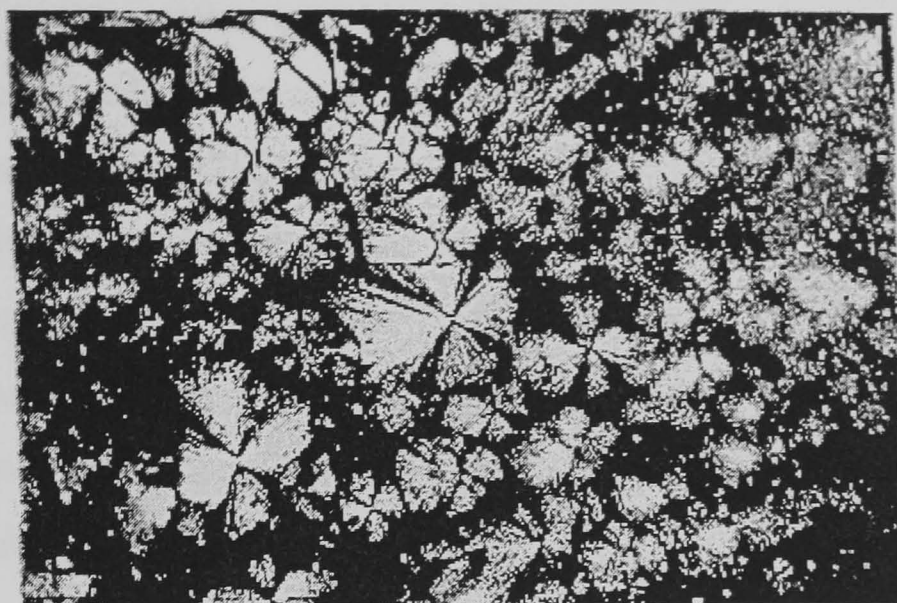
50 μm

Figure 5.29 Polarised light micrograph (X 200) for SPBT (7.9)
in the SPBT/PC 50/50 composition melted on hot plate.
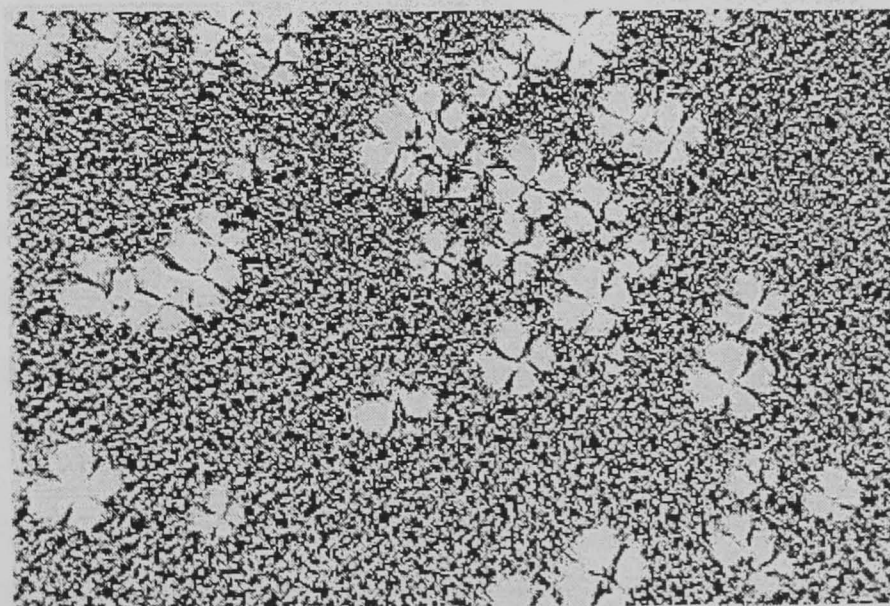
50 μm

Figure 5.30 Polarised light micrograph (X 200)
for SPBT (11.1) Solution Cast.

crystalline morphology to a great extent[8]. Figure 5.32 shows the morphology of SPBT(11.1)/PC 50/50 solution cast blend. Phase separation is seen with PBT rich phases distributed evenly in circular fashion. A reduction in the spherulite size, compared to that of a pure SPBT 11.1 mole % is evident. Remarkable similarity in the formation of SPBT-rich circular phases is seen to that found in the SPBT(7.9)/PC 50/50 solution cast blend shown in Figure 5.27. Both blends have the same wt. % ratio with PC, reduced spherulites with larger diameter of SPBT-phase, small gaps between the phases. Amorphous phase shows no sign of crystallites of any kind. It is therefore likely their miscibility is similar.

SPBT(11.1)/PC 50/50 blend melted on hot plate is shown in the Figure 5.33. Compared to the same sample before melting, (Figure 5.32) spherulite morphology is lost upon melting. The crystalline spherulites are almost completely melted and are seen aggregated in a dense, well spaced, circular shaped units of different diameters of the diameter of about 150 μm. three large, regular black spots are likely to be an artefact due to not perfectly clean glass slide or PC (being amorphous) rich region.

Finally Figure 5.34 shows the micrograph of SPBT(11.1)/PC 75/25 blend solution cast film. The structure is rather interesting in that large spherulites of one phase are again observed in the matrix of PBT/PC amorphous phase. The restricted growth of spherulites is seen in the micrograph with PC particles surrounded by the tiny spherulites of PBT/SPBT particles. PC particles are also found segregated on the outer surfaces of the large spherulites. Comparing this figure with Figure 5.28 which shows SPBT(7.9)/PC 75/25 one can observe that dispersed PC particles have resisted the growth of spherulites even in the PBT-rich phase. Moreover, the dispersion and segregation of PC particles as well as particle size has increased to some extent. In Figure 5.28 PC particles are captivated in the amorphous background, whereas PC particles are seen captivated by SPBT particles in the amorphous background in this micrograph. This phenomena can be interpreted as a change in miscibility is somewhere between these two compositions and degrees of sulphonation.
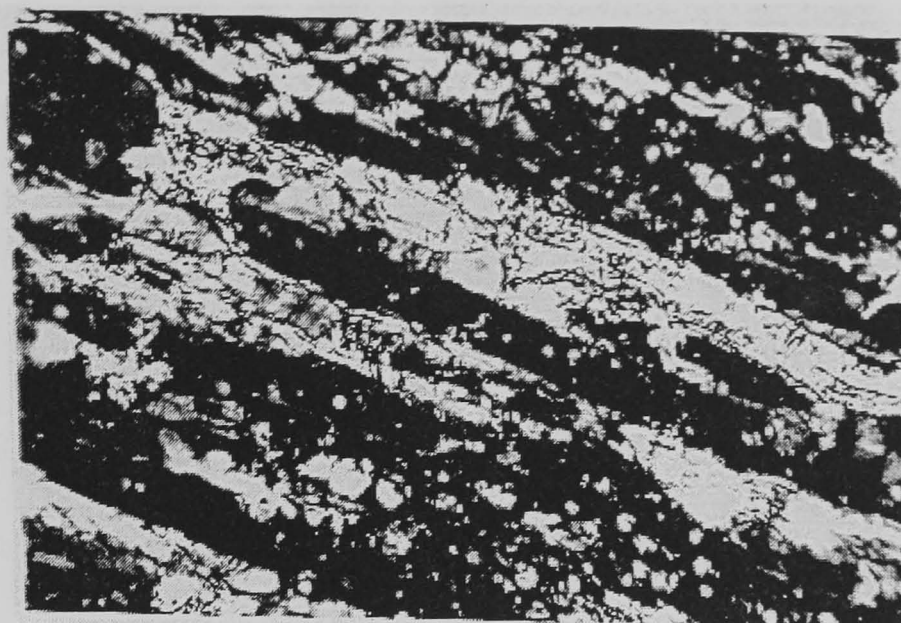
50 μm

**Figure 5.31 Polarised light micrograph (X 200) for SPBT (11.1)
in the SPBT/PC 25/75 composition.**
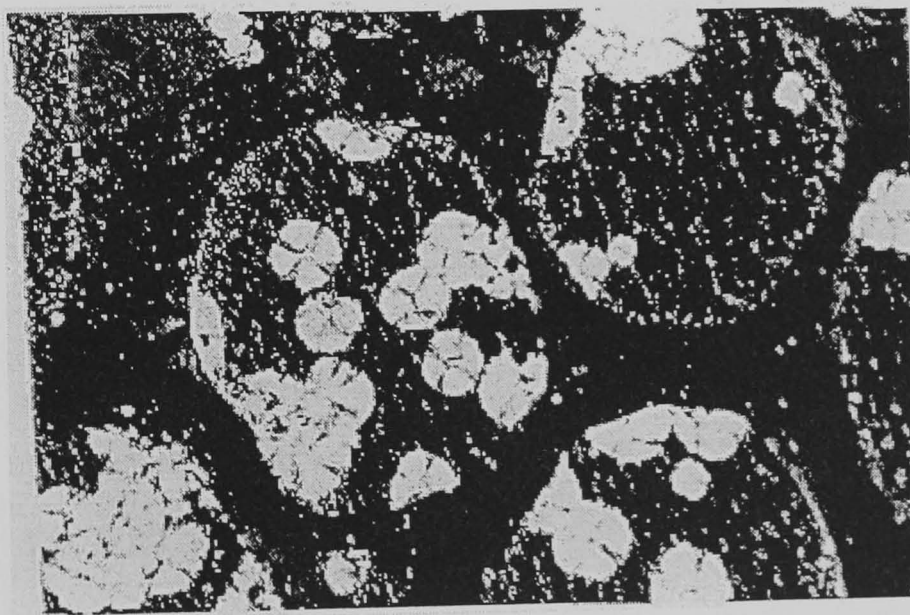
50 μm

**Figure 5.32 Polarised light micrograph (X 200) for SPBT (11.1)
in the SPBT/PC 50/50 composition.**
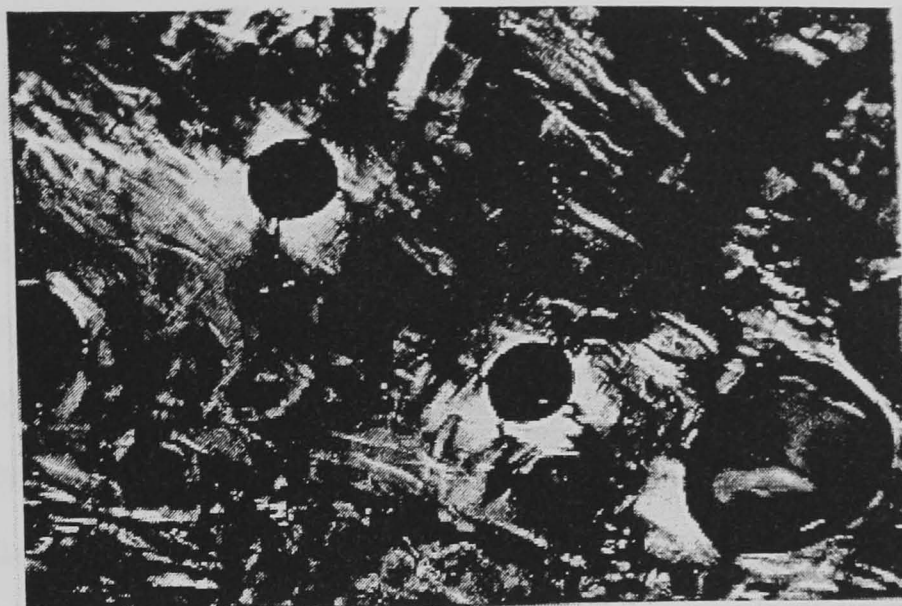
50 μm

**Figure 5.33 Polarised light micrograph (X 200) for SPBT (11.1)
in the SPBT/PC 50/50 composition melted on hot plate.**
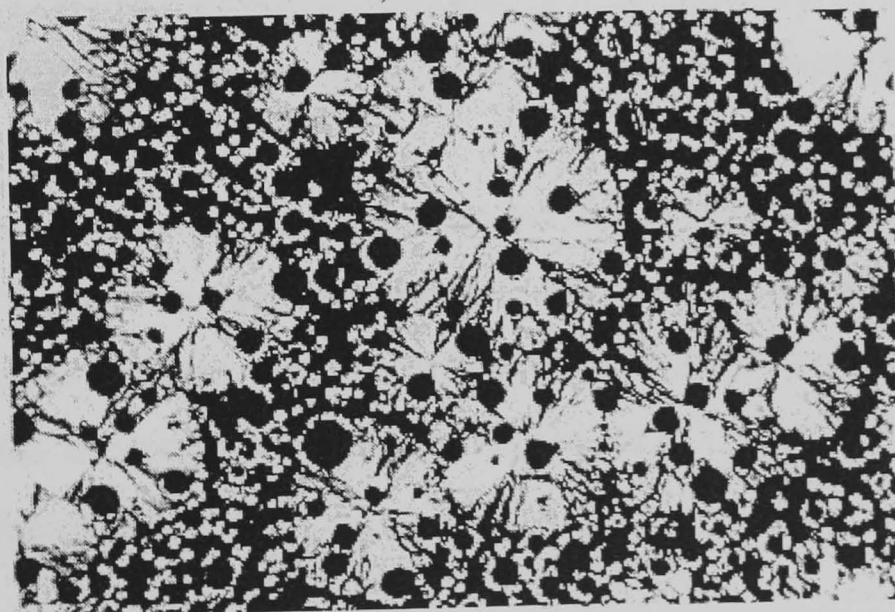
50 μm

**Figure 5.34 Polarised light micrograph (X 200) for SPBT (11.1)
in the SPBT/PC 75/25 composition.**

5.5   Conclusions

The morphology (molecular order) upon sulphonation of PBT and SPBT films was studied by WAXD and optical microscopy. The WAXD results indicate that both PBT and SPBT (powder and film) are in a partially ordered state. For SPBT of the degree of sulphonation higher than 3.5 mole %, the molecular order and overall crystallinity decrease as compared to unfunctionalised PBT. SPBT with the highest levels of sulphonation showed a marked reduction in the crystallinity. A significant decrease in the crystallite size was noticed in the samples with ion content larger than 5 mole %.

PS ionomers also showed a significant decrease in the crystallinity upon sulphonation up to 10.5 mole %. However % crystallinity increased for fully sulphonated iso-PS (94.5 mole %). Iso-tactic polystyrene and syndiotactic polystyrene, non-sulphonated, were both found to be partially crystalline compared to atactic polystyrene, which was found to be amorphous.

Optical microscopy results on the SPBT/PC blends with level of sulphonation 0.0 to 11.1 mole % of SPBT and several composition (25/75, 50/50 and 75/25) displayed the influence of the sulphonate groups on the crystalline and amorphous phases.

Furthermore, optical microscopy studies support DSC results obtained for SPBT 3.5 mole % with respect to high temperature double melting endotherms. Optical microscopy provided a direct evidence of two types of spherulites, usual and unusual. However, for the degree of sulphonation higher than 5 mole % only one type of isolated spherulites is seen.

It has been found that overall loss of crystallinity with sulphonation and the subsequent dilution of PBT with an amorphous polymer PC corresponds well to DSC results obtained for these blends. In addition, phases with two different levels of sulphonation are formed, un-sulphonated which is crystalline and sulphonated, amorphous phase. Finally, it is concluded from these results that sulphonated groups form amorphous phases in the PBT semi crystalline material.

References

1   M Yokouchi, Y Sakakibara, Y Chatani, H Tadokoro, T Tanaka and K Yoda, *Macromolecules*, **9** 226 (1976).

2   M Ree and T L Nunes, *Polym*, **6** 1148 (1994).

3   G Voyiatzis, G Petekidis, D Vlassopoulos, E Kamitsos and A Bruggeman, *Macromolecules*, **29** 2244 (1996).

4   B Gabrys, D G Peiffer, J. S Higgins, C. W Lantman, W J MacKnight, A M Pedley and A R Rennie, *Macromolecules*, **22** 3748 (1989).

5   X Zhang and A Eisenberg, *Polym. for Advance Tech*, **1** 14 (1989).

6   A N Wilkinson and S B Tattum, *Polym*, **38** 1927 (1997).

7   R B Moore, and C R Martin, *Macromolecules*, **21** 9 (1989).

8   R E Prud'Homme and R S Stein, *Eur. Polym*, **13** 365 (1977).

9   I A Nyrkova, A R khokhlov, and M Doi, *Macromolecules*, **26** 3601 (1993).

10   A Eisenberg, B Hird and R B Moore, *Macromolecules*, **23** 4098 (1990).

11   L Alexander, "X-Ray Diffraction Methods in Polymer Science", Krieger, New York (1979).

12   K Tandano, E Hirasawa, H Yamamoto and S Yano, *Macromolecules*, **22** 752 (1989).

13   K Heesub, S B Park, C J Jin and C Z Wang, *Polymer* **37** 2445 (1996).

14   R P Sundararajan and N J Tyrer, *Macromolecules*, **15** 1004 (1982).

15   M Melchiors, H Keul, and H Hocker, *Polymer*, **37** 1519 (1996).

16   S Karim and A V Tobolsky, *J. Text. Res*, **21** 805 (1951).

17   T Hatakeyama, *J. Macromol Sci. Phys*, **10** 1167 (1977).

18   K L Mittal, "Metallized plastics : Fundamentals and Applications" Mercel Dekker New York (1998).

19   C E Sroog, *J. Polym. Sci, Macromol. Rev*, **11** 161 (1976).

20   M D Sefcik, E O McKay and R E Schaefer, *Macromolecules*, **12** 423 (1979).

21   K S Seshardi, P A Antonopolos and W J Heilman, *J. Polym. Sci. Chem. Ed*, **18** 2469 (1980).

22   S Zhaohui, L Xuan and L H Shaw, *Macromolecules*, **27** 291 (1994).

23   B Gabrys, O Scharpf and D G Peiffer, *J. Polym. Sci. Part B, Polym. Phys*, **31**

1891 (1993).

24   D Delimony, B Goffaux, J Devaux and R Legras, _Polymer_, **36** 3255 (1995).

25   C E Williams, "Structure and properties of ionomers", M Pineri and
A Eisenberg (1987).

26   J Wu and Y W Mai, _J. Mater. Sci_, **28** 6167 (1993).

CHAPTER 6

CONCLUSIONS

6.1   Conclusions

The aim of this thesis was two fold. Firstly, to investigate the structural and thermal properties of a semicrystalline ionomer poly (butylene terephthalate), PBT and its sulphonate analog. Secondly, to study its blends with amorphous polycarbonate (PC) in order to determine the best composition from the view point of miscibility and optical clarity. It was determined, as briefly summarised below, that the optimal composition of the SPBT/PC blend would be made with an estimated degree of sulphonation around 9-mole %. That was the region yielding transparent blends, which is important for commercial applications such as car windshields. To this end, a number of SPBT samples in the powder and film forms, with degree of sulphonation ranging from 0.0 mole % to 13.5 mole % was investigated. Furthermore, a series of blends of SPBT/PC, made varying the degree of sulphonation of SPBT and the amount of PC, was studied. In order to differentiate between the effects of sulphonation on PBT and mixing with PC, a comparative series of blends made with non-sulphonated PBT was investigated. It has been concluded that the process of sulphonation improves the PBT/PC blend miscibility considerably, as shown by increased optical clarity of SPBT/PC blends compared to those of PBT/PC.

The optical clarity increases, since the crystallite structure of PBT is gradually destroyed upon sulphonation, as by wide angle X-ray scattering studies. Both PBT and SPBT (powder and film) were found to be in a partially ordered state. For SPBT highest level of ion content, the molecular order and overall crystallinity have decreased compared to unfunctionalised PBT. SPBT with the highest levels of sulphonation showed marked reduction in crystallinity. For the highest degree of sulphonation, the crystallinity was apparently destroyed. Investigations of thermal properties confirmed this result

In the case of PBT powder samples the crystallinity was reduced from 40 % to 30 % upon sulphonation (for samples with <5.0 mole % ionic content). In samples with > 5.0 mole % 24-30 % crystallinity was found. Multiple melting endotherms were recorded for samples with <5.0 mole %, which was attributed to two distinct crystallite forms and single melting peak for samples with >5.0 mole %. Data obtained can be explained in terms of Flory's model for melting of random copolymers. For SPBT/PC blends the crystallinity of PBT fraction remained at the same level of 40 % (for samples with <5.0 mole %). Samples with level of sulphonation > 5.0 mole % the crystallinity ranging from 20-30 % was found.

SPBT/PC blends with the sulphonation level less than 5.0 mole % were found not to be miscible due to high level of crystallinity. However, blends with the sulphonation level greater than 5.0 mole % were found partially miscible. Furthermore, it was found by the DSC investigations that SPBT/PC 7.9 mole % 25/75 and 11.1 mole % 50/50 blends are the best composition for greater degree of transparency and miscibility compared with other blend compositions and level of sulphonation or non sulphonated blends.

For comparison, a series of polystyrene ionomers was studied. It was found that the isotactic and syndiotactic, non-sulphonated PS both were partially crystalline compared to atactic polystyrene, which was found to be amorphous. The iso-PS 0.0 mole % was found to be partially crystalline. Main melting peak only appeared in the first scan for iso-PS 0.0 mole %, which is characteristic of the material. All the iso-PS, PS samples exhibited glass transition temperatures. However, increase in the level of sulphonation for iso-PS samples resulted in disorder in the material i. e. transition from the partial crystalline state to amorphous one. The similar behaviour of PS ionomers to that of PBT ionomers gives an additional support to this study.

Optical microscopy results obtained on the SPBT/PC blends have shown the influence of the sulphonate groups on both the crystalline and amorphous phases. Furthermore, optical microscopy studies support DSC results obtained for SPBT 3.5 mole % as far as the interpretation of high temperature double melting endotherms is concerned.

SPBT/PC 7.9 mole % 25/75 blend was found partially miscible. This blend composition and the level of ionic content resulted in a remarkable reduction in the crystallite size in the blend compared with functionalised and unfunctionalised blends of different compositions and the level of ionic content. Optical microscopic investigations also provided direct evidence of two types of spherulites, usual and unusual. However, for the degree of sulphonation higher than 5 mole % only one type of isolated spherulites were seen. An alternative explanation about the existence of only one type of spherulites is offered in the attached paper.

This research project also demonstrates the utility of a number of techniques for the study of ionomers and their blends, and the effect of ionic content on the structural properties in these materials.

(i)   Differential scanning calorimetry was the main experimental technique used to study the thermal behaviour of the polymers and their blends. Through the measurement of glass transition temperature, melting point, and the crystallinity of various polymers and blends was determined. For blends with well-determined glass transition temperature T_g, DSC was used to confirm miscibility of the blends and to search for an optimal composition and functionality for miscible blends. The multiple melting behaviour investigated by DSC studies was complimented by optical microscopy measurements on the blends of SPBT/PC.

(ii)   Wide angle X-ray diffraction was used to detect changed structural properties of the ionomers, such as a transition from the semicrystalline to amorphous state upon the increase of ionic content. For samples with highest level of sulphonation a diffused X-ray pattern was obtained due to disorder setting in.

(iii)   Optical light microscopy was used to investigate miscibility of phases, morphology of spherulites, spherulite size and to provide direct evidence for the existence of two types of spherulites. Optical microscopic studies on blends are consistent with the interpretation of DSC results.

In summary one of the important goals in studying ionomer blends is to be able to relate the effect of ionic content with the reduction of crystallinity and further dilution with amorphous polymer PC to improve optical clarity. It is hoped that this work demonstrated this possibility fully.

6.2   Recommendations for future work

It is clear that the progress in the ionomer field is accelerating, and it is anticipated that development of new and interesting ionomer blends will continue to be a major activity in the near future. The present and most likely future widespread use of the PBT/PC blend system in the automobile industry world-wide suggests that active research into this and similar blend systems will continue. In the particular case of the sulphonated PBT/PC blend it is important to have a better understanding of the influence of the ionic content on the physical and mechanical properties of the new polymer blend system. Future work should focus on three distinct but complementary directions: (i) materials and microstructural characterisation, (ii) modelling the SPBT/PC blend system for different level of sulphonation molecular simulation and (iii) collection of experimental data to validate the computer simulation for example using small angle neutron scattering technique.

To enhance our knowledge in the area of sulphonated PBT/PC blend system, the next significant work has to concentrate on the mechanisms involved in the formation of ionic aggregates. Using auger electron probe (AES), nuclear magnetic resonance (NMR) and small angle neutron scattering (SANS) could study this.

Dynamics of chains in ionomer blends would be another area of study. It has been found that in most non-ionic polymer blends, the local chain dynamics of the two components are very different, even in the miscible blend. The effect of coulombic interactions on chain dynamic is thus of special interest. The dynamical information can be obtained from ^{13}C and ^{2}H NMR relaxation measurements. The possibilities of utilising ionic interactions to prepare 'ionic block' and 'graft' copolymers and to enhance the miscibility of molecular composites certainly deserve further exploration.

Although most of the present studies are concentrated on binary systems, interesting ternary and quaternary systems can, in principle, be developed by the use of coulombic interactions.